

MODEL DEVELOPMENT FOR FREIGHT CAR
DYNAMIC CURVING SIMULATION

by

SUSAN MARIE KROLEWSKI

B. S., Massachusetts Institute of Technology

September 1980

SUBMITTED IN PARTIAL FULFILLMENT OF THE
REQUIREMENTS FOR THE DEGREE OF
MASTER OF SCIENCE

at the

MASSACHUSETTS INSTITUTE OF TECHNOLOGY

June 1982

© MASSACHUSETTS INSTITUTE OF TECHNOLOGY

Signature of Author.....
Department of Mechanical Engineering
March 1, 1982

Certified by.....
J. K. Hedrick
Thesis Supervisor

Accepted by.....
Warren M. Rohsenow
Chairman, Committee of Graduate Students

Archives
MASSACHUSETTS INSTITUTE
OF TECHNOLOGY

JUL 30 1982

LIBRARIES

MODEL DEVELOPMENT FOR FREIGHT CAR
DYNAMIC CURVING SIMULATION

by

SUSAN MARIE KROLEWSKI

Submitted to the Department of Mechanical Engineering
on March 1, 1982, in partial fulfillment of the requirements
for the degree of Master of Science.

ABSTRACT

A mathematical model of a freight car has been developed to simulate the dynamic response of a vehicle during curve entry and exit. The carbody and each truck have three degrees of freedom. Each wheelset has two degrees of freedom. Nonlinearities included are wheel/rail geometry, coulomb friction and creep force saturation. Solution of the equations to initial conditions are found by fourth order Runge-Kutta integration. Parametric studies investigated the effects of wheel/rail geometry, curve entry geometry, coulomb friction and suspension design.

Thesis Supervisor: J. Karl Hedrick

Title: Associate Professor of
Mechanical Engineering

ACKNOWLEDGEMENT

I would like to thank Professor J. Karl Hedrick for his continual assistance and encouragement throughout the past year. I would also like to thank the countless people who helped me along the way.

Special thanks to Robin Rohlicek for his hours of help in preparing the manuscript.

TABLE OF CONTENTS

	PAGE
ABSTRACT.....	2
ACKNOWLEDGMENTS.....	3
LIST OF FIGURES.....	7
LIST OF TABLES.....	10
NOMENCLATURE.....	11
 CHAPTER 1 - INTRODUCTION.....	 16
1.1 Motivation.....	16
1.2 Previous Work.....	18
1.3 Research Approach.....	19
 CHAPTER 2 - MODEL DEVELOPMENT.....	 21
2.1 Model Description.....	21
2.2 Wheel/Rail Characteristics.....	31
2.2.1 Wheel/Rail Geometry.....	31
2.2.2 Wheel/Rail Forces and Moments.....	36
2.3 Nonlinear Suspension Characteristics.....	40
2.4 Curve Geometry.....	43
2.5 Track Flexibility Model.....	45
2.6 Equations of Motion.....	50
2.7 Model Evaluation.....	50

CHAPTER 3 - PARAMETRIC STUDIES.....	53
3.1 Introduction.....	53
3.2 Performance of Vehicle.....	54
3.3 Spiral Length.....	57
3.4 Degree Curve.....	62
3.5 Rail Flexibility.....	62
3.6 Wheel/rail Profile.....	66
3.7 Interconnection of Wheelsets.....	66
3.8 Coulomb Friction.....	70
CHAPTER 4 - CONCLUSIONS AND RECOMMENDATIONS.....	77
REFERENCES.....	79
APPENDIX A - DERIVATION OF WHEELSET DYNAMIC CURVING	
EQUATIONS OF MOTION.....	82
A.1 Introduction.....	82
A.2 Axis System.....	82
A.3 Acceleration of Wheelset.....	84
A.4 Angular Momentum of the Wheelset.....	85
A.5 Forces and Moments.....	86
A.5.1 Normal Forces.....	89
A.5.2 Creep Forces.....	90

APPENDIX B - DERIVATION OF THE EQUATIONS OF MOTION

FOR FREIGHT CAR MODEL.....	95
B.1 Introduction.....	95
B.2 Axis Systems.....	97
B.3 Acceleration.....	100
B.3.1 Sideframes.....	100
B.3.2 Bolster.....	101
B.3.3 Carbody.....	102
B.4 Angular Momentum.....	102
B.4.1 Sideframes.....	102
B.4.2 Bolster.....	103
B.4.3 Carbody.....	104
B.5 Forces and Moments.....	105
B.5.1 Roller Bearing Connections.....	105
B.5.2 Interwheelset Connections.....	109
B.5.3 Secondary Suspension.....	110
B.5.4 Centerplate.....	111
B.6 Equations of Motion.....	111
B.6.1 Wheelset.....	111
B.6.2 Truck Frame.....	113
B.6.3 Carbody.....	116
APPENDIX C - LISTING OF PROGRAM.....	119

LIST OF FIGURES

2.1	Schematic of Freight Car Model.....	22
2.2	Three-Piece Truck.....	24
2.3	Scheffel's Radial Truck.....	26
2.4	List's Radial Truck.....	27
2.5	Schematic of Equilibrium Configuration of Truck.....	28
2.6	Schematic of Disturbed Configuration of Truck.....	29
2.7	Schematic of Freight Car Model.....	30
2.8	Schematic of Wheelset Interconnection Model.....	32
2.9	Wheel/Rail Contact Geometry Parameters.....	33
2.10	Contact Geometry for <u>New Wheel</u>	34
2.11	Contact Geometry for <u>Worn Wheel</u> on <u>Worn Rail</u>	35
2.12	Creep Force as a Function of Creepage.....	39
2.13.a	Warp Suspension Characteristic.....	41
2.13.b	Lateral Suspension Characteristic.....	41
2.13.c	Vertical Suspension Characteristic.....	41
2.14.a	Ideal Coulomb Friction Element.....	42
2.14.b	Piecewise Linear Coulomb Friction Approximation.....	42
2.15.a	Definition of Superelevation.....	44
2.15.b	Definition of Degree Curve.....	44
2.16	Superelevation and Track Curvature as a Function of Distance.....	46

2.17	Schematic of Rail Flexibility Model.....	48
2.18	Rail Deflection as a Function of Lateral Load.....	49
2.19.a	Response of Model below Critical Speed.....	52
2.19.b	Response of Model above Critical Speed.....	52
3.1	Lateral Excursion of the Wheelsets of the Baseline Vehicle.....	56
3.2	Angle of Attack of the Wheelsets of the Baseline Vehicle.....	58
3.3	Lateral Component of Normal Force on Left Wheel of Baseline Vehicle.....	59
3.4	Work on Wheelsets of Baseline Vehicle.....	60
3.5	Effect of Spiral Length on Maximum Flange Force.....	61
3.6	Effect of Final Degree Curve on the Lateral Excursion of the Wheelsets.....	63
3.7	Effect of Final Degree Curve on the Lateral Component of Normal Force on the Left Lead Wheel.....	64
3.8	Effect of Rail Flexibility on Maximum Flange Forces.....	65
3.9	Effect of Worn Wheel on Worn Rail Profile on Wheelset Lateral Excursion.....	67
3.10	Effect of Worn Wheel on Worn Rail Profile on Angle of Attack.....	68
3.11	Effect of Worn Wheel on Worn Rail Profile on Lateral Component of the Normal Force on the Left Wheel.....	69
3.12	Effect of Wheelset Interconnection on Angle of Attack of Lead Wheelset.....	71
3.13	Effect of Wheelset Interconnection on Lateral Component of the Normal Force on the Left Wheel.....	72

3.14	Effect of Coulomb Friction on Wheelset Angle of Attack.....	75
3.15	Effect of Coulomb Friction on the Lateral Component of Normal Force on the Left Wheel.....	76
A.1	Definition of Coordinate Systems.....	83
A.2	Freebody Diagram of Wheelset.....	87
A.3	Definition of Contact Plane Axis System....	91
B.1	Definition of Coordinate Systems.....	98
B.2	Freebody Diagram of Wheelset Suspension Forces.....	106
B.3	Freebody Diagram of Sideframes and Bolster.....	107
B.4	Freebody Diagram of Carbody.....	108

LIST OF TABLES

3.1	Baseline Freight Car Parameter.....	55
3.2	Nonlinear Suspension Parameters.....	74

NOMENCLATURE

a	Half the rail gauge, ft
\bar{a}_B	Inertial acceleration of the bolster, ft/sec ²
\bar{a}_C	Inertial acceleration of the carbody, ft/sec ²
\bar{a}_S	Inertial acceleration of the sideframes, ft/sec ²
\bar{a}_T	Inertial acceleration of the track reference frame, ft/sec ²
\bar{a}_W	Inertial acceleration of the wheelset, ft/sec ²
b	Half the truck wheelbase, ft
b_T	Rail damping, lb-sec/ft
d	Half horizontal spacing between sideframes, ft
d_{CP}	Effective centerplate damping, ft-lb-sec/rad
d_{PX}	Longitudinal primary suspension damping, lb-sec/ft
d_{PY}	Lateral primary suspension damping, lb-sec/ft
d_{SY}	Lateral secondary suspension damping, lb-sec/ft
d_{SZ}	Vertical secondary suspension damping, lb-sec/ft
d_W	Effective warp damping, ft-lb-sec/rad
f_{11}	Lateral creep coefficient, lb/wheel
f_{12}	Lateral/spin creep coefficient, ft-lb/wheel
f_{22}	Spin creep coefficient, ft ² -lb/wheel
f_{33}	Longitudinal creep coefficient, lb/wheel
F_{GRAV}	Gravitational stiffness force, lb
\bar{F}_L	Creep force on left wheel, lb

\bar{F}_R	Creep force on right wheels, lb
\bar{F}_{SUSP}	Suspension force on wheelset, lb
F_{YO}	Lateral friction breakout force between bolster and sideframes, lb
F_{ZO}	Vertical friction breakout force between bolster and sideframes, lb
g	Acceleration due to gravity, 32.2 ft/sec ²
h	Height of external weight above the axle, ft
h_B	Height of the bolster center of gravity above the axle, ft
h_C	Height of the carbody center of gravity above the bolster, ft
h_S	Height of the sideframe center of gravity above the axle, ft
h_T	Height of the carbody hinge point above the bolster, ft
\bar{H}_B	Angular momentum of the bolster about its center of gravity, slugs-ft ² /sec
\bar{H}_C	Angular momentum of the carbody about its hinge point, slugs-ft ² /sec
\bar{H}_O	Angular momentum of the carbody about its center of gravity, slugs-ft ² /sec
\bar{H}_S	Angular momentum of the sideframes about its center of gravity, slugs-ft ² /sec
\bar{H}_W	Angular momentum of the wheelset about its center of gravity, slugs-ft ² /sec
\bar{I}_B	Moment of inertia of the bolster, slug-ft ²
\bar{I}_C	Moment of inertia of the carbody, slug-ft ²
\bar{I}_S	Moment of inertia of the sideframes, slugs-ft ²
\bar{I}_W	Moment of inertia of wheelset, slugs-ft ²

k_B	Interaxle bending stiffness, ft-lb/rad
k_{CP}	Effective centerplate stiffness, ft-lb/rad
k_{PX}	Longitudinal primary suspension stiffness, lb/ft
k_{PY}	Lateral primary suspension stiffness, lb/ft
k_{SY}	Lateral secondary suspension stiffness, lb/ft
k_{SZ}	Vertical secondary suspension stiffness, lb/ft
k_T	Rail stiffness, lb/ft
k_S	Interaxle shear stiffness, lb/ft
k_W	Effective warp stiffness, ft-lb/rad
L	Half the distance between truck centerplates, ft
\bar{L}_A	Axle load, lb
m_B	Mass of the bolster, slugs
m_C	Mass of the carbody, slugs
m_S	Mass of the sideframes, slugs
m_W	Mass of the wheelset, slugs
\bar{M}_L	Creep moment on the left wheel, ft-lb
\bar{M}_R	Creep moment on the right wheel, ft-lb
M_{GRAV}	Gravitational stiffness moment, ft-lb
\bar{M}_{SUSP}	Suspension moment on the wheelset, ft-lb
\bar{N}_L	Normal force on the left wheelset, lb
\bar{N}_O	Nominal normal force, lb
\bar{N}_R	Normal force on the right wheelset, lb
r_L	Wheelset left rolling radius, ft
r_O	Nominal wheelset rolling radius, ft
r_R	Wheelset right rolling radius, ft

R	Vehicle radius of curvature, ft
\bar{R}_B	Displacement of the bolster center of gravity, ft
\bar{R}_C	Displacement of the carbody center of gravity, ft
\bar{R}_L	Position vector of the left wheel contact point, ft
\bar{R}_O	Displacement of the carbody hinge point, ft
\bar{R}_R	Position vector of the right contact point, ft
\bar{R}_S	Displacement of the sideframe center of gravity, ft
\bar{R}_W	Displacement of the wheelset center of gravity, ft
t	Time, sec
T_{CPO}	Centerplate friction breakaway torque, ft-lb
T_{WO}	Warp friction breakaway torque, ft-lb
V	Forward speed of the vehicle, ft/sec
W_{EXT}	External weight acting on the wheelset, lb
Y_L	Lateral displacement of the left rail, ft
Y_R	Lateral displacement of the right rail, ft
δ_L	Contact angle of left wheel, rad
δ_O	Nominal contact angle, rad
δ_R	Contact angle of right wheel, rad
ϵ	Nonlinear creep saturation coefficient
ϕ_d	Cant deficiency, radians
ϕ_{SE}	Superelevation angle, radians
ϕ_W	Wheelset rollangle, radians
μ	Coefficient of friction between wheel and rail
$\bar{\omega}_{AXIS}$	Angular velocity of wheelset axis system, rad/sec
$\bar{\omega}_B$	Angular velocity of bolster, rad/sec

$\bar{\omega}_C$	Angular velocity of carbody, rad/sec
$\bar{\omega}_S$	Angular velocity of sideframe, rad/sec
$\bar{\omega}_T$	Angular velocity of the track reference frame, rad/sec
$\bar{\omega}_W$	Angular velocity of the wheelset, rad/sec
Ω	Nominal wheelset spin velocity, rad/sec
ξ_X	Longitudinal creepage
ξ_Y	Lateral creepage
ξ_Z	Vertical creepage
ξ_{SP}	Spin creepage

CHAPTER 1

INTRODUCTION

1.1 MOTIVATION

The dynamic performance of a railway vehicle can be characterized by its stability and curving behavior. Above a certain critical value of forward speed, small disturbances to the vehicle will result in coupled lateral and yaw oscillations that will grow until the wheels of the vehicle hit against the rails. This behavior, called hunting, is accompanied by large dynamic loads which cause damage to both the vehicle and the track. The most effective way to suppress hunting and increase stability is to stiffen the primary suspension. For good curve negotiation, it is desirable that the wheels align themselves radially to reduce wear, noise and lateral forces. Unfortunately stiffening the primary suspension restrains the wheelset to remain parallel causing curving performance to deteriorate.

This conflict between stability and curving performance has been a problem in all rail vehicle designs. Overcoming this conflict has become a major design goal. As a result, a new concept in truck design, called the radial truck, has been introduced. Interconnecting the wheelsets of the truck by radial arms or springs can improve the ability of the wheelsets to align themselves radially in curves without

decreasing stability.

The North American three-piece freight truck suffers from particularly poor curving performance and stability. Due to its simple and inexpensive construction, its design has remained unchanged for years despite its poor dynamic performance. The three-piece truck has no primary suspension. The motion of the wheelset relative to the truck is very restricted by roller bearings. As the truck enters a curve, the wheelsets are prevented from aligning radially with the track and are forced to move laterally to achieve equilibrium. The truck assumes a skewed parallelogram shape which allows the wheelsets some yaw flexibility. It is not, however, enough to significantly enhance the curving performance. High flange forces develop, resulting in increasing stress levels, wear and noise. With the advent of the radial truck, however, there exists a way of improving existing trucks by the use of radial connections.

Most previous work has been concerned with tangent track stability and steady state curving. These results however cannot be used to predict vehicle performance on changing radius track. In many situations, steady state conditions are never met due to the transient effects of track alignments and irregularities and transition curves. Most derailments, in fact, occur in spiral entries. Tests have observed large dynamic force variations even on constant radius curves. The

aim of this thesis is to create a simulation program capable of predicting forces and displacements during transition curve entry and exit. The performance of both three-piece and radial freight trucks will be investigated.

1.2 PREVIOUS WORK

The first analytical studies of rail vehicle curving date back to the nineteenth century. The early work of Porter [1] was based on a friction center method. This method assumes that the vehicle is rigid, the wheelsets are cylindrical and that one or more wheelsets are in flange contact. As a result, this theory is useful only for vehicles with stiff primary suspensions on tight radius curves.

It was not until the work of Vermulen and Johnson [2] and Kalker [3] that a proper understanding of the wheel/rail friction mechanism needed to accurately describe stability and curving was developed. Since then numerous steady-state models have been proposed. Boocock [4] and Newland [5] independently used linear analysis to study the effects of primary stiffness on curving performance. Nonlinear curving theory was developed by Elkins and Gostling [6], Law and Cooperrider [7] and Bell [8]. The model by Elkins and Gostling considers nonlinear wheel/rail profiles with large contact angles and nonlinear Kalker creep theory [3]. Law and Cooperrider formulated a model which includes "heuristic"

nonlinear creep [9], nonlinear wheel/rail geometry and secondary yaw breakaway. Bell investigated the stability/curving tradeoff in conventional and radial vehicles.

In the past several years a few dynamic models have been proposed to study the effect of curve entry and exit. Smith [10] formulated a dynamic curving model to study the effect of spiral length, curvature and initial vehicle position on the response of freight cars. Although a nonlinear suspension was considered, his model uses conical wheels and an unbanked track. Law and Cooperrider [11] have used a model with nonlinear suspension, creep forces and wheel/rail geometry to study the influence of track curvature, superelevation angle and irregularities on the response of conventional and radial trucks. Clark [12] conducted studies of the dynamic response of rail vehicles to lateral track irregularities. His model includes nonlinear wheel/rail geometry, creep saturation and rail flexibility.

1.3 RESEARCH APPROACH

Despite its simple design, the three-piece truck is a difficult system to analyze due to its nonlinear nature. A model capable of predicting the dynamic curving performance of conventional three-piece trucks and radially steered trucks is initially developed. The equations of motion of the model are

derived and simulated by digital integration to find time histories of the state variables, lateral forces, lateral/vertical (L/V) ratios, angle of attack and work in the contact patch. Nonlinear wheel/rail geometry, coulomb friction, creep saturation and rail flexibility will be considered.

Chapter 2 describes the development of the analytical model. Chapter 3 examines the influences of spiral length, degree curve, cant deficiency, radial connections, rail flexibility, wheel/rail profile and coulomb friction on the response of the vehicle. Chapter 4 summarizes the results and includes suggestions for future work. Appendices A, B and C contain detailed derivations of the equations of motion and the program listing.

CHAPTER 2

MODEL DEVELOPMENT2.1 MODEL DESCRIPTION

The typical North American freight car, shown schematically in Figure 2.1 consists of a carbody supported by a pair of dual axle three-piece trucks.

Each wheelset consists of two wheels rigidly attached to an axle. The wheels are tapered outwards to provide self-centering action. As the wheelset is displaced laterally from the track centerline, the difference in wheel rolling radii tends to steer the wheelset back to the centered position. To provide lateral guidance in tight curves, wheels are equipped with flanges on the inner edge. The wheelset motion is described in terms of lateral and yaw degrees of freedom. An extra state describing the spin rate perturbation about the axle centerline is necessary to describe the change in nominal spin rate during curving. The wheelsets are assumed never to lose contact with the rail, thus the roll angle is a function of wheelset lateral displacement.

The wheelsets are attached to the truck frame by roller bearings. Since there is usually no resilient material between bearings and the truck, the lateral and yaw motion of the wheelset relative to the truck is generally restricted. As a result, the axle connections of freight cars do not

TRACK CENTERLINE

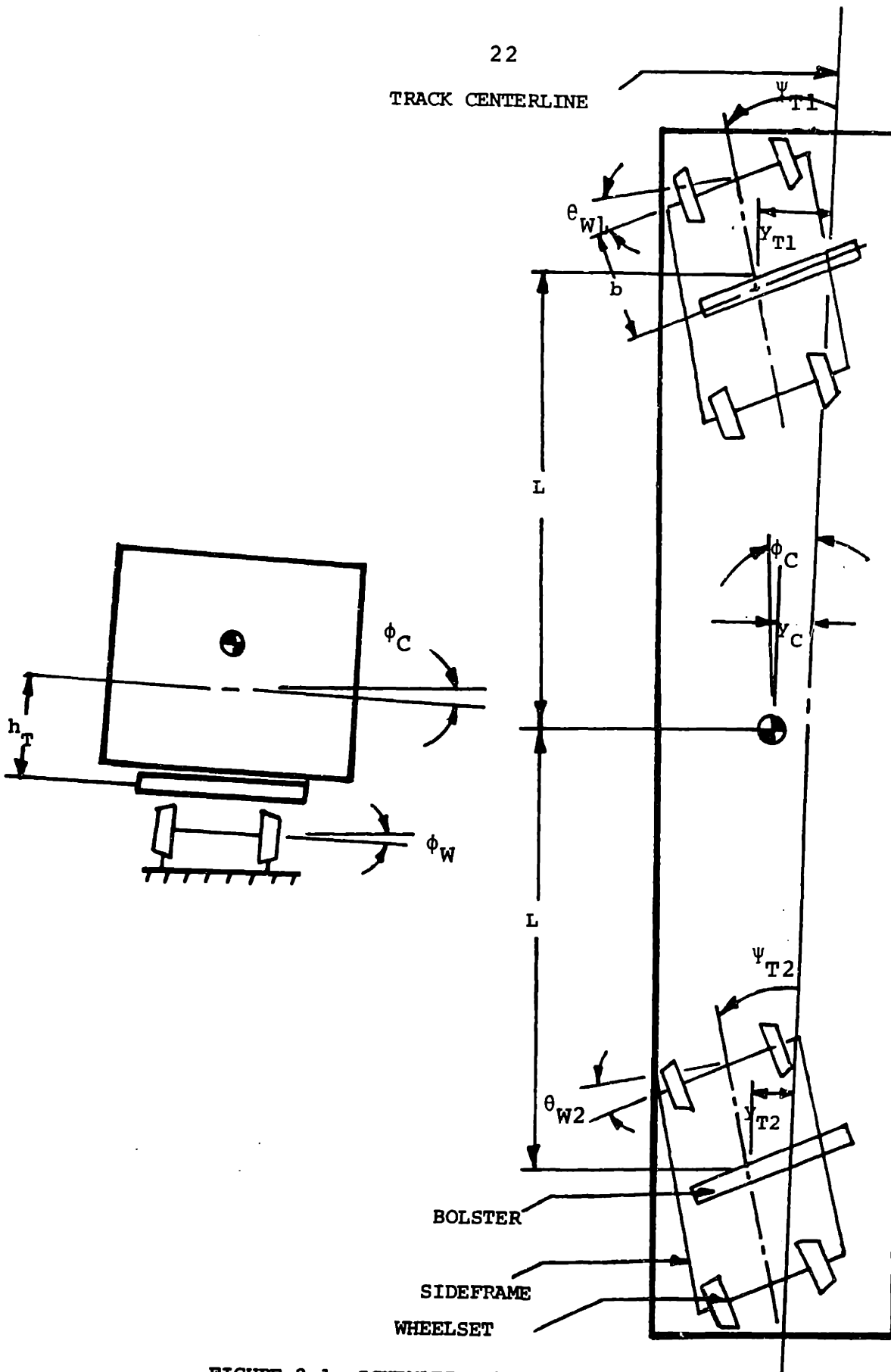


FIGURE 2.1 SCHEMATIC OF FREIGHT CAR [14]

provide the yaw flexibility and soft primary suspension needed for satisfactory curve negotiation.

A conventional three piece truck shown in Figure 2.2 consists of two sideframes and a bolster. The sideframes rest directly on the wheelset bearing adapters. The bolster is supported by vertical coil springs which rest in the sideframes. The coil springs oppose the lateral and roll motions of the bolster relative to sideframes. Very little longitudinal motion is possible between the bolster and the sideframes. The relative yaw of the bolster with respect to the sideframes causes the sideframes to rotate about the truck centerline and assume a skewed "parallelogram" shape. This type of deformation, referred to as warping, is resisted by friction between the bolster and sideframes and is usually limited to an angle of two and a half degrees [13] by the contact of the ends of the bolster against the sideframes. The warping motion of the truck frame provides the wheelset with some yaw flexibility. Three degrees of freedom: lateral, yaw and warp are used to represent the truck motion. The roll angle of truck is assumed to be the average of the roll angle of the two wheelsets.

The freight carbody rests directly on the bolster centerplate. The carbody also is modelled by three degrees of freedom: lateral, roll and yaw. Carbody lateral flexibility and torsion are neglected. The carbody is assumed to roll and

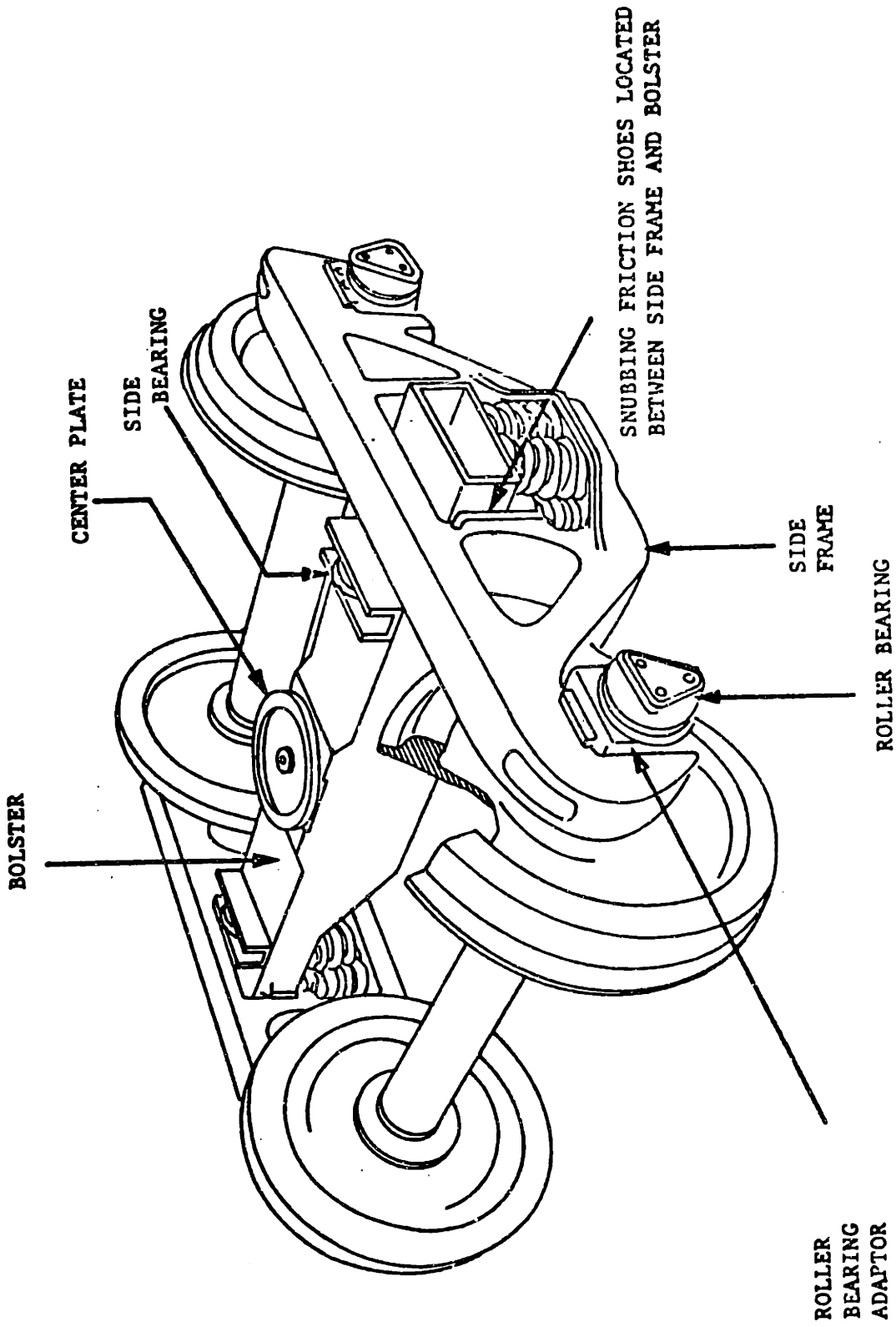


FIGURE 2.2 THREE-PIECE TRUCK [15]

translate with the bolster. Yaw rotation of the carbody relative to the bolster is resisted by coulomb friction.

A radial truck is a conventional truck with an additional direct connection between the wheelsets by means of springs or radial arms. Interconnecting the wheelsets causes a yaw moment or lateral force to be transmitted between the wheelsets. As the truck negotiates a curve, the wheelsets tend to align themselves more radially in a curve. Two different radial truck designs proposed for freight vehicles by Scheffel [16] and List [17] are shown in Figures 2.3 and 2.4.

The model adopted for this study is an extension of a linear model developed by Hadden [13]. Nonlinear wheel/rail geometry and creep force saturation have been added. External forces such as aerodynamics are not included. All rigid bodies are represented as lumped masses and inertias. The connections between rigid bodies are modelled by linear springs in parallel with either coulomb friction elements or linear viscous dampers [14]. The wheelsets are assumed to run freely in the bearings without friction or applied torques due to tractive or braking effects. The rails are assumed to be flexible and perfectly aligned. Vertical and pitch degrees of freedom are not considered and are assumed to have negligible effect on the lateral dynamics. Schematics of the conventional vehicle model are shown in Figures 2.5-2.7. The

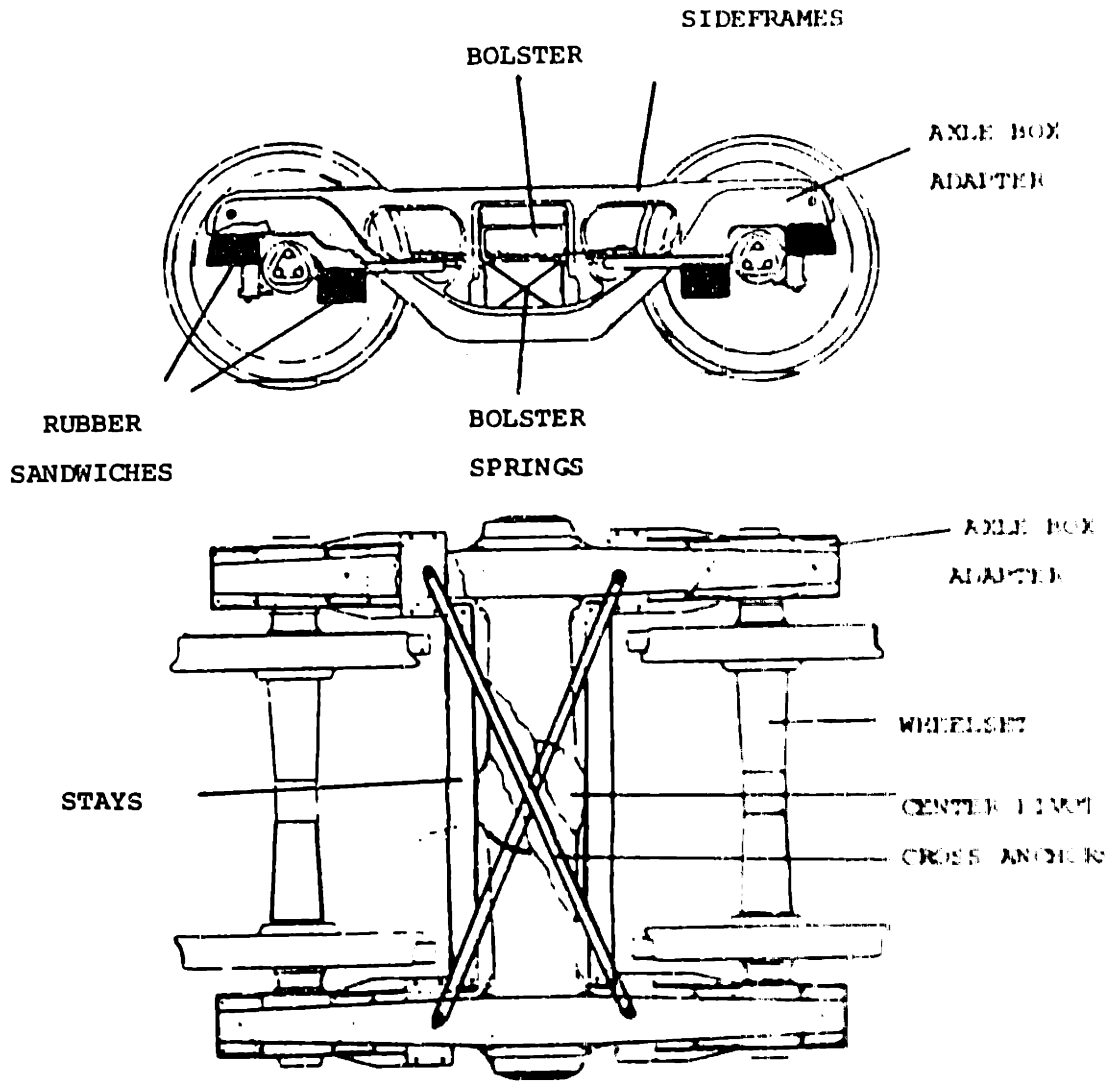
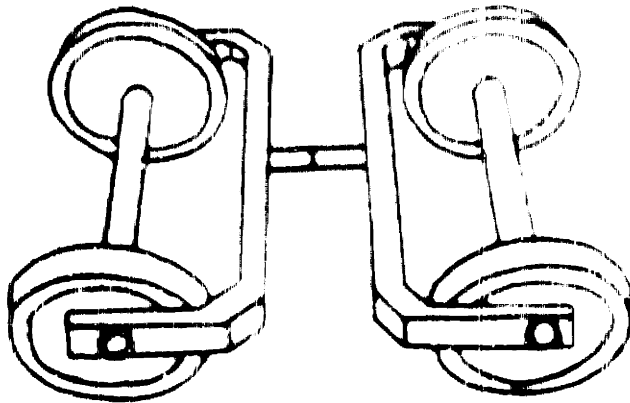


FIGURE 2.3 SCHEFFEL'S RADIAL TRUCK (16)



MODEL OF STEERING ARM APPLICATION

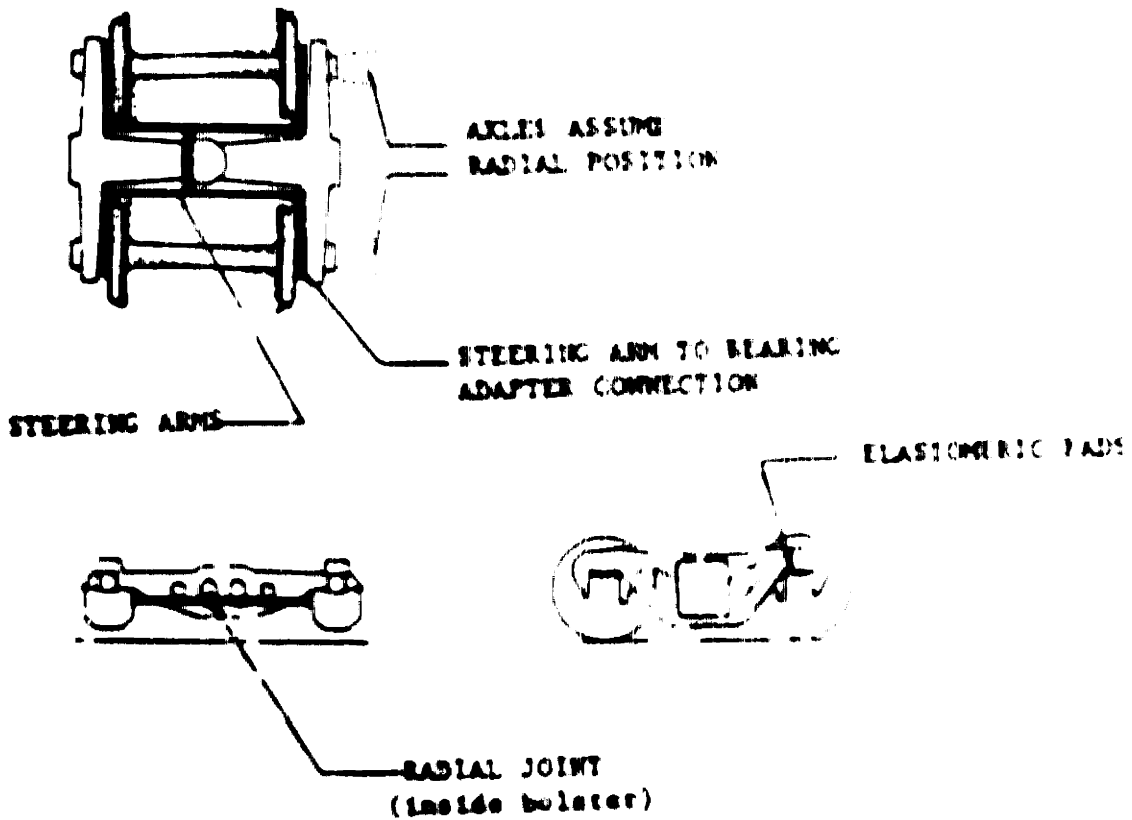


FIGURE 2.4 LIST'S RADIAL TRUCK [17]

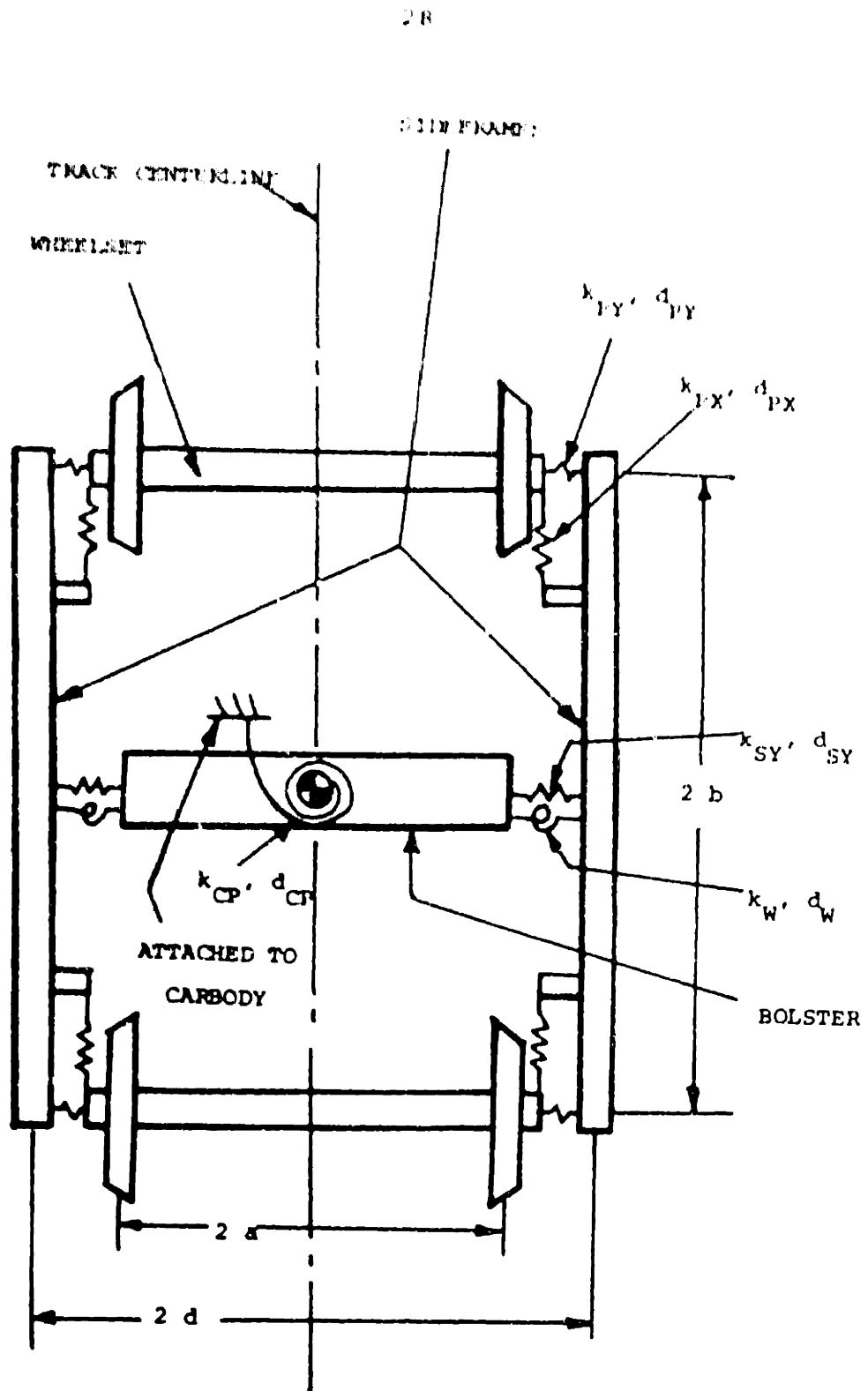


FIGURE 2.5 SCHEMATIC OF EQUILIBRIUM CONFIGURATION OF TRUCK [13]

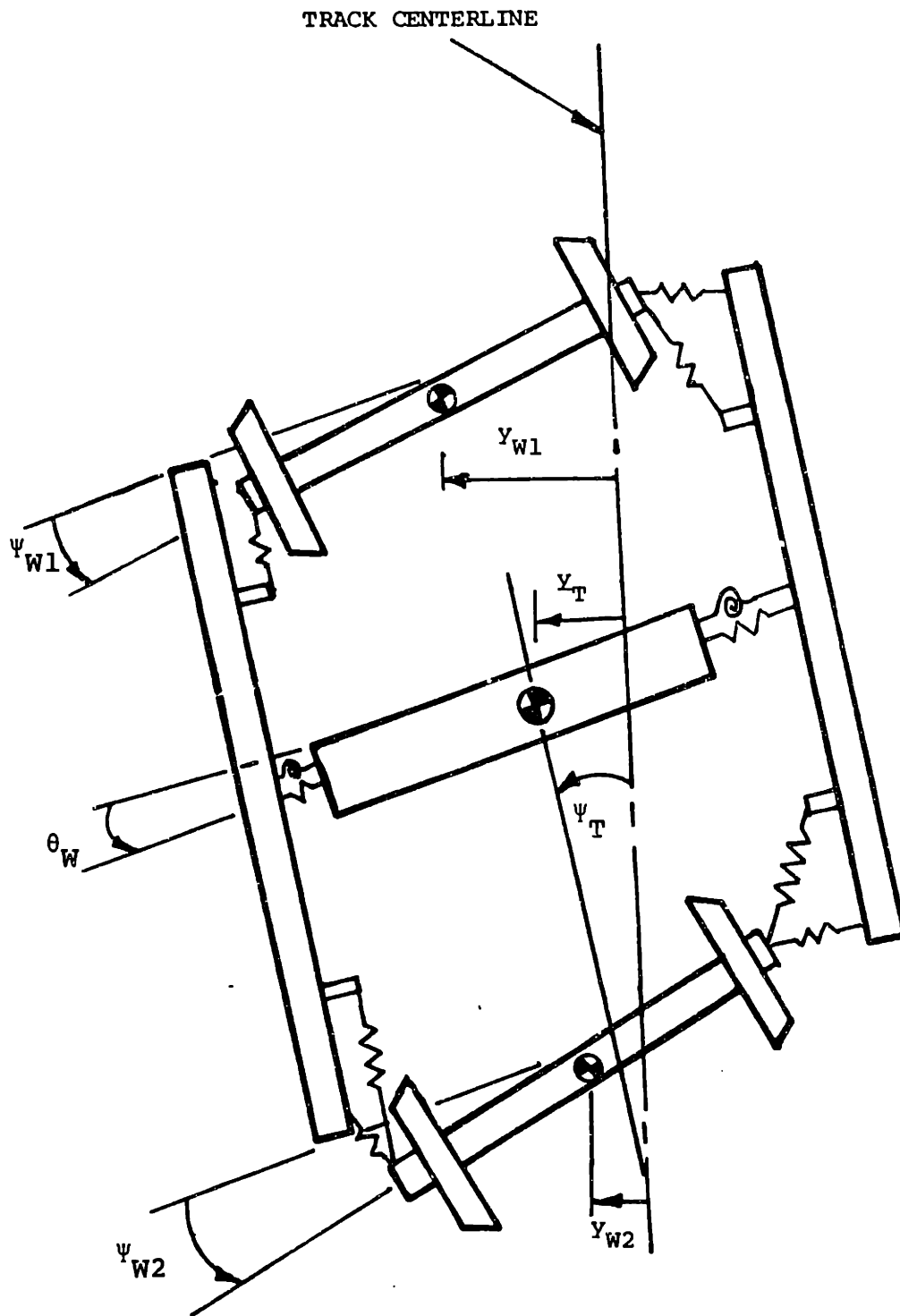
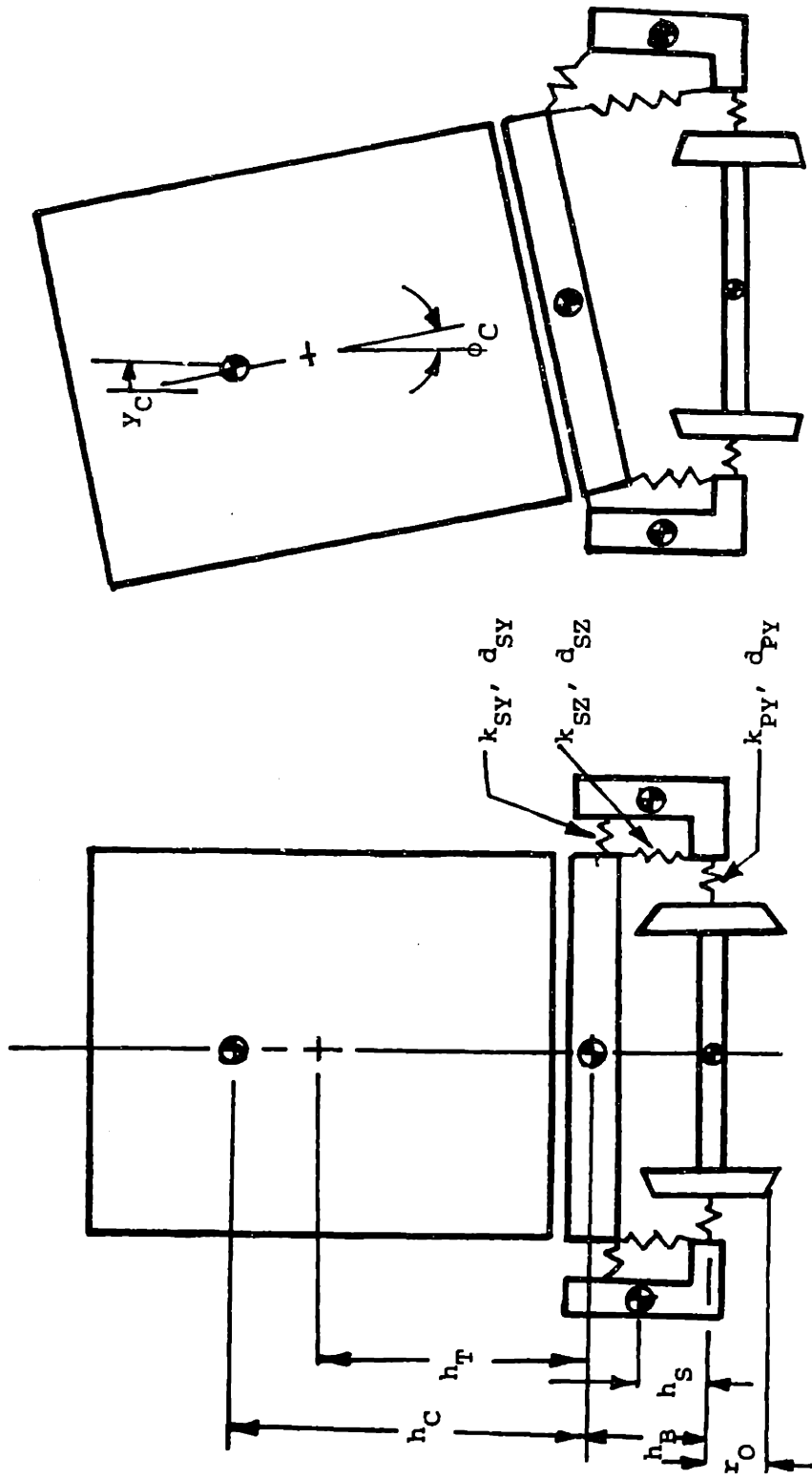


FIGURE 2.6 SCHEMATIC OF DISTURBED CONFIGURATION OF TRUCK [13]



B) DISTURBED CONFIGURATION

A) EQUILIBRIUM CONFIGURATION

FIGURE 2.7 SCHEMATIC OF FREIGHT CAR MODEL [13]

radial vehicle includes the wheelset interconnections modelled in Figure 2.8.

2.2 WHEEL/RAIL CHARACTERISTICS

2.2.1 WHEEL/RAIL GEOMETRY

The wheel/rail geometry shown in Figure 2.9 is described by the wheelset roll angle, the rolling radii of the wheels and the contact angles between the wheels and the rails. Knowledge of this contact geometry is essential to the accurate calculation of wheel/rail forces. Within the tread region, the contact parameters can be expressed as linear functions of the wheel lateral excursion. Rapid changes and sudden discontinuities in contact geometry, however, are associated with flange contact. Since flanging is common during curving, linear profiles do not accurately describe the contact geometry.

Tabulated wheel/rail profiles developed by Cooperrider and Law [18] are used to determine rolling radii, roll angle and contact angles. The first and second derivatives of roll angle are approximated using first order differences of data points and the time derivatives of wheelset excursions. The vertical velocity of the wheelset has been neglected. Figures 2.10 and 2.11 show geometric relationships for two wheel/rail configurations, New Wheel and Worn Wheel on a Worn Rail.

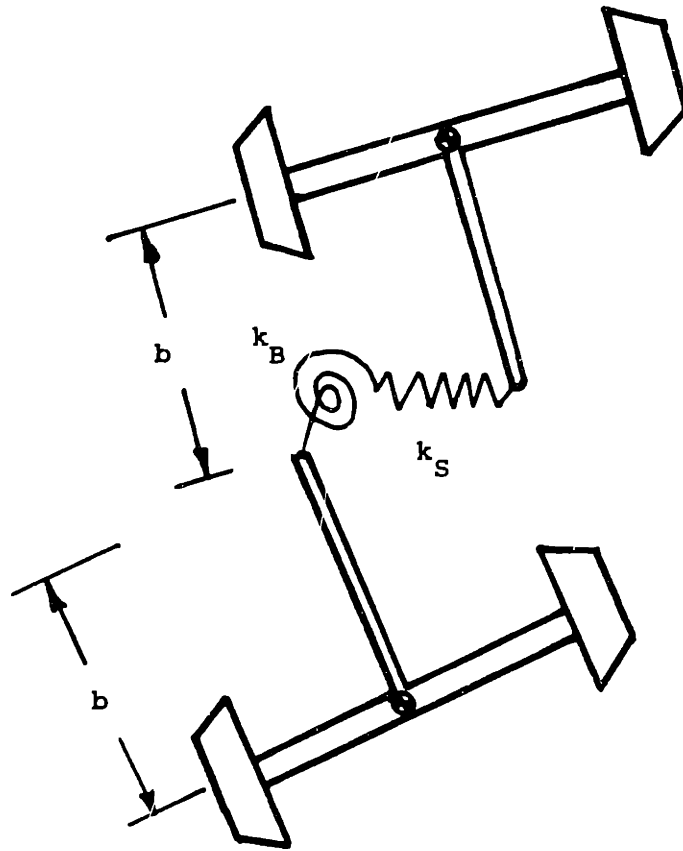


FIGURE 2.8 SCHEMATIC OF WHEELSET INTERCONNECTION MODEL [13]

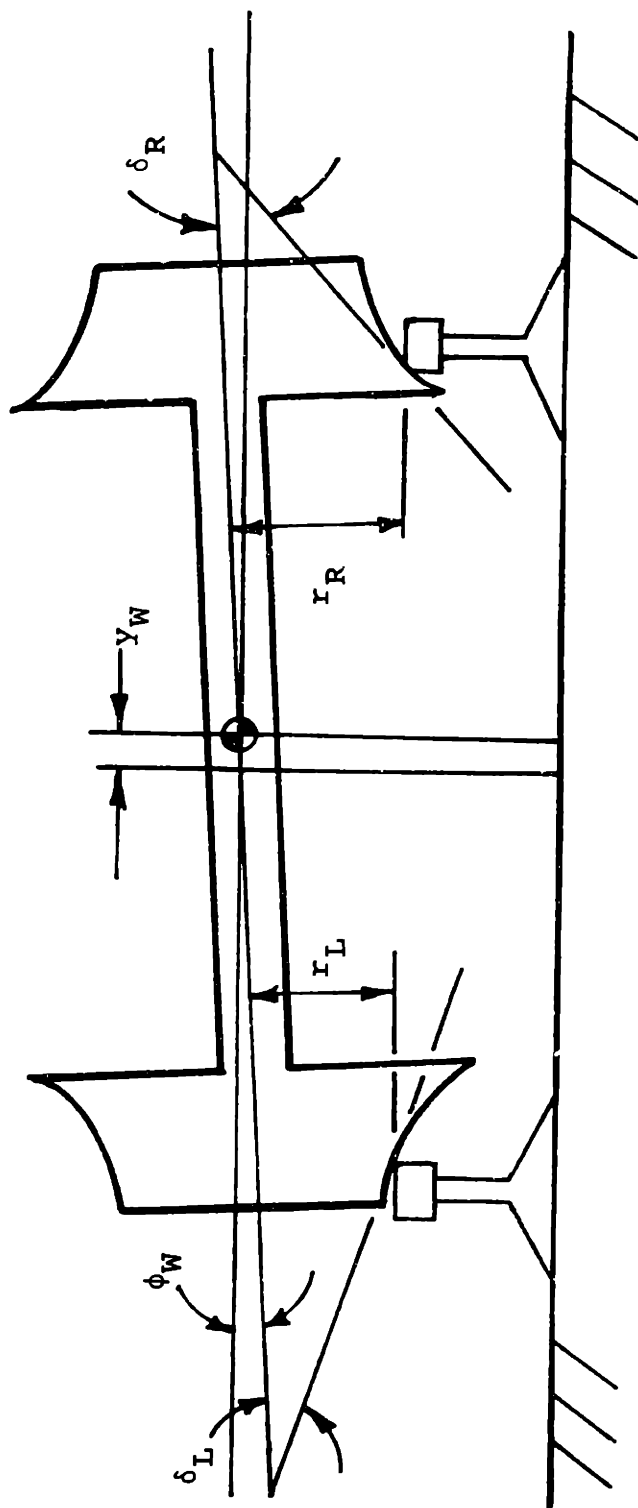
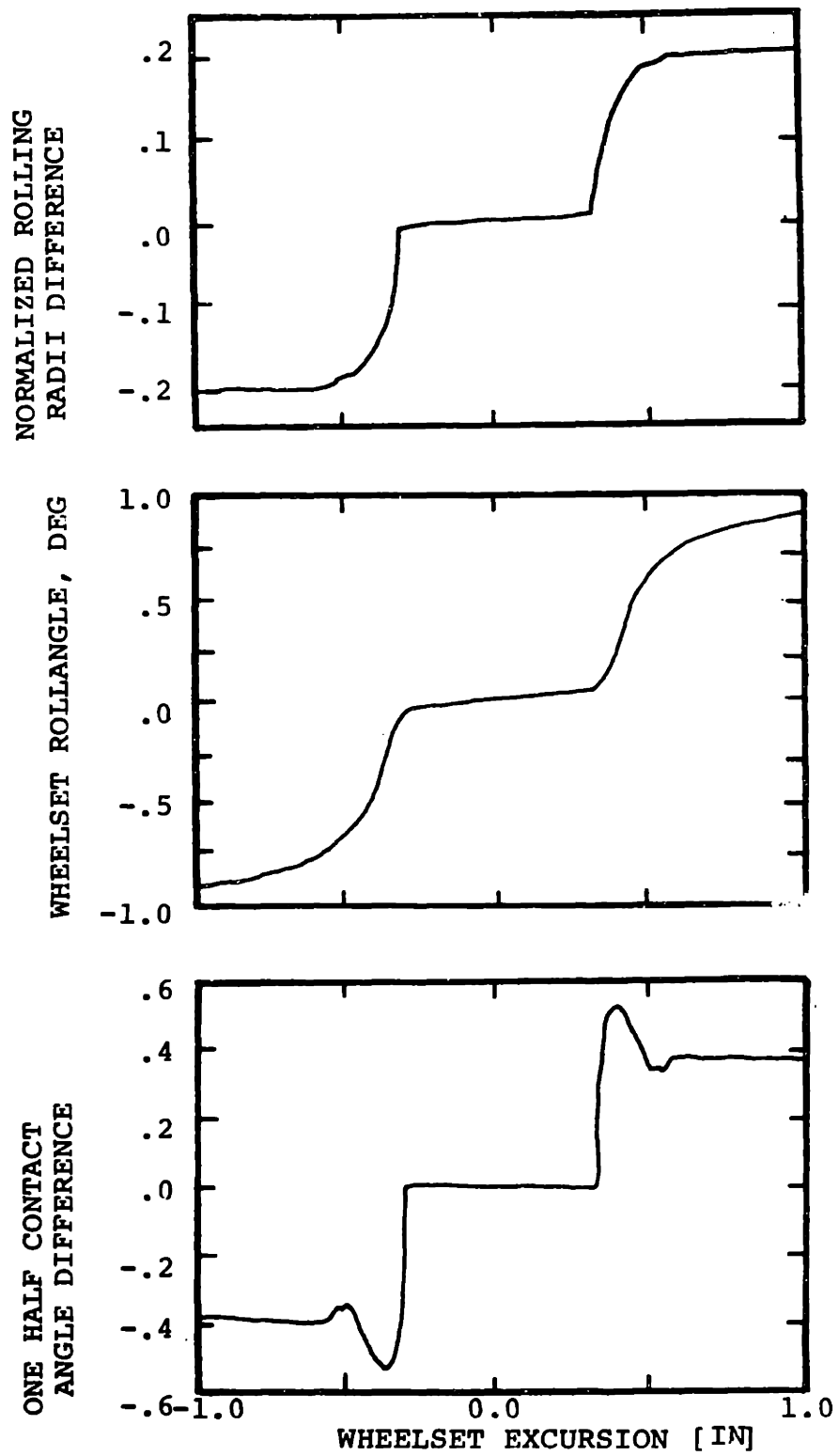


FIGURE 2.9 WHEEL/RAIL CONTACT GEOMETRY PARAMETERS

FIGURE 2.]0 CONTACT GEOMETRY FOR NEW WHEEL

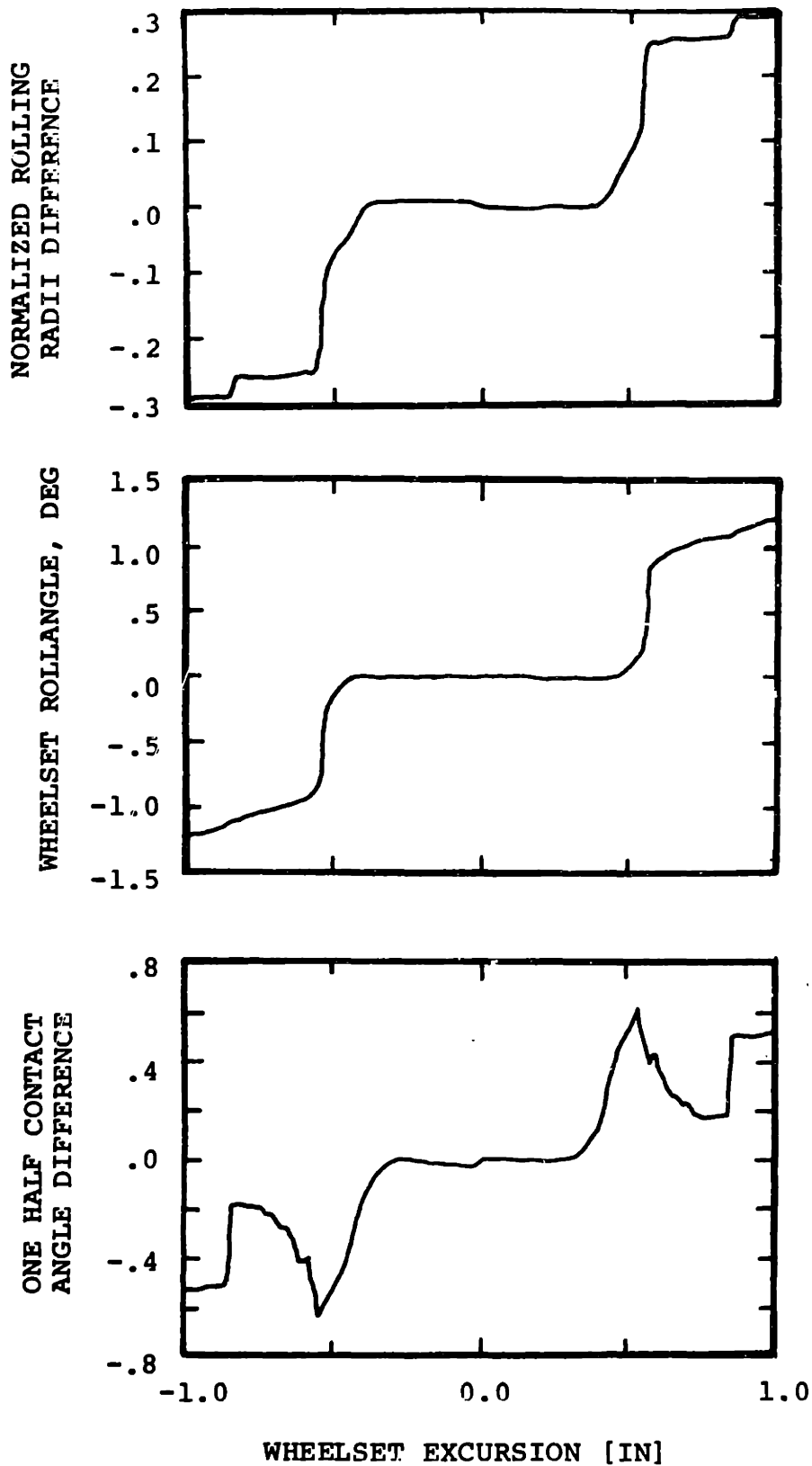


FIGURE 2.11 CONTACT GEOMETRY FOR WORN WHEEL
ON WORN RAIL

2.2.2 WHEEL/RAIL FORCES AND MOMENTS

When the wheelset is displaced from a centered position, the difference between rolling radii at the left and right rails requires that the velocities of the wheels at their contact points differ. This results in partial slip or creepage of the wheels relative to the rail. The action of the normal forces upon the slipping wheelset will result in generation of creep forces. Creepage is defined as the relative velocity between the wheels and rails at the contact point normalized to the forward velocity of the wheelset. Expressions for the creepage as functions of vehicle state variables are given in Appendix A.

Many theories [2,3,9,19] have been developed to describe the tangential or creep forces between two elastic bodies in rolling contact. One of the simplest of these, Kalker linear creep theory [19], relates the linear creep forces to creepage by the relations

Lateral Creep Force

$$F_Y = -f_{11} \xi_Y - f_{12} \xi_{SP} \quad (2 . 1)$$

Longitudinal Creep Force

$$F_X = -f_{33} \xi_X \quad (2 . 2)$$

Spin Creep Moment

$$M_Z = f_{12} \xi_Y - f_{22} \xi_{SP} \quad (2 . 3)$$

where

- ξ_Y = lateral creepage
- ξ_X = longitudinal creepage
- ξ_{SP} = spin creepage
- f_{11} = lateral creepage coefficient
- f_{12} = lateral/spin creep coefficient
- f_{22} = spin creep coefficient
- f_{33} = longitudinal creep coefficient

Linear creep coefficients are functions of the normal load given by the following relations:

$$f_{11} = f_{110} \left(\frac{N}{N_0} \right)^{2/3} \quad (2.4)$$

$$f_{12} = f_{120} \left(\frac{N}{N_0} \right) \quad (2.5)$$

$$f_{22} = f_{220} \left(\frac{N}{N_0} \right)^{4/3} \quad (2.6)$$

$$f_{33} = f_{330} \left(\frac{N}{N_0} \right)^{2/3} \quad (2.7)$$

where

- $N_0 = g(m_w + \frac{1}{2}m_B + \frac{1}{4}m_C) / \cos \delta_0$
- f_{ij0} = nominal values creep coefficients for a nominal normal load

Linear creep theory fails to consider the physical limitations imposed on the magnitude of the resultant creep force by the amount of available adhesion between the wheel and rail. When the creepages become too large, gross sliding of the wheel over the rail occurs and the creep forces are no longer proportional to the creepage but are determined by the level of saturation. The nonlinear effect of the adhesion limit is approximated by using a cubic saturation expression developed by Vermullen and Johnson [5] and shown in Figure 2.12. Modifying this approach to include spin creep

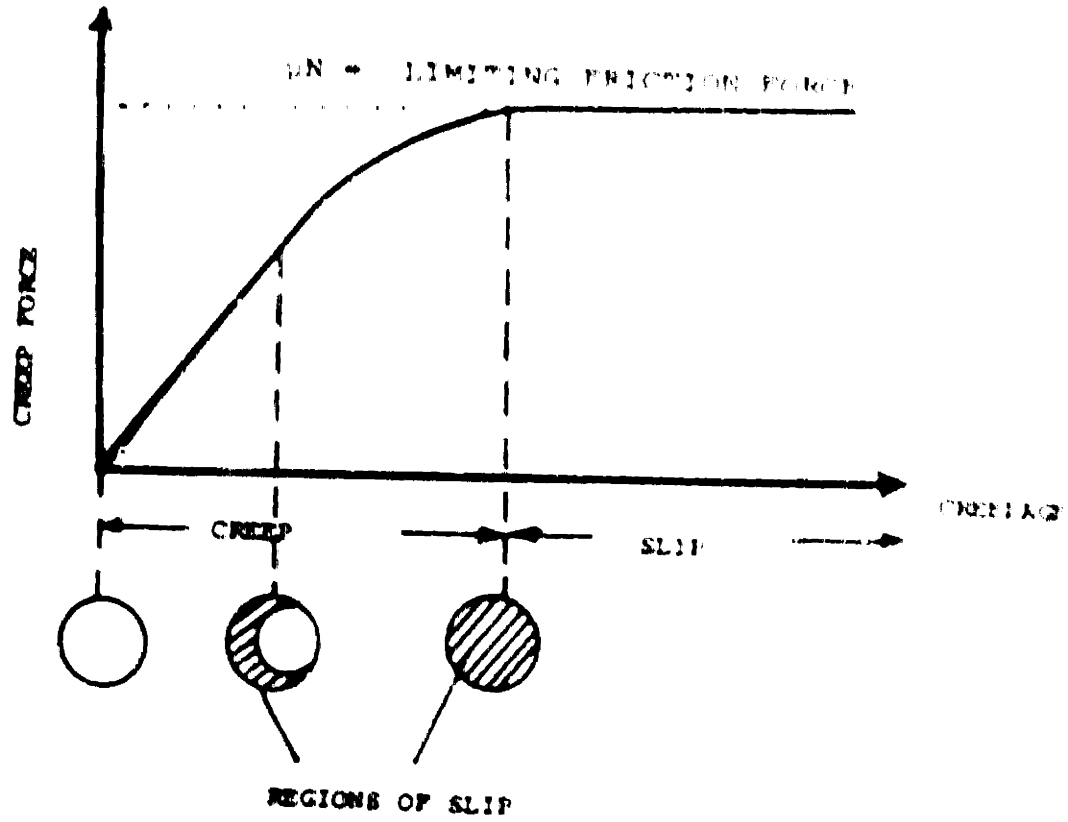


FIGURE 2.12 CREEP FORCE AS A FUNCTION OF CREEPAGE

terms, a saturation coefficient is determined by

$$c = \begin{cases} \frac{\mu N}{|F|} \left(\frac{|F|}{\mu N} - \frac{1}{3} \left(\frac{|F|}{\mu N} \right)^2 + \frac{1}{27} \left(\frac{|F|}{\mu N} \right)^3 \right) & \text{for } |F| \leq 3\mu N \\ \frac{\mu N}{|F|} & \text{for } |F| > 3\mu N \end{cases}$$

where $|F| = (F_X^2 + F_Y^2)^{1/2}$ (2 . 8)

The saturated creep forces and moments are then defined by

$$F_Y = c (-f_{11} \zeta_Y - f_{12} \zeta_{SP}) \quad (2 . 9)$$

$$F_X = c (-f_{33} \zeta_X) \quad (2 . 10)$$

$$M_Z = c (f_{12} \zeta_Y - f_{22} \zeta_{SP}) \quad (2 . 11)$$

In linear analysis, the normal force is usually assumed to be equivalent to half the axle load. During rail vehicle curving, however, the normal forces acting at the wheel/rail interface exhibit nonlinear behavior dependent on longitudinal and lateral creep forces. The weight distribution is usually asymmetrical. Also, as the wheels flange, the contact angle increases and the lateral components of normal force, called the flange forces, become quite large. Since normal and creep forces are functions of one another, an iterative approach must be used at each integration step to calculate the wheel/rail forces. The iteration is terminated when successive values for normal force vary by less than 10 percent.

2.3 NONLINEAR SUSPENSION CHARACTERISTICS

Modelling the vehicle suspension system is particularly difficult for freight cars due to their complexity and nonlinearity [14]. The effects of these suspension nonlinearities are often more pronounced in curve negotiation than in tangent track operation. The only intentional suspension components are the coil springs and friction wedges between bolster and sideframes. The lateral, vertical and warp motions of the truck are resisted by dry friction at each sideframe/bolster connection. Each of these connections is modelled by linear springs in parallel with a coulomb friction element. The characteristics are shown in Figures 2.13a-c. The rotation of the bolster centerplate relative to the carbody is resisted by friction. This resistance is represented by a breakout torque.

A mathematical representation of a ideal coulomb friction element [19] is illustrated in Figure 2.14a. In order to simulate coulomb friction digitally, the model must include a small velocity region about the origin where friction force or moment will take on values below the breakout force or moment. The piecewise linear model of Figure 2.14b enables the approximation of friction levels below breakout during stopped conditions. The selection of the width of the linear viscous band is important. Too wide a band will produce viscous damping results. If the band is too narrow the discrete

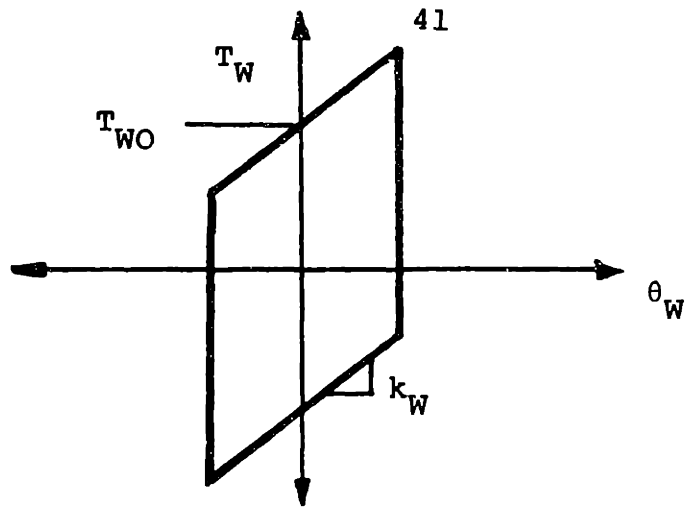


FIGURE 2.13.a. WARP SUSPENSION CHARACTERISTIC [14]

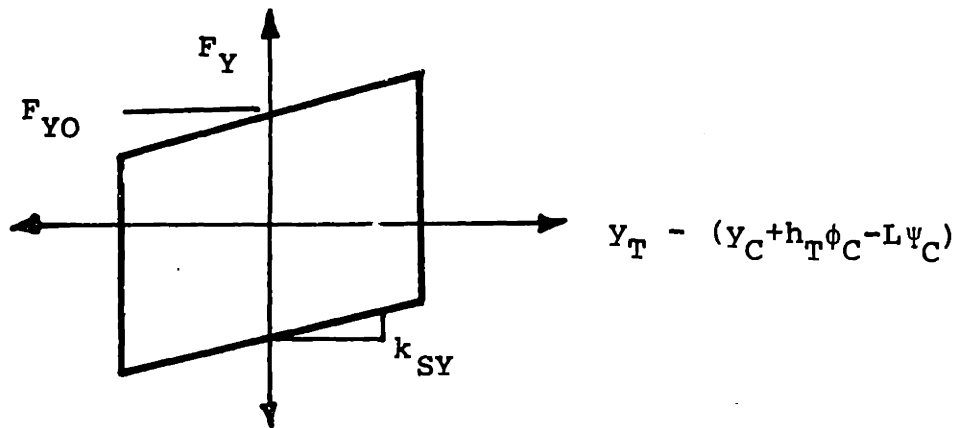


FIGURE 2.13.b. LATERAL SUSPENSION CHARACTERISTIC [14]

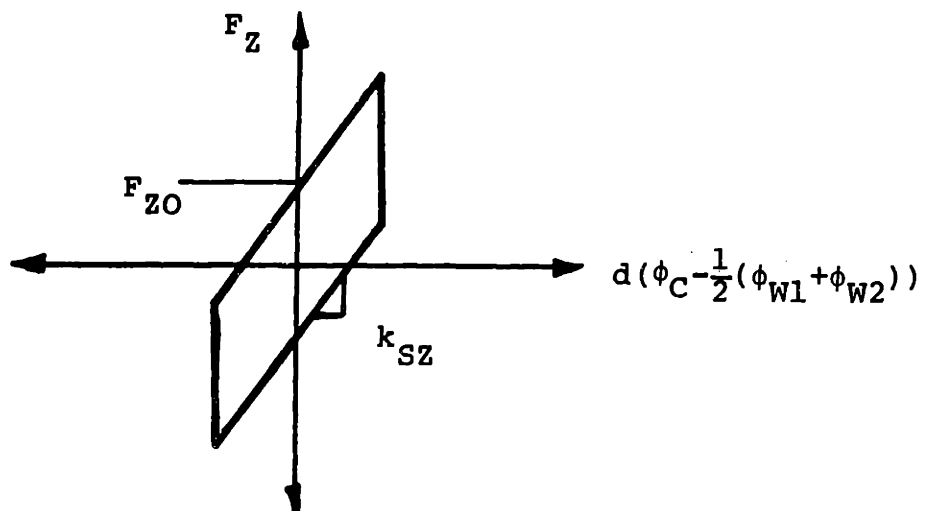


FIGURE 2.13.c. VERTICAL SUSPENSION CHARACTERISTIC [14]

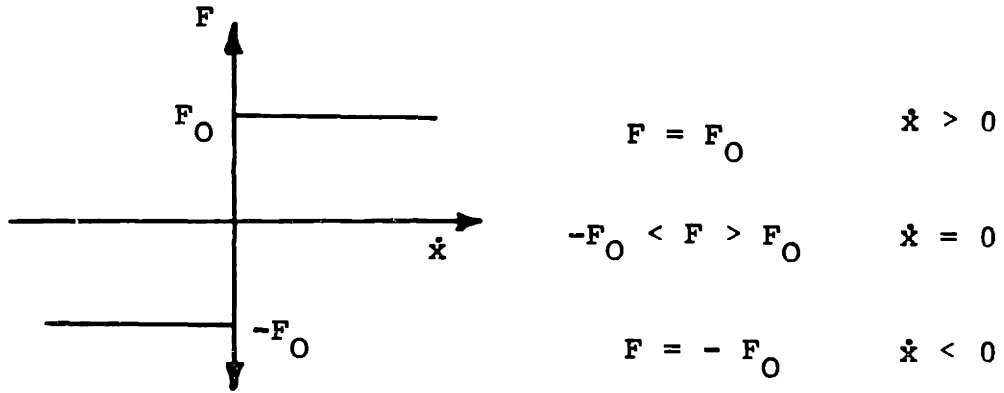


FIGURE 2.14.a. IDEAL COULOMB FRICTION ELEMENT [19]

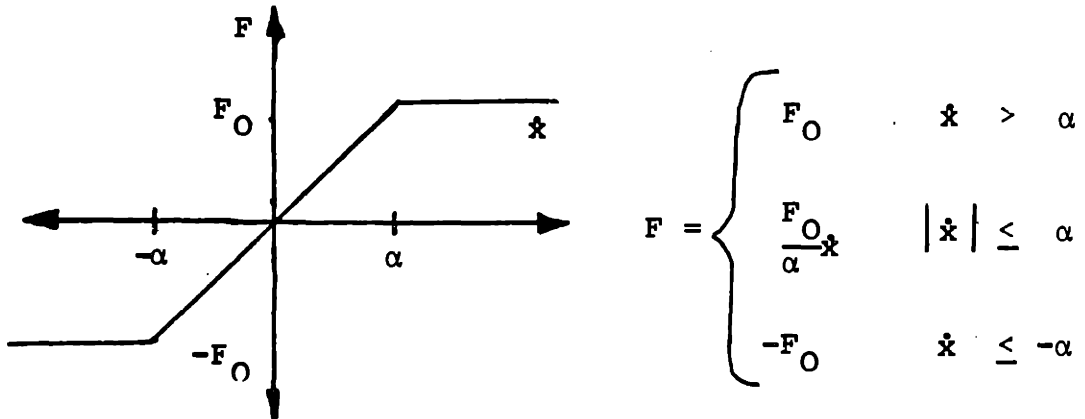


FIGURE 2.14.b. PIECEWISE LINEAR COULOMB FRICTION APPROXIMATION [19]

integration method may miss the stopped condition.

Since coulomb friction is difficult to simulate digitally, an alternative linear suspension was also studied. The connections between the bolster and sideframe and bolster and carbody were modelled as linear springs in parallel with linear viscous dampers. Coulomb friction is approximated by a viscous damper equivalent. This method also has drawbacks. The phenomenon of gross slipping that can occur for actual friction cannot occur for equivalent viscous damping.

2.4 CURVE GEOMETRY

Superelevation angle, track curvature and track irregularities constitute the inputs to the vehicle dynamic system. The superelevation, shown in Figure 2.15a, is defined as the angle between the track and the horizontal. The track curvature, usually expressed in degrees, corresponds to the degrees of arc spanned by a hundred foot cord as illustrated in Figure 2.15b. The curvature, superelevation and vehicle speed are often combined into the cant deficiency. The cant deficiency is used as a measure of the imbalance between the centrifugal and gravitational forces and is defined by

$$\phi_d = \frac{v^2}{gR} - \phi_{SE} \quad (2 . 12)$$

Balanced running or zero cant deficiency corresponds to the condition where the lateral component of weight cancels the

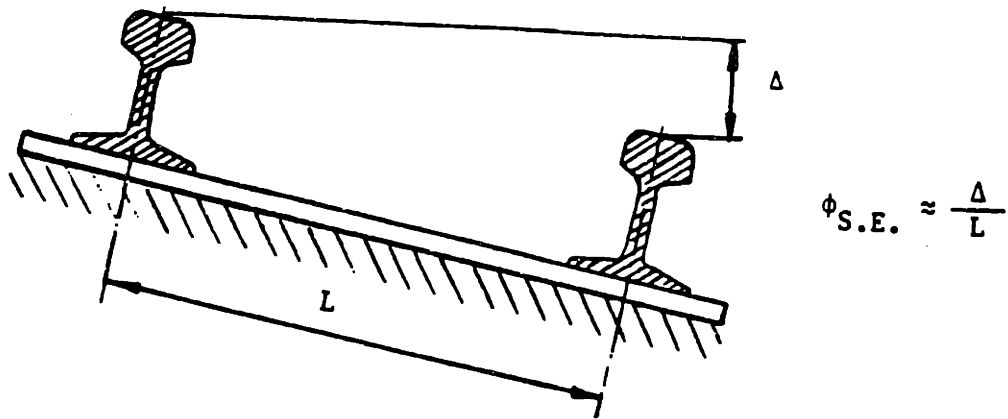


FIGURE 2.15.a. DEFINITION OF SUPERELEVATION [20]

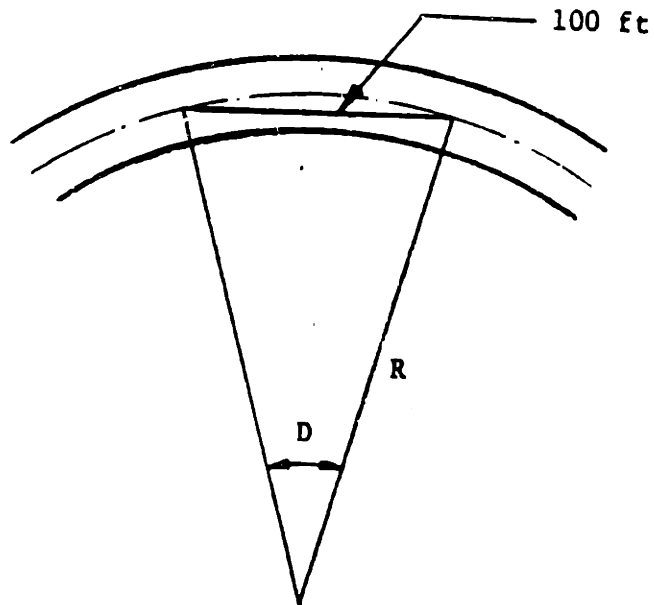


FIGURE 2.15.b. DEFINITION OF DEGREE CURVE [20]

centrifugal force generated during the curve negotiation.

Track irregularities are due to a combination of installation error and gradual degradation. Four irregularities are universally used to define track geometry [20]. Gauge is the horizontal distance between two rails. Crosslevel is the difference between the elevations of the rails. Alignment is the average of two rail lateral positions. Vertical profile is the average of two rail elevations.

The simulation track in this study is composed of three distinct sections: tangent, transition spiral and constant radius curve. Along the transition spiral, the superelevation angle and radius of curvature vary quadratically as shown in Figure 2.16. The purpose of the spiral is to reduce the magnitude of the peak flange force during the transition to constant radius curved track. Track irregularities have been neglected in this study. Implementation of crosslevel and alignment irregularities is possible by the addition of a random disturbances to the superelevation angle and the lateral excursion term in wheel/rail geometry respectively.

2.5 TRACK FLEXIBILITY MODEL

During flange contact, the net lateral force may become considerably larger than the lateral track stiffness. Under

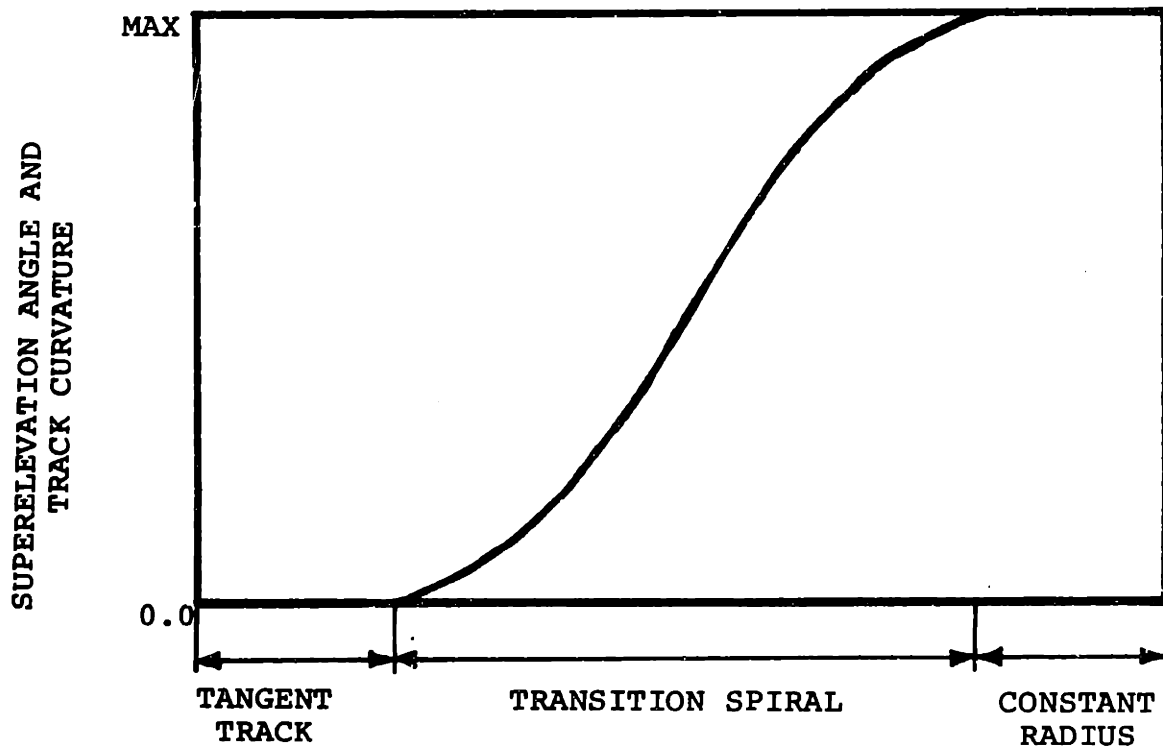


FIGURE 2.16 SUPERELEVATION AND TRACK CURVATURE AS FUNCTION OF DISTANCE

these conditions, the assumption that the rail remains perfectly rigid is not valid. Allowances must be made for rail lateral displacement to avoid prediction of excessive lateral forces during flanging [12].

The track in effect acts as the final element in the vehicle suspension. Rail movement at each of the four wheels is assumed to be resisted by a linear spring in parallel with viscous damper model shown in Figure 2.17. Neglecting the mass of rails, the motion of the left and right rails is determined by the expressions:

$$b_T \dot{Y}_L + k_T Y_L = F_{LY} + N_{LY} \quad (2 . 13)$$

and

$$b_T \dot{Y}_R + k_T Y_R = F_{RY} + N_{RY} \quad (2 . 14)$$

An effective lateral excursion, found by subtracting the rail deflection from the wheelset lateral excursion, is used to determine the wheel/rail contact geometry described in Section 2.2.1. This method ignores the inertia of rails and the influence of rail velocity on lateral creepage [12]. Since the lateral creep force is generally saturated during flange contact, this approximation is justified.

Values for track stiffness and damping vary for different types of track and loading. Track lateral force/deflection data [21] shown in Figure 2.18 illustrates the highly nonlinear dependence of lateral stiffness on both the lateral

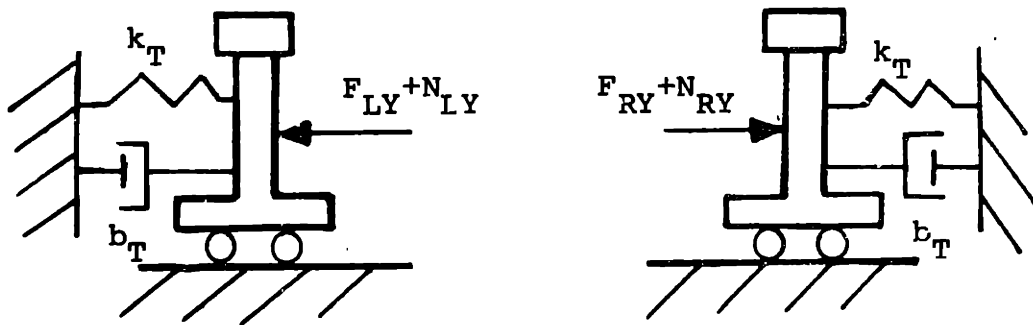
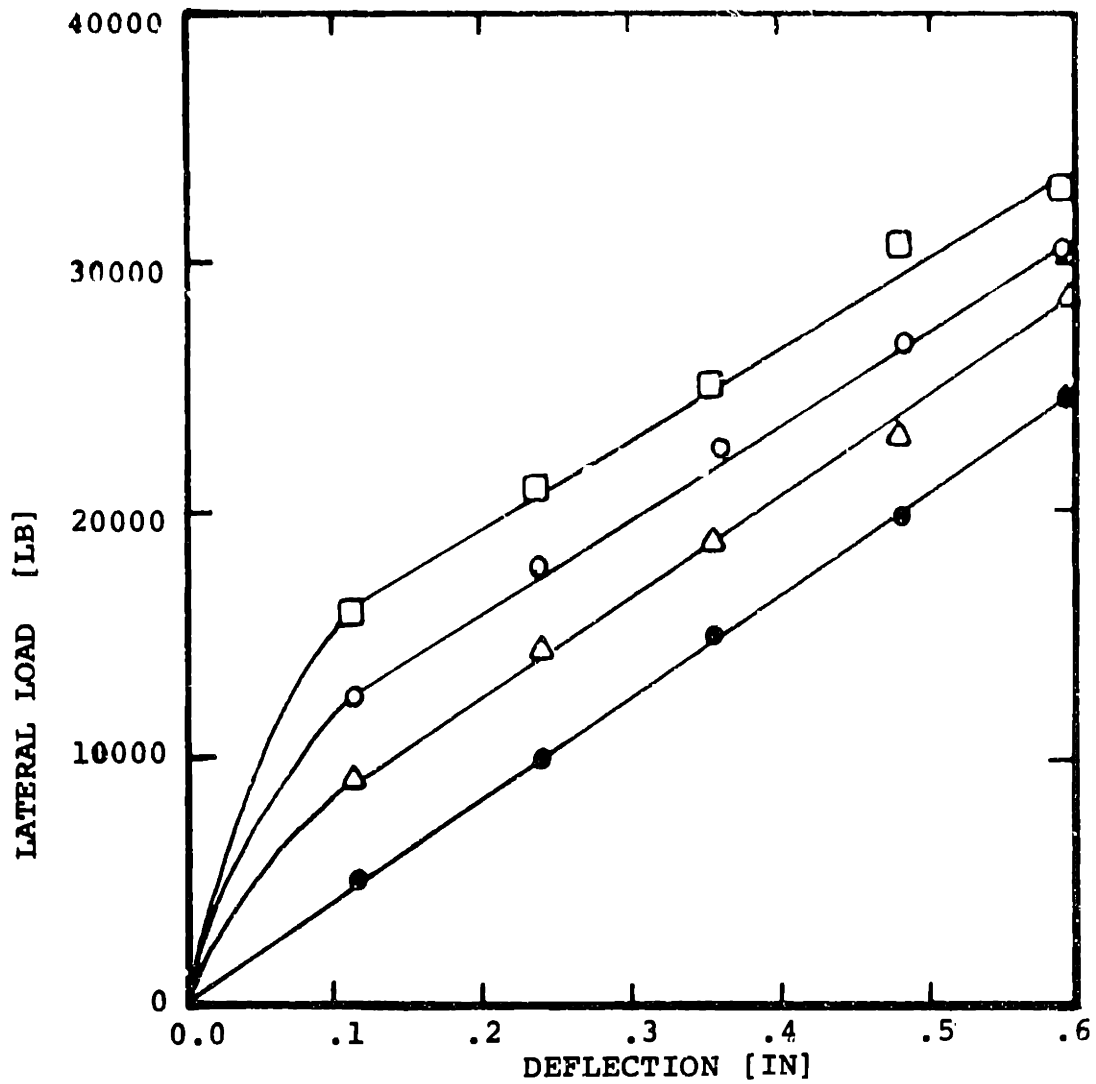


FIGURE 2.17 SCHEMATIC OF RAIL FLEXIBILITY MODEL



VERTICAL LOAD KEY

● 0 LB

○ 20,000 LB

△ 10,000 LB

□ 30,000 LB

FIGURE 2.18 RAIL DEFLECTION AS A FUNCTION OF LATERAL LOAD [21]

and vertical load as well as the type and condition of rails, ties, fasteners and roadbed.

2.6 EQUATIONS OF MOTION

The essential dynamic element of a rail vehicle is the wheelset. It is therefore important to describe its curving behaviour accurately. The wheelset motion is represented by two degrees of freedom: lateral and yaw and its spin perturbation rate. The forces acting on the wheelset arise from the weight it supports, creep forces from wheel/rail interaction and suspension elements. A detailed derivation of the wheelset equations, following similar derivations by Arslan [22] and Nagurka [23], is presented in Appendix A. This nonlinear wheelset model has been incorporated into the full freight truck model. The equations of motion for the complete freight vehicle, an extension of then model developed by Hadden [13], are derived in Appendix B.

2.7 MODEL EVALUATION

Preliminary evaluation studies were performed to compare the present model to a nonlinear steady-state curving model developed by Bell [8] for passenger vehicles and a tangent track linear freight car model developed by Hadden [13].

For comparison with the steady-state curving results of Bell, the present model was simulated along a constant radius track. With the initial conditions corresponding to the previously predicted steady state model, the model approximately maintained this state. Equilibrium forces were also found to be consistent.

To enable comparison with the linear tangent track model, nonlinear effects in the present model were eliminated. These included creep forces saturation, coulomb friction and nonlinear wheel/rail profiles. System parameters were chosen to correspond to the LIMRV vehicle. The LIMRV vehicle has a softer primary suspension and a resulting critical speed of 139ft/sec [13]. This modified model was run on tangent track at different speeds to empirically determine the critical speed. Figures 2.19a and 2.19b show the vehicle response to small perturbations below and above this empirical critical speed. The result was consistent with the eigenvector analysis of the linear model.

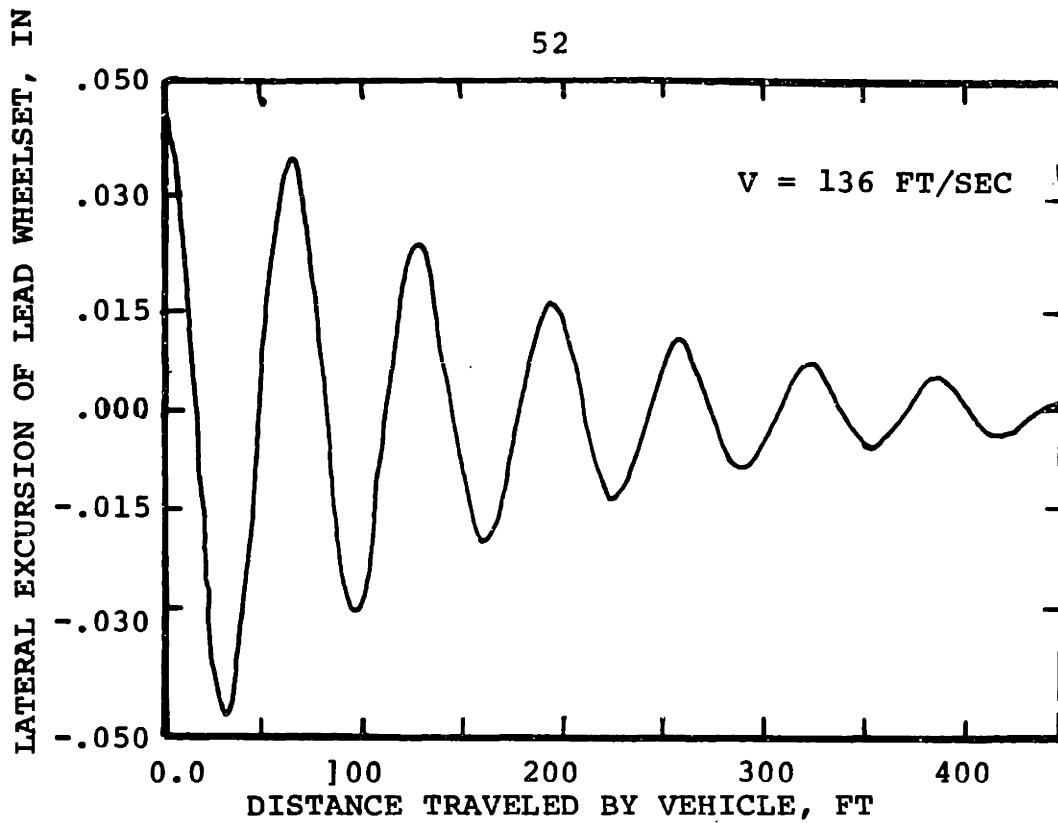


FIGURE 2.19.a. RESPONSE OF VEHICLE BELOW CRITICAL SPEED

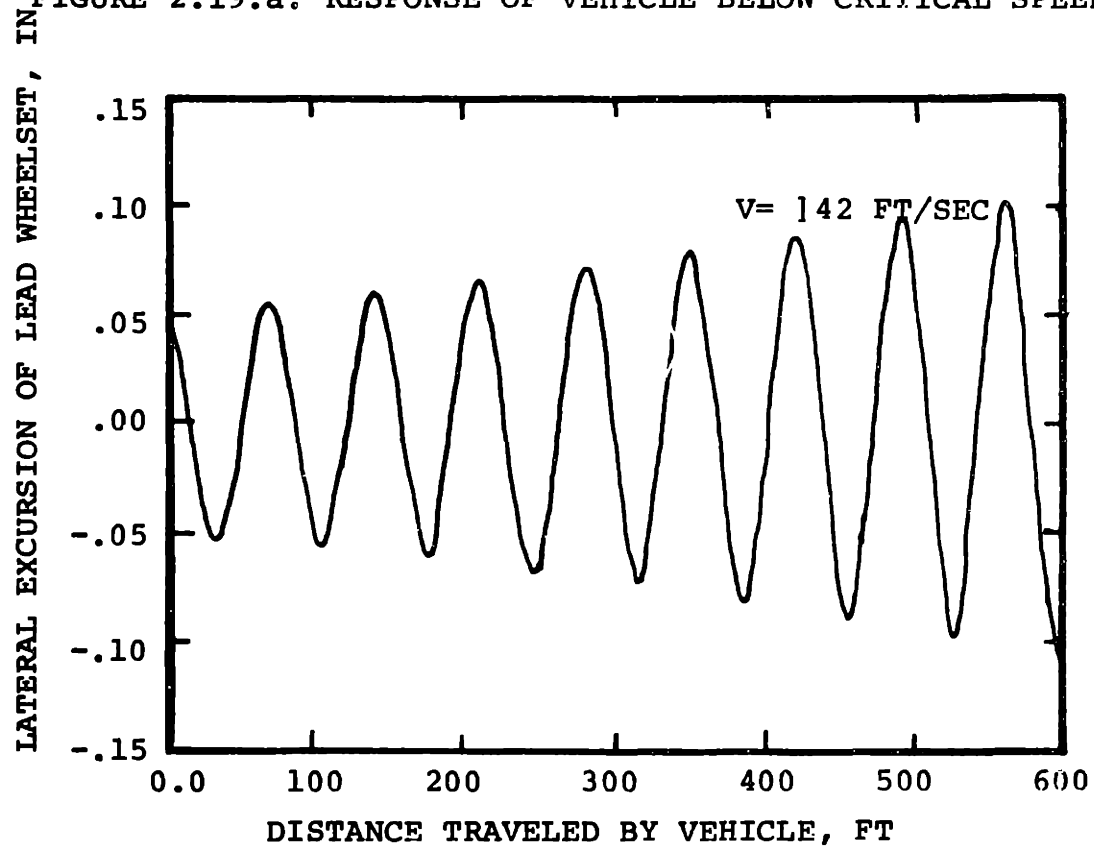


FIGURE 2.19.b. RESPONSE OF VEHICLE ABOVE CRITICAL SPEED

CHAPTER 3

PARAMETRIC STUDIES3.1 INTRODUCTION

In this chapter, the influence of vehicle parameters and operating conditions on dynamic curving performance are examined. These conditions are characterized by the roadbed and wheel/rail geometries, rail flexibility and suspension design. The curving performance of the rail vehicle is judged by the lateral forces, L/V ratios, angles of attack and work in the contact regions. These values determine the possibility of wheel climb, rail rollover and lateral track shift and the amount of wear.

The equations of motion presented in Appendix B are transformed into forty-six first order nonlinear differential equations. Solutions of the equations subject to initial conditions were obtained by a fourth order Runge-Kutta integration algorithm. The results are time histories of the state variables, wheel/rail forces and work. Appendix C contains a listing of the computer program.

Due to the restricted movement between the wheelset and the sideframes, the three-piece freight truck is a very stiff system. A time step of 0.00075 seconds was required to maintain a stable integration. A variable time step approach was therefore used to reduce the computation time. Since the

nonlinear characteristics of the model are most important during flange contact, it is necessary to use small timesteps in this region. During off flange operation, the time step can be increased without any loss of accuracy.

3.2 PERFORMANCE OF BASELINE VEHICLE

A set of baseline vehicle parameters which correspond to a unloaded hopper freight car [13] are summarized in Table 3.1. The baseline vehicle model is simulated through a one hundred and fifty foot transition spiral (Figure 2.16) into a two and a half degree curve at a balanced running velocity of 50 ft/sec. The results obtained are used to evaluate the effects of changing operating conditions. The wheel/rail profile, New Wheel, described in Section 2.2.1 is used. The carbody, initially centered on the track, runs along tangent track for ten feet before entering the spiral. The vehicle critical speed is approximately seventy-two feet/second.

Figure 3.1 shows the lateral excursion of the wheelsets as the vehicle travels along the track. The outer wheel of the lead wheelset of the lead truck impacts the rail 1.15 seconds after entering the curve and continues to flange as the vehicle moves into the constant radius portion of the curve. None of the other wheelsets contact the flange. After the impact of the lead wheelset against the flange,

TABLE 1BASELINE FREIGHT CAR PARAMETERS [13]

MASSES AND INERTIAS:

m_W	=	76.6 SLUGS	m_B	=	36.1 SLUGS
m_S	=	24.0 SLUGS	m_C	=	1102.0 SLUGS
I_{WY}	=	53.1 SLUGS-FT ²	I_{WZ}	=	448.5 SLUGS-FT ²
I_{BZ}	=	178.6 SLUGS-FT ²	I_{BX}	=	178.6 SLUGS-FT ²
I_{SZ}	=	77.6 SLUGS-FT ²	I_{CX}	=	13000.0 SLUGS-FT ²
I_{CZ}	=	234000.0 SLUGS-FT ²	L_A	=	344.1 SLUGS

GEOMETRY:

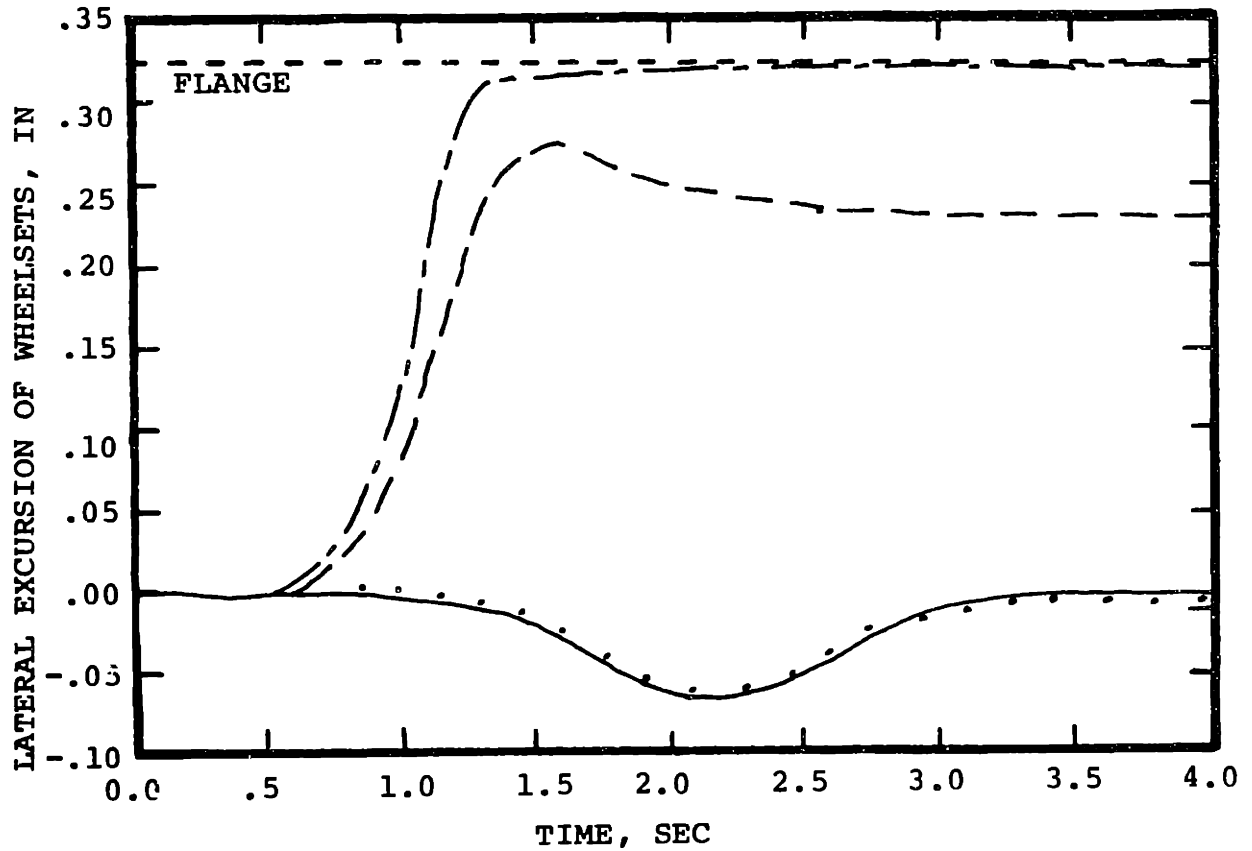
b	=	2.800 FT	d	=	3.250 FT
a	=	2.460 FT	h_S	=	.824 FT
h_S	=	.824 FT	h_T	=	2.994 FT
h_C	=	2.994 FT	L	=	18.600 FT

FRICTION AND KALKER CREEP COEFFICIENTS:

f_{11}	=	994670.0 LB/WHEEL	f_{12}	=	4607.0 FT-LB/WHEEL
f_{22}	=	77.5 FT ² -LB/WHEEL	f_{33}	=	1153000.0 LB/WHEEL

SUSPENSION PARAMETERS:

k_{PX}	=	38000000.0 LB/FT	d_{PX}	=	0.0 LB-SEC/FT
k_{PY}	=	29000000.0 LB/FT	d_{PY}	=	0.0 LB-SEC/FT
k_S	=	0.0 LB/FT	k_B	=	0.0 FT-LB/RAD
k_{SZ}	=	265800.0 LB/FT	d_{SZ}	=	7587.0 LB-SEC/FT
k_{SY}	=	24000.0 LB/FT	d_{SY}	=	12645.0 LB-SEC/FT
k_{CP}	=	50.0 LB-FT/RAD	d_{CP}	=	2409.0 FT-SEC-LB/RAD
k_W	=	4011000.0 FT-LB/RAD	d_W	=	9318.0 FT-LB-SEC/RAD



- | | | |
|-----------|------------|---------------|
| ----- | WHEELSET 1 | 2.5° CURVE |
| - - - - - | WHEELSET 2 | 150 FT SPIRAL |
| | WHEELSET 3 | 50 FT/SEC |
| ————— | WHEELSET 4 | $\phi_d = 0$ |

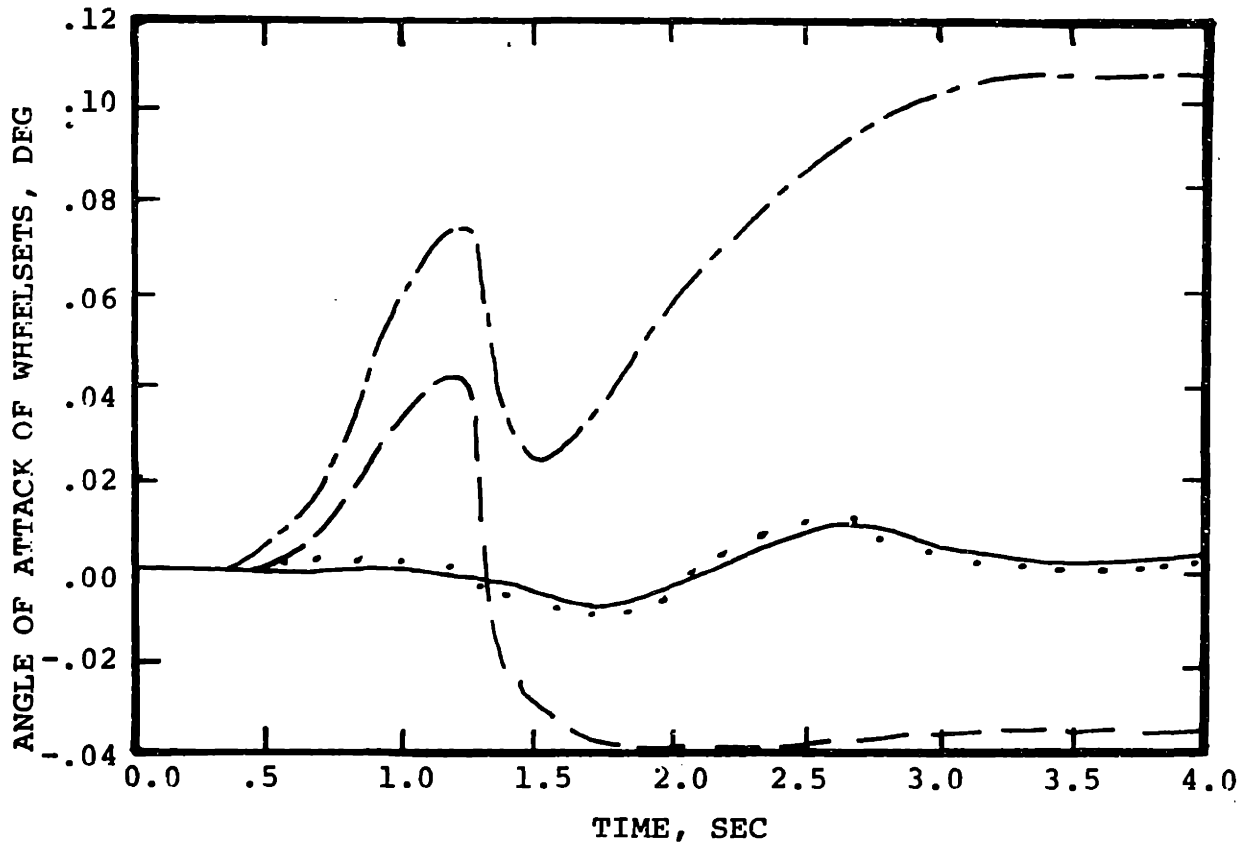
FIGURE 3.1 LATERAL EXCURSION OF THE WHEELSETS OF THE BASELINE VEHICLE

oscillations in the wheelset angles of attack occur as shown in Figure 3.2. These oscillations are much less severe for the trailing wheelsets. The carbody and the lead truck experience their peak lateral accelerations coincident with the initial flange impact. The lead truck also warps at this time.

Figures 3.3 and 3.4 show time histories of lateral component of normal force on the left wheel and work for the four wheelsets. The impact of the lead wheelset flange against the rail results in a large lateral component of normal force called the flange force. This flange force is of short duration and is associated with a corresponding increase in work. The flange force and work of the trailing wheelsets do not exhibit this behavior and are significantly lower in magnitude.

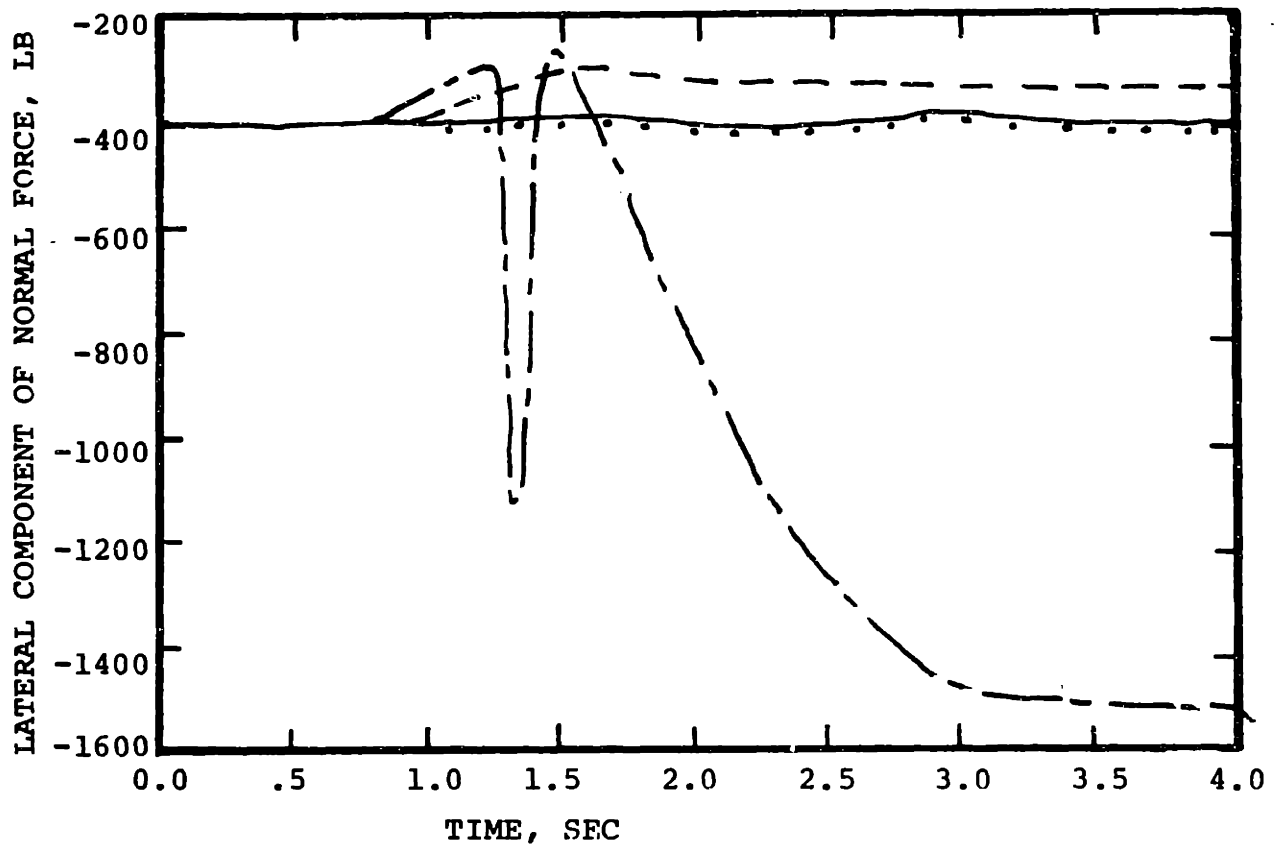
3.3 SPIRAL LENGTH

The length of the transition curve effects the peak lateral force of the lead wheelset. This is illustrated by Figure 3.5. Reducing the spiral length increases the peak force resulting from the initial flange contact. For spirals up to a critical length, this peak force exceeds the steady state curving values. corresponds to the maximum force during curving. Beyond this length, the steady state force is of greater magnitude. This effect was also observed by Law and



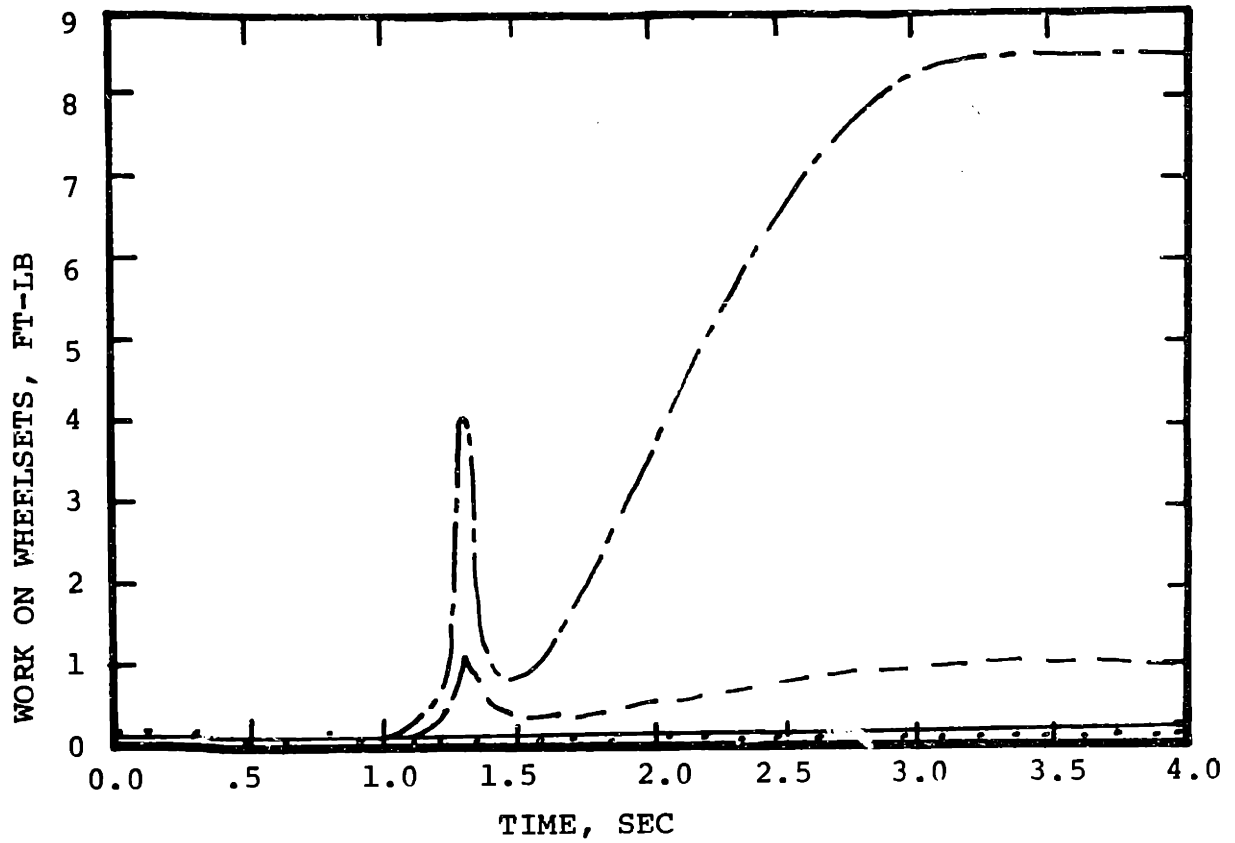
- - - - - WHEELSET 1 2.5° CURVE
 - - - - - WHEELSET 2 150 FT SPIRAL
 WHEELSET 3 50 FT/SEC
 _____ WHEELSET 4 $\phi_d = 0$

FIGURE 3.2 ANGLE OF ATTACK OF THE WHEELSETS OF THE BASELINE VEHICLE



-----	WHEELSET 1	2.5° CURVE
—————	WHEELSET 2	150 FT SPIRAL
.....	WHEELSET 3	50 FT/SEC
—————	WHEELSET 4	$\phi_d = 0$

FIGURE 3.3 LATERAL COMPONENT OF NORMAL FORCE ON LEFT WHEELS OF BASELINE VEHICLE



-----	WHEELSET 1	2.5° CURVE
-----	WHEELSET 2	150 FT SPIRAL
.....	WHEELSET 3	50 FT/SEC
-----	WHEELSET 4	$\phi_d = 0$

FIGURE 3.4 WORK ON WHEELSETS OF BASELINE VEHICLE

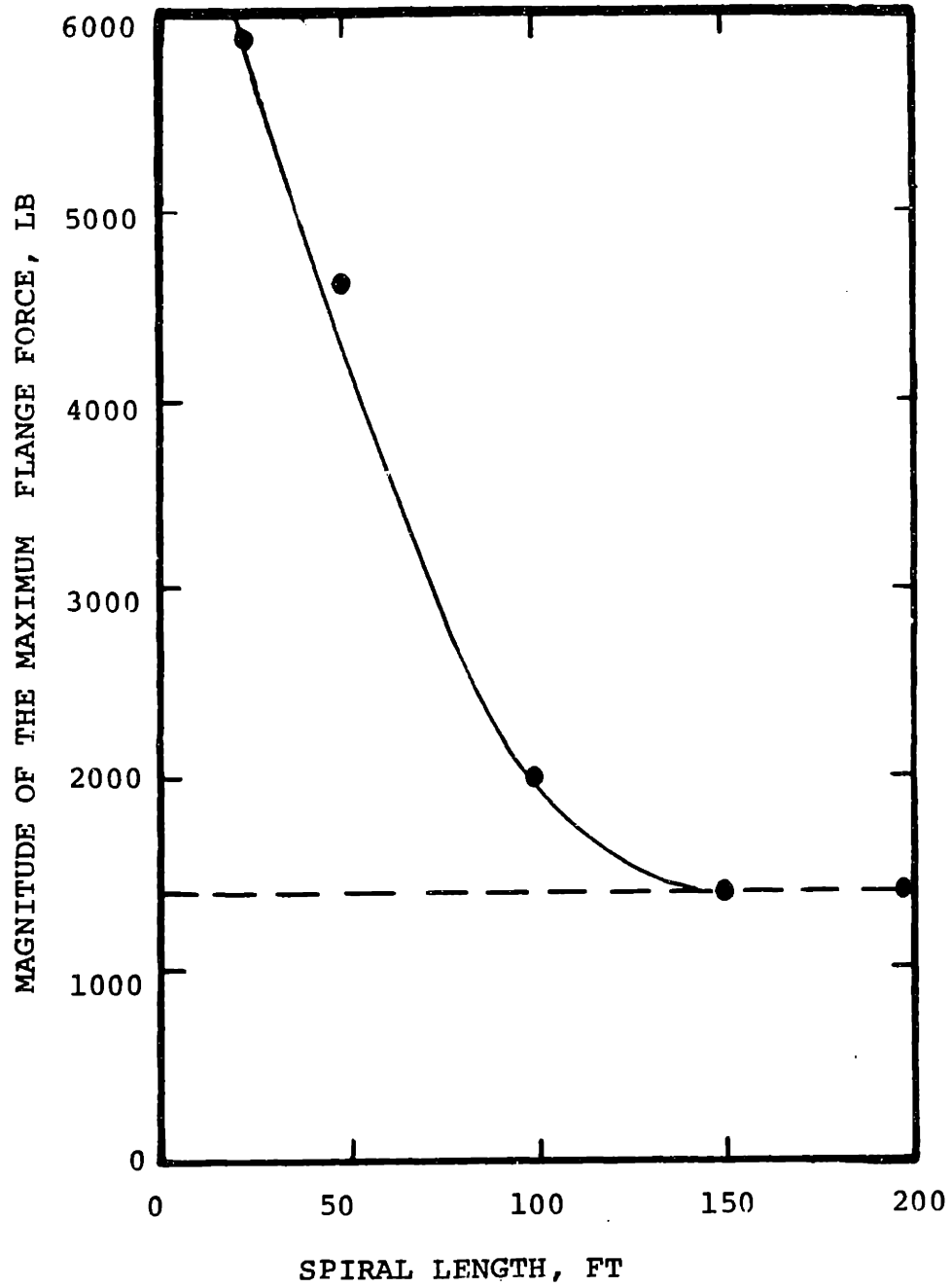


FIGURE 3.5 EFFECT OF SPIRAL LENGTH ON MAXIMUM FLANGE FORCE

Cooperrider [11]. For this model the critical length is approximately one hundred and fifty feet.

3.4 DEGREE CURVE

Curving studies were conducted with the baseline vehicle for several final degree curves at their associated balance running speeds. The length of the transition spiral was held constant. Figures 3.6 and 3.7 show the lateral excursion and flange force respectively of the lead wheelset as a function of final degree curve. For tight curves, the wheel flange impacts the rail soon after curve entry and remains in contact for the duration of the curve. High flange forces are associated with this behavior. As the radius of the curve increases, the wheelset oscillates laterally after initial flange contact. The corresponding lateral forces are lower. Further increase in radius results in low flange forces and no flanging.

3.5 RAIL FLEXIBILITY

During curving, the lateral flexibility of the rail, illustrated in Figure 2.17, has an important effect on the modelled vehicle response. Figure 3.8 shows the effect of rail stiffness on the peak lateral force of a vehicle negotiating a five degree curve at balanced running speed. As the flexibility of the track increases while maintaining

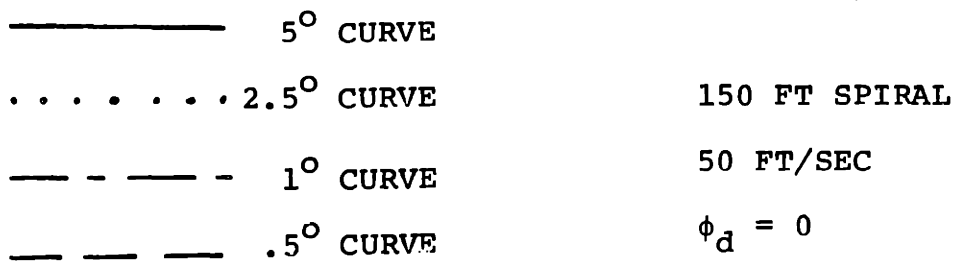
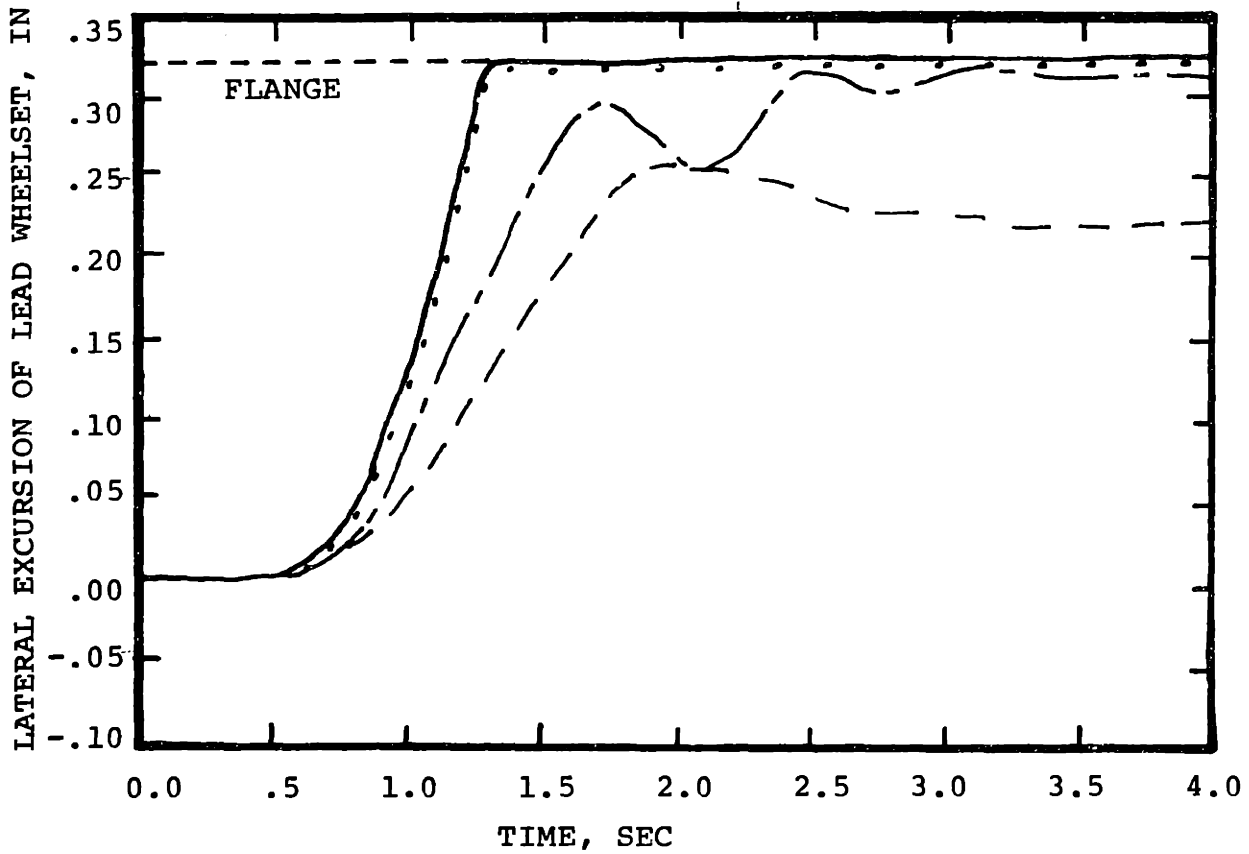
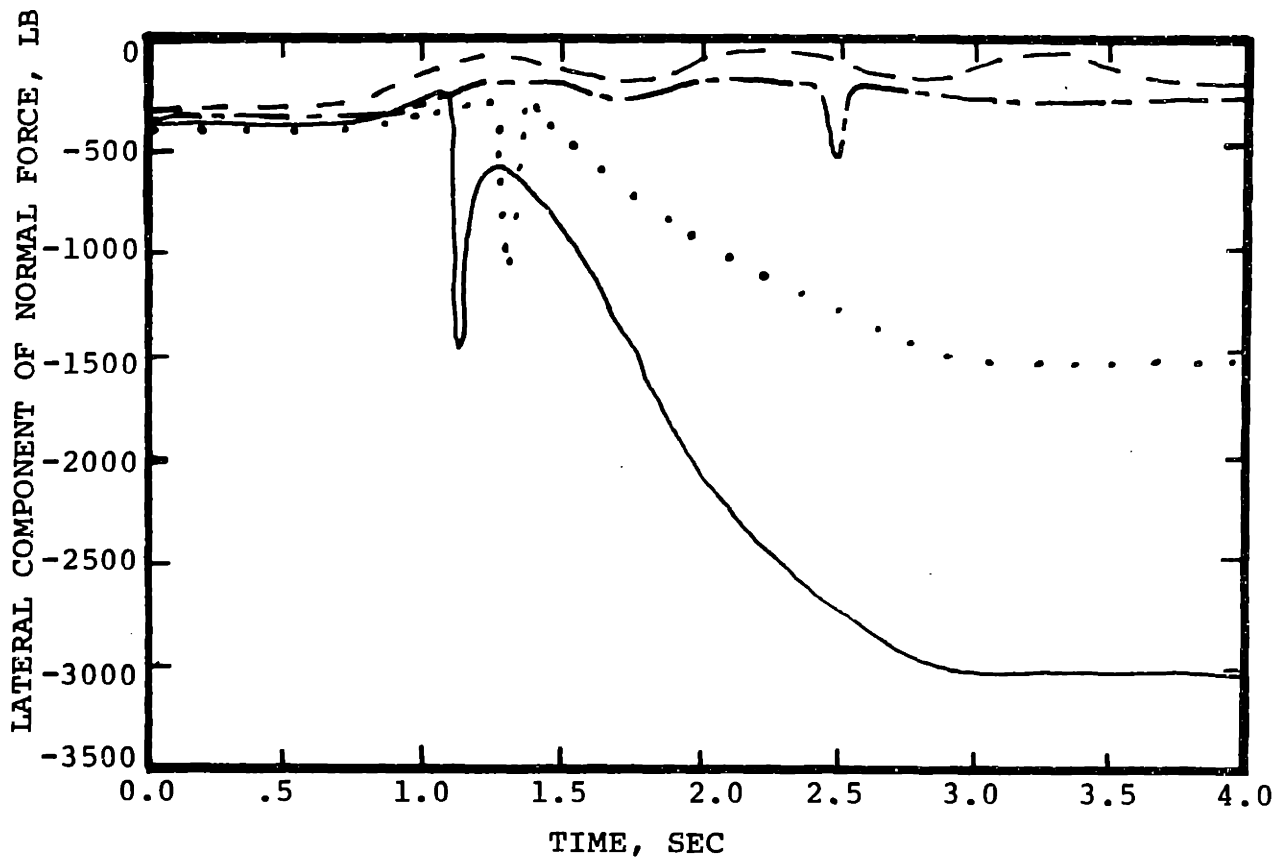


FIGURE 3.6 EFFECT OF FINAL DEGREE CURVE ON THE LATERAL EXCURSION OF THE WHEELSETS



————— 5° CURVE
 2.5° CURVE
 - - - - - 1° CURVE
 - - - - - .5° CURVE

150 FT SPIRAL
 50 FT/SEC
 $\phi_d = 0$

FIGURE 3.7 EFFECT OF FINAL DEGREE CURVE ON THE LATERAL COMPONENT OF NORMAL FORCE ON THE LEFT LEAD WHEEL

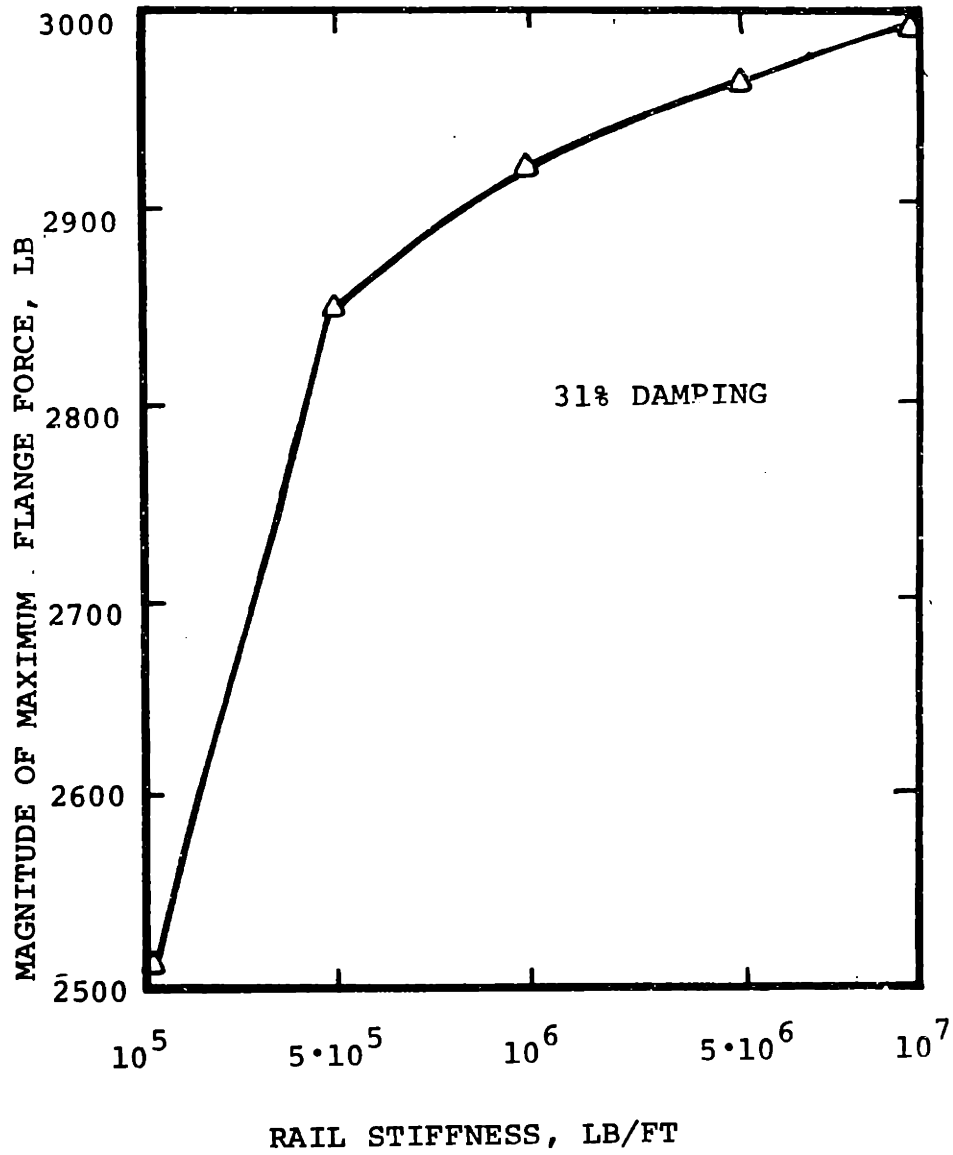


FIGURE 3.8 EFFECT OF RAIL FLEXIBILITY ON MAXIMUM FLANGE FORCE

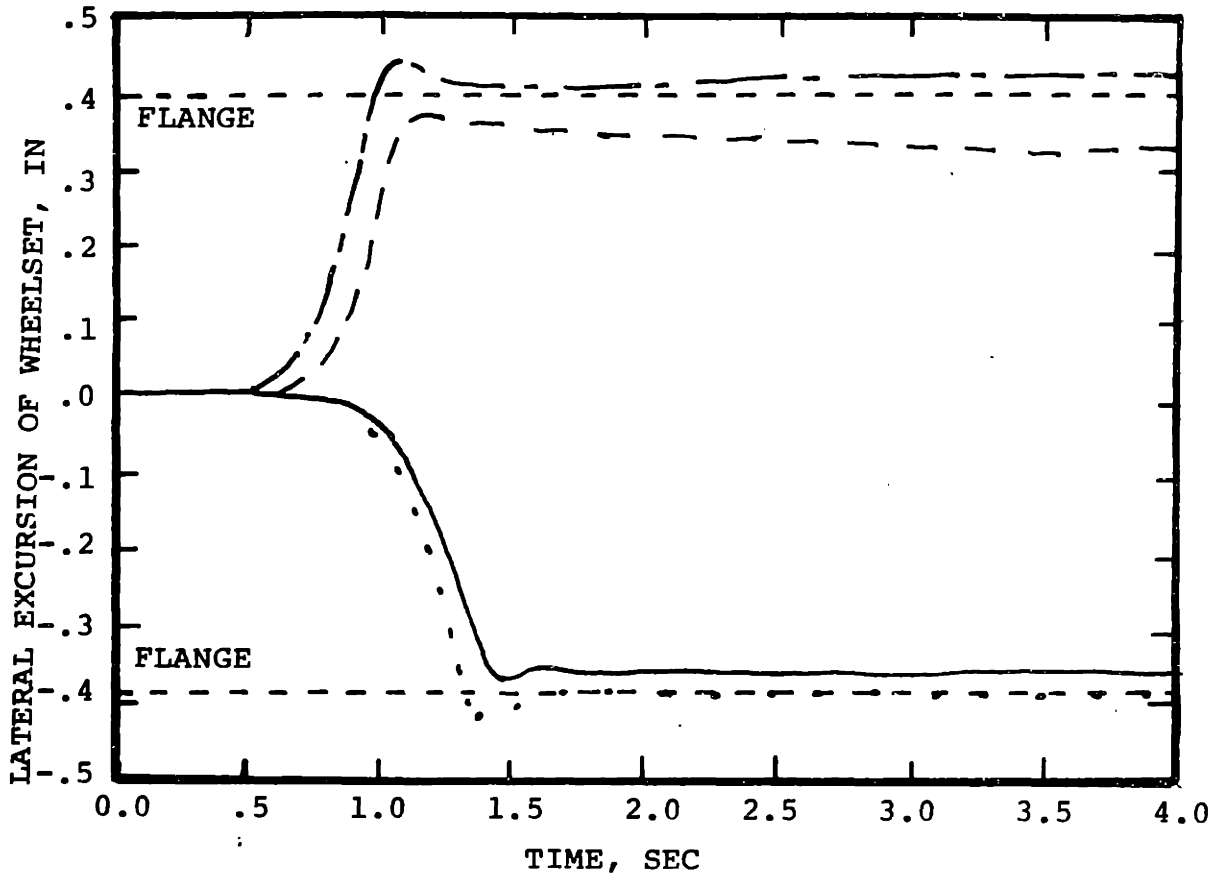
thirty one percent damping [22], the net lateral flange force experienced by the vehicle decreases. Net lateral force predicted by a rigid rail model is significantly greater than that predicted by typical values for rail stiffness.

3.6 WHEEL/RAIL PROFILE

As wheels and rails become worn with service, the geometry of the wheel/rail interface changes as illustrated in Figure 2.10 and 2.11. The baseline vehicle conditions described in Section 3.2 were repeated with the Worn Wheel on Worn Rail profile. In this case both lead wheelsets flange and the angles of attack are much greater as seen in Figures 3.9 and 3.10. The flange force, shown in Figure 3.11, resulting from the initial flange contact is nearly twice as large as with new wheelsets. The steady state flange force increases to a lesser extent. Therefore the critical spiral length, at which the flange force resulting from the initial contact exceeds the steady state flange force, is shorter. Since the rolling radius difference is less for a given gravitational stiffness [8], worn wheels do not produce as great a steering moment as new wheels.

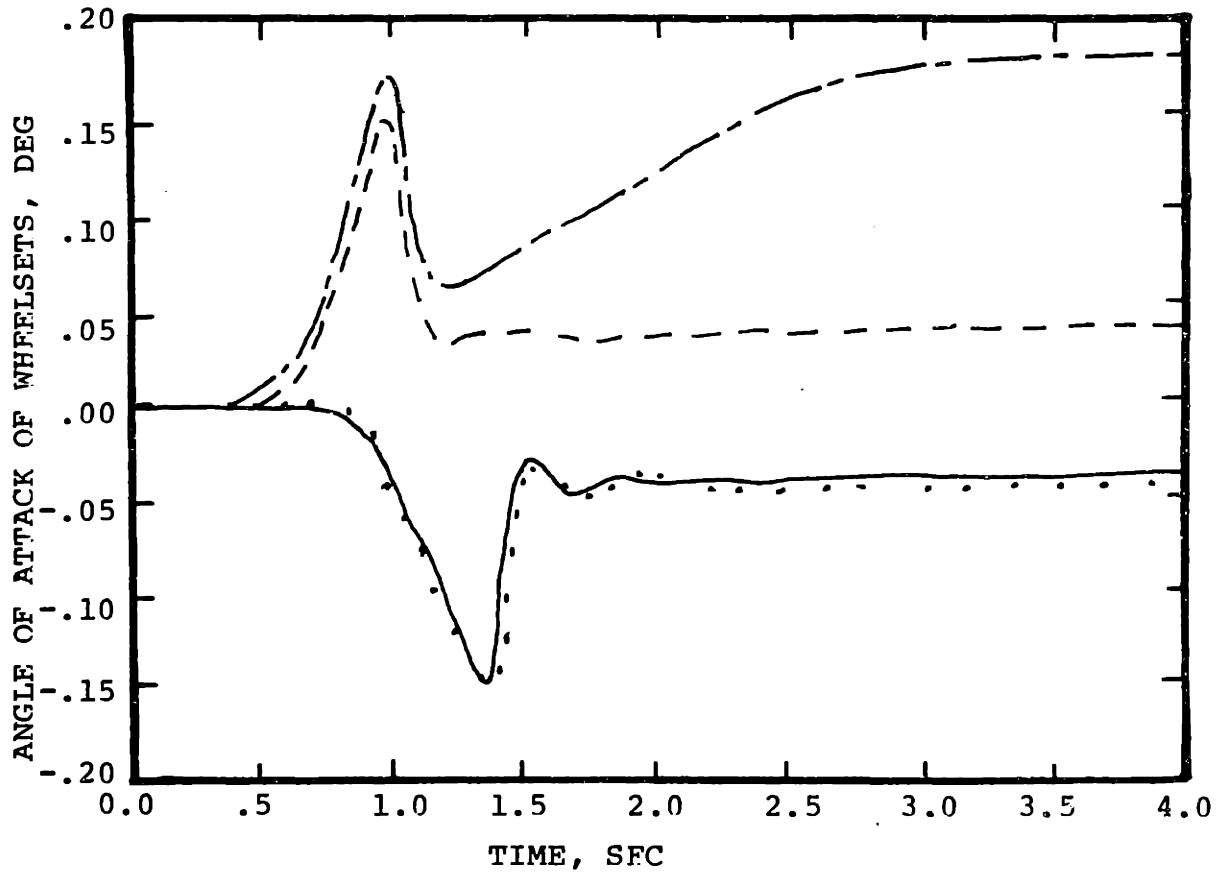
3.7 INTERCONNECTION OF THE WHEELSETS

Interconnecting the wheelsets of a conventional freight truck results in a significant improvement in the curving



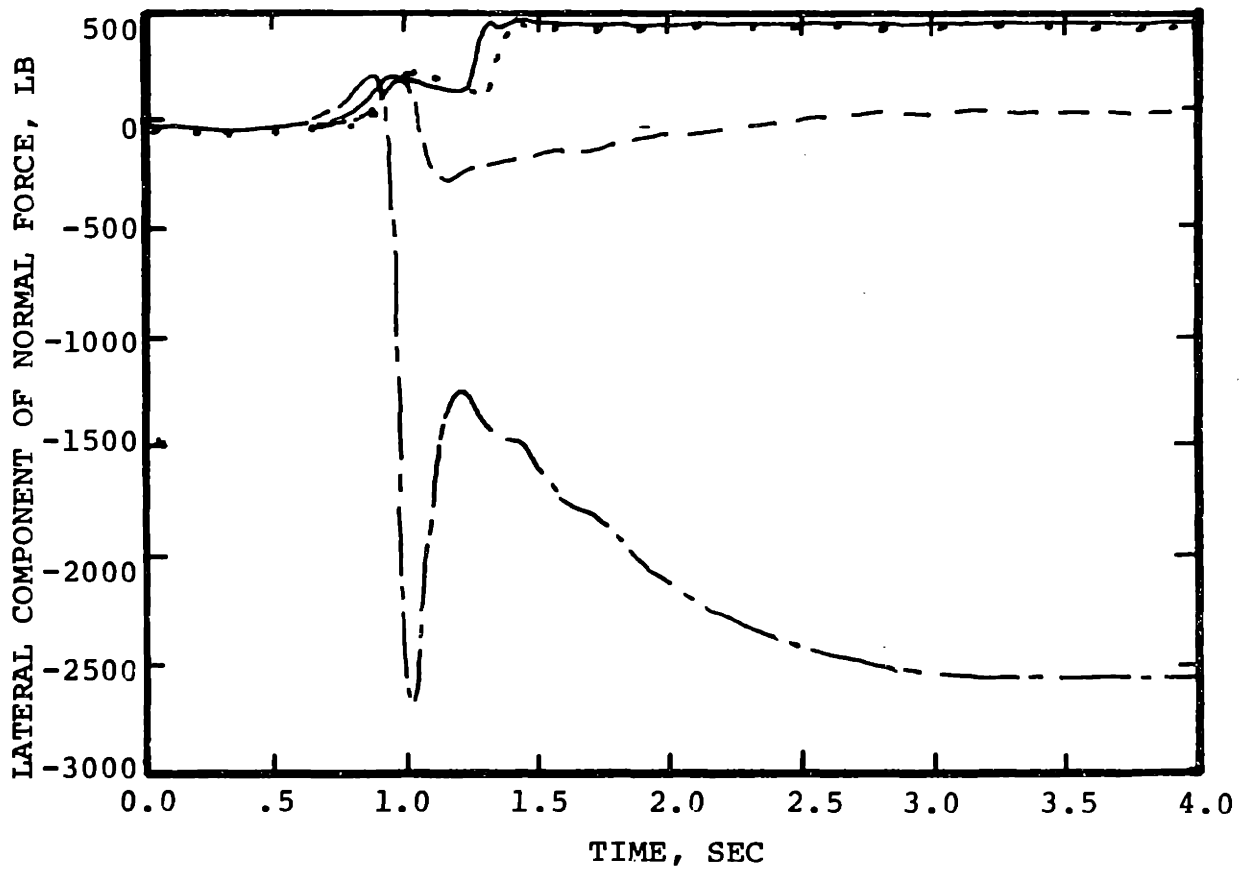
— — — — —	WHEELSET 1	2.5° CURVE
- - - - -	WHEELSET 2	150 FT SPIRAL
• • • • •	WHEELSET 3	50 FT/SEC
—————	WHEELSET 4	$\phi_d = 0$

FIGURE 3.9 EFFECT OF WORN WHEEL WORN RAIL PROFILE ON WHEELSET LATERAL EXCURSION



— — — —	WHEELSET 1	2.5° CURVE
- - - - -	WHEELSET 2	150 FT SPIRAL
.	WHEELSET 3	50 FT/SEC
—————	WHEELSET 4	$\phi_d = 0$

FIGURE 3.10 EFFECT OF WORN WHEEL WORN RAIL PROFILE
ON WHEELSET ANGLE OF ATTACK



— — — — —	WHEELSET 1	2.5° CURVE
- - - - -	WHEELSET 2	150 FT SPIRAL
.	WHEELSET 3	50 FT/SEC
—————	WHEELSET 4	$\phi_d = 0$

FIGURE 3.11 EFFECT OF WORN WHEEL WORN RAIL PROFILE ON LATERAL COMPONENT OF THE NORMAL FORCE ON LEFT LEAD WHEEL

performance. The angles of attack and flange forces of a conventional three-piece truck and radial trucks with varying shear stiffnesses are compared. In each case, the vehicle travels through a one hundred and fifty foot spiral into a constant two and a half degree curve. The mass and the yaw moment of inertia of each wheelset of the radial trucks are increased by about twenty percent due to the addition of radial arms [13]. The primary stiffnesses are decreased to allow the wheelsets to assume a radial position. The bending stiffness of the radial trucks are held constant.

Figures 3.12 and 3.13 compare angles of attack and flange forces of the lead wheelset of the conventional three-piece truck and a radial truck. The lower angle of attack of the radial truck indicates that the wheelset is aligned in a more radial position. Dynamic flange forces of the radial truck are also lower. Increasing the shear stiffness of the radial truck by one hundred percent had very little effect on the angle of attack, work or flange force levels.

3.8 COULOMB FRICTION

To accurately model the motion of freight vehicles, it is necessary to consider coulomb friction. The linear viscous damping elements of the baseline vehicle are replaced with coulomb friction elements, discussed in Section 2.3, to determine their effect on the response of the model. Values

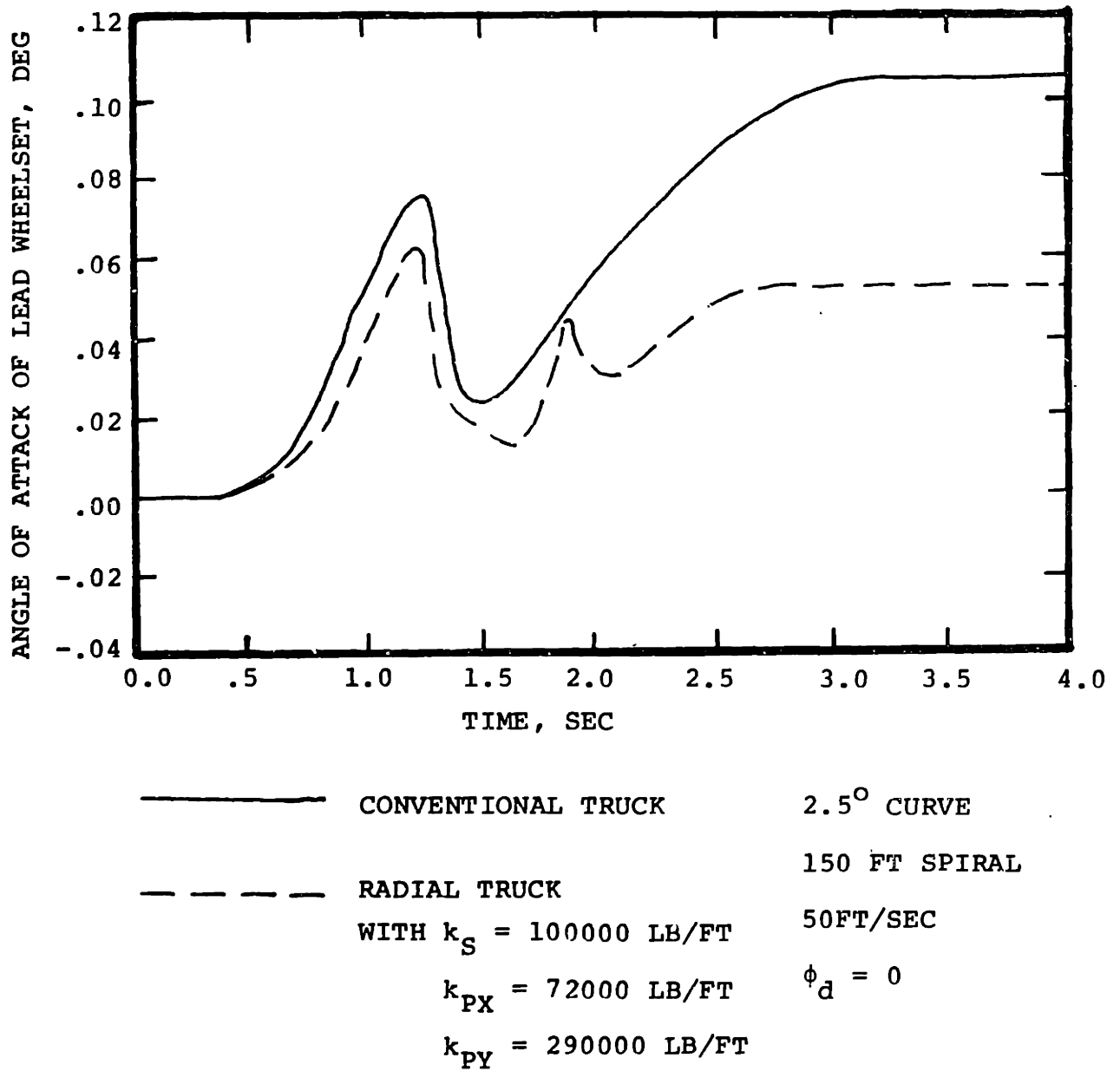
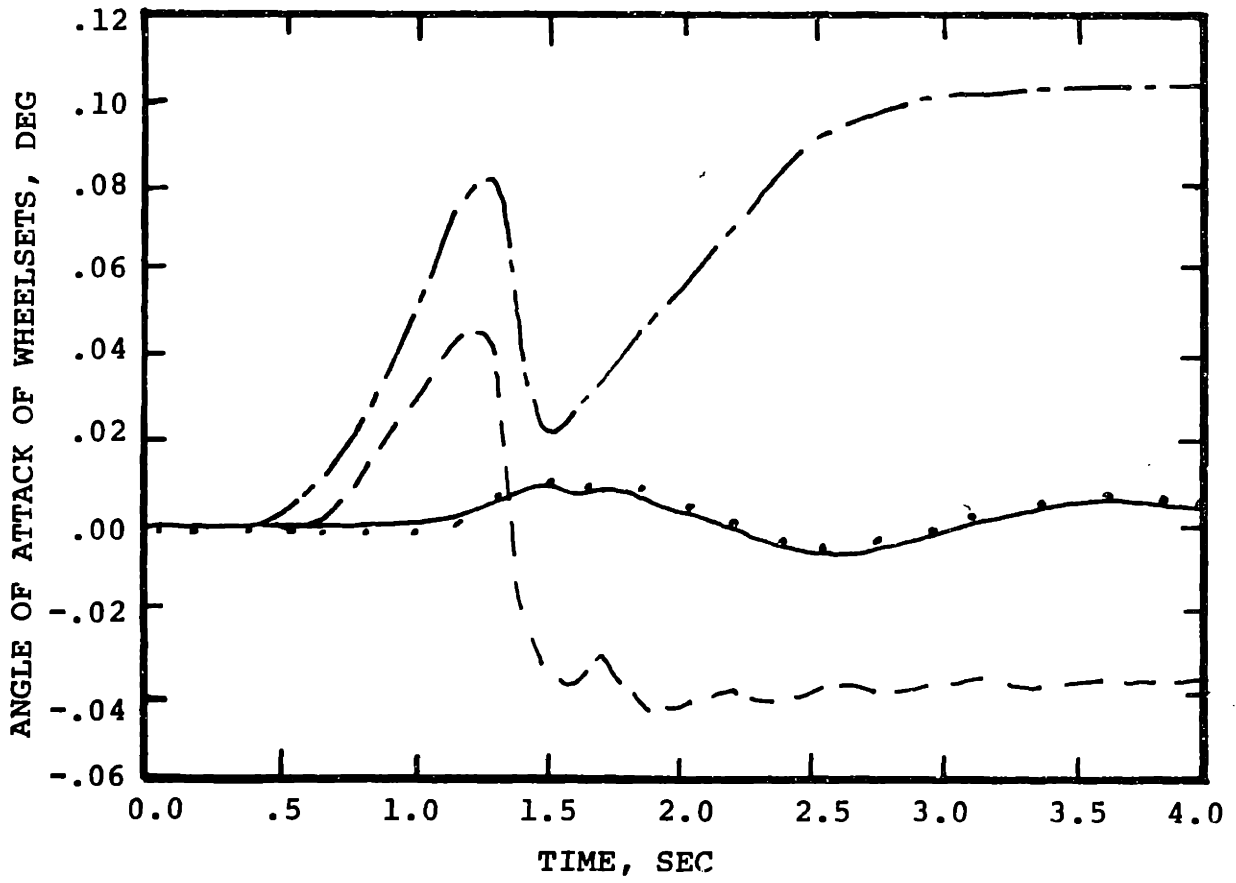


FIGURE 3.12 EFFECT OF WHEELSET INTERCONNECTION ON ANGLE OF ATTACK OF LEAD WHEELSET

for the breakout forces and moments and spring constants are given in Table 3.2 [24]. Figures 3.14 and 3.15 show the angles of attack and flange forces as the vehicle travels through the spiral. The magnitudes predicted by the model with coulomb friction are approximately the same as those predicted by the model with linear suspension. The flange force, however, is much more oscillatory than the baseline vehicle predicts.

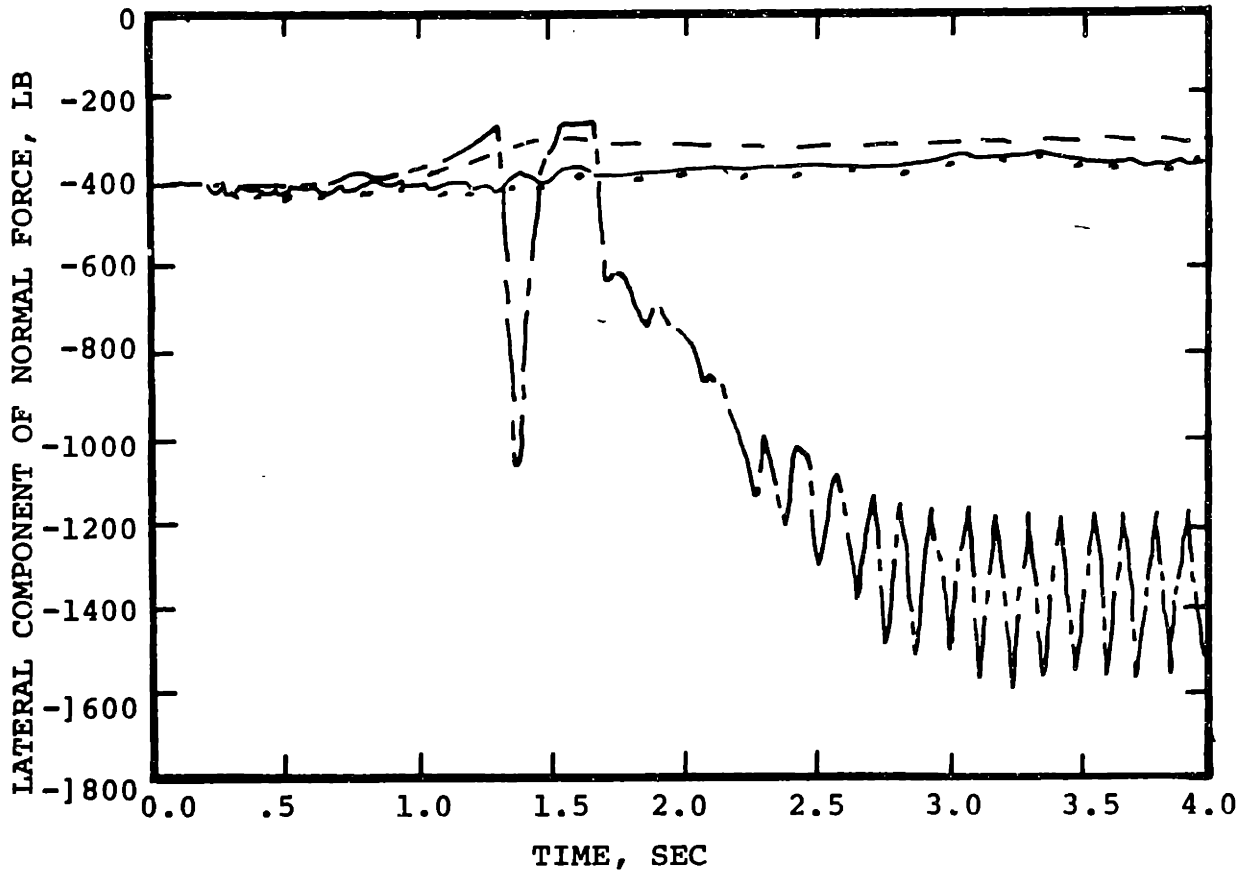
TABLE 2NONLINEAR SUSPENSION PARAMETERS [24]

F_{YO}	=	3669.0 LB	k_{SY}	=	61932.0 LB/FT
T_{CPO}	=	606.0 FT-LB	k_{SZ}	=	257150.0 LB/FT
T_{WO}	=	4687.0 FT-LB	k_W	=	3729000.0 LB/FT
F_{ZO}	=	3500.0 LB			



-----	WHEELSET 1	2.5° CURVE
- - - - -	WHEELSET 2	150 FT SPIRAL
.....	WHEELSET 3	50 FT/SEC
—————	WHEELSET 4	$\phi_d = 0$

FIGURE 3.14 EFFECT OF COULOMB FRICTION ON WHEELSET ANGLE OF ATTACK



— · — · — · —	WHEELSET 1	2.5° CURVE
— — — — —	WHEELSET 2	150 FT SPIRAL
· · · · ·	WHEELSET 3	50 FT/SEC
—————	WHEELSET 4	$\phi_d = 0$

FIGURE 3.15 EFFECT OF CO LOMB FRICTION ON THE LATERAL COMPONENT OF NORMAL FORCE ON THE LEFT WHEEL

CHAPTER 4

CONCLUSIONS AND RECOMMENDATIONS

A model capable of predicting the dynamic behavior of a freight car during curve entry and exit was developed. The model includes nonlinear wheel/rail geometry, coulomb friction and creep force saturation. By varying the interaxle bending and shear stiffnesses, both conventional and radial trucks can be modelled. Previous curving studies have been predominately concerned with steady state constant radius analyses which are unable to predict the dynamic effects of nonuniform track curvature and cant deficiency.

Solution to the set of nonlinear equations describing the model were found numerically using a fourth order Runge-Kutta algorithm. This model behaves consistently with previous results. With parameters chosen to correspond to previously developed models, this model predicted similiar results.

Preliminary results demonstrate the ability of this model to evaluate the effects of roadbed and wheel/rail geometry, rail stiffness and suspension design. Force levels exceeding maximum steady-state values have been predicted. This indicates the importance of continued dynamic analysis.

This model was developed primarily as a design tool. A useful modification of the program would incorporate track

irregularities either as explicit data or as a statistical description. Experimental data should also be obtained to validate the theoretical analysis. This study indicated the utility of further dynamic simulations to analyze the curving behavior of freight trucks.

REFERENCES

1. Porter, S. R. M., "The Mechanics of a Locomotive on Curved Track", The Railway Gazette, 1935.
2. Vermuelen, P. J. and Johnson, K. L., "Contact of Nonspherical Elastic Bodies Transmitting Tangential Forces", Journal of Applied Mechanics, Volume 86, June 1964, pp 338-340.
3. Kalker, J. J., "On the Rolling Contact of Two Elastic Bodies in the Presence of Dry Friction", Ph.D. Thesis, Technische Hogeschool, delft, Netherlands, 1967.
4. Boocock, D., "Steady State Motion of Railway Vehicles on Curved Track", Journal of Mechanical Engineering Science, Volume 11, No. 6, December 1969, pp 556-566.
5. Newland, D. E., "Steering a Flexible Railway Truck on Curved Track", Journal of Engineering for Industry, A.S.M.E. Transactions, Series B, Volume 91, No. 3, August 1969, pp. 908-918.
6. Elkins, J. A. and Gostling, R. J., "A General Quasi-Static Curving Theory for Railway Vehicles", Proc. 5th VSD-2nd IUTAM Symposium on the Dynamics of Vehicles on Roads and Tracks, 1978.
7. Law, E. H. and Cooperrider, N. K., "Nonlinear Dynamic and Steady State Curving of Rail Vehicles", presented at the 1980 A.S.M.E. Winter Annual Meeting, San Francisco, Ca., December 1981.
8. Bell, C. E., "Curving Mechanics of Rail Vehicles", Ph.D. Thesis, Department of Mechanical Engineering, M. I. T., September 1981.
9. Hedrick, J. K., et al, "Nonlinear Analysis and Design Tools for Rail Vehicles", Final Report for AAR, January 1, 1979.
10. Smith, K. "Curve Entry and Curve Negotiation Characteristics of Two-axle Trucks", M.S. Thesis, Illinois Institute of Technology, December 1975.

11. Cooperrider, N. K. and Law, E. H. "The Nonlinear Dynamics of Rail Vehicles in Curve Entry and Negotiation", presented at the 7th IAVSD-IUTAM Symposium on the Dynamics of Vehicles on Road and Tracks, Cambridge, U.K., September 7-11, 1981.
12. Clark, R. A., Eikhoff, B. M. and Hunt, G. A., "Prediction of the Dynamic Response of Vehicles to Lateral Track Irregularities", presented at the 7th IAVSD-IUTAM Symposium on the Dynamics of Vehicles on Road and Tracks, Cambridge, U.K., September 7-11, 1981.
13. Hadden, J. A., "The Effects of Truck Design and Component Flexibility on the Lateral Stability of Railway Freight Vehicles", M.S. Thesis, Clemson University, December 1976.
14. Hedrick, J. K., et al. "The Application of Quasi-Linearization Techniques to Rail Vehicle Dynamic Analyses", report No. FRA/ORD-78/56 prepared under U. S. Department of Transportation Contract DOT/TSC-902, November 1977.
15. Briggs, M., "Nonlinear Analysis of Rail Vehicles", M.E. Thesis, Department of Mechanical Engineering, M.I.T., September 1977.
16. Scheffel, H., "Wheelset Suspensions Designed to Eliminate the Detrimental Effects of Wear on the Hunting Stability of Railroad Vehicles", A.S.M.E. Symposium on Railroad Equipment Dynamics, Chicago, 1976.
17. List, H. A., "Design System Approach to Problem Solving", 12th Annual Railroad Engineering Conference on the Effects of Heavy Axle Loads on Track, 1975, p.79.
18. Cooperrider, N. K., and Law, E. H., "Wheel/Rail Geometry for Five Wheel Profiles and Three Rail Profiles", Report No. ERC-R-76009 prepared under U.S. Department of Transportation Contract DOT-OS-40018, March 1976.
19. Heller, R. et al., "Analog and Digital Computer Simulation of Coulomb Friction", Report No. FRA-ORD-78/07 prepared under U. S. Department of Transportation Contract No. DOT-OS-40018, December 1977.
20. Hedrick, J. K., et al. "Performance Limits of Rail Passenger Vehicles: Evaluation and Optimization", Final Report No. DOT/RSPA/DPB-50/79/12, prepared under U. S. Department of Transportation Contract DOT-OS-70052, December 1979.

21. Ahlbeck, D. R., "The Effects of Track Modulus on Vehicle-Track Dynamic Interaction", submitted for presentation at the A.S.M.E./I.E.E.E. Joint Railroad Conference, April 1982.
22. Arslan, A. V., "The Application of Statical Linearization to Nonlinear Rail Vehicle Dynamics", Ph.D. Thesis, M.I.T., June 1980.
23. Nagurka, M., "Dynamic Curving of Rail Vehicles", Ph.D. Thesis, M.I.T., 1983.
24. Cooperrider, N. K., "Freight Car Dynamics: Field Test Results and Comparison with Theory", Report No. FRA/ORD-81/46, prepared under U. S. Department of Transportation Contract DOT-OS-40018, June 1981.

APPENDIX A

DERIVATION OF THE WHEELSET DYNAMIC CURVINGEQUATIONS OF MOTIONA.1 INTRODUCTION

This section contains the derivation of the equations of motion for a single wheelset negotiating an arbitrarily changing radius curve. The wheelset is connected through a suspension system to a moving reference frame which travels at a constant forward speed along the track. The outer rail of the track is superelevated relative to the inner rail. The wheelset has two degrees of freedom for yaw and lateral motion and an extra state to describe the spin perturbation of the wheelset. The wheelset is assumed to be a rigid body which does not lift from the track.

A.2 AXIS SYSTEMS

Figure A.1 defines the two moving coordinate systems used to develop this model. A track reference axis system, \hat{i}_T , \hat{j}_T and \hat{k}_T , moves along the centerline of a superelevated track at a constant tangential speed. The \hat{i}_T axis is directed along the track centerline. The \hat{j}_T axis is perpendicular to the track centerline. The \hat{k}_T axis is normal to the track plane. The \hat{i}_W , \hat{j}_W and \hat{k}_W axes are fixed to the center of gravity of an isolated wheelset. The \hat{i}_W axis is positioned along the

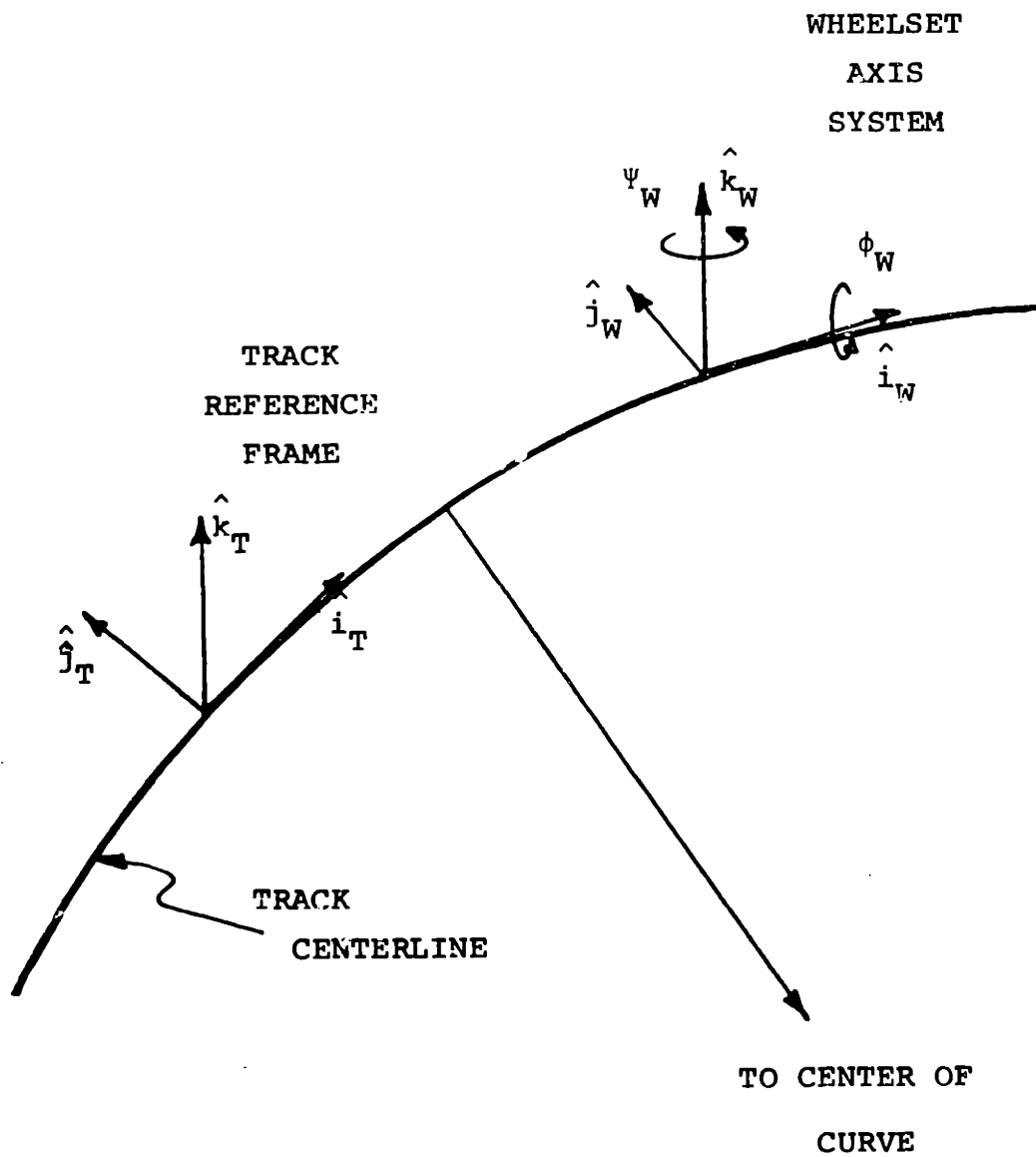


FIGURE A. 1 DEFINITION OF COORDINATE SYSTEMS

track centerline. The \hat{j}_W axis lies along the axle centerline parallel to the track plane. The \hat{k}_W is normal to and directed upward from the \hat{i}_W - \hat{j}_W plane. The w-axis system translates, yaws and rolls but does not spin with the wheelset center of gravity. Assuming small roll and yaw angles the coordinate transformations between axes are given by

$$\begin{bmatrix} \hat{i}_W \\ \hat{j}_W \\ \hat{k}_W \end{bmatrix} = \begin{bmatrix} 1 & \psi_W & 0 \\ -\psi_W & 1 & \phi_W \\ 0 & -\phi_W & 1 \end{bmatrix} \begin{bmatrix} \hat{i}_T \\ \hat{j}_T \\ \hat{k}_T \end{bmatrix} \quad (A.1)$$

A.3 ACCELERATION OF WHEELSET

The inertial acceleration of a wheelset is defined by the expression

$$\bar{a}_W = \bar{a}_T + \dot{\bar{\omega}}_T \times \bar{R}_W + \bar{\omega}_T \times (\bar{\omega}_T \times \bar{R}_W) + 2\bar{\omega}_T \times \dot{\bar{R}}_W + \ddot{\bar{R}}_W \quad (A.2)$$

$$\text{where } \bar{\omega}_T = \dot{\phi}_{SE} \hat{i}_T + \frac{V}{R} \phi_{SE} \hat{j}_T - \frac{V}{R} \hat{k}_T$$

$$\bar{a}_T = \frac{V^2}{R} \hat{j}_T + (a_{SE} + \frac{V^2}{R} \phi_{SE}) \hat{k}_T$$

$$\bar{R}_W = x_W \hat{i}_T + y_W \hat{j}_T + (z_W + r_0) \hat{k}_T$$

Substitution yields the expression

$$\bar{a}_W = \ddot{x}_W \hat{i}_T + \left(\ddot{y}_W - \frac{V^2}{R} - r_0 \ddot{\phi}_{SE} \right) \hat{j}_T + \left(\ddot{z}_W + a \ddot{\phi}_{SE} + \frac{V^2}{R} \phi_{SE} \right) \hat{k}_T \quad (A.3)$$

A.4 ANGULAR MOMENTUM OF THE WHEELSET

The angular velocity of the wheelset is defined by

$$\bar{\omega}_W = \dot{\phi}_{SE} \hat{i}_I - \frac{V}{R} \hat{k}_I + \dot{\phi}_W \hat{i}_W + (\Omega + \beta) \hat{j}_W + \dot{\psi}_W \hat{k}_T \quad (A.4)$$

Small angle approximations reduce this equation to

$$\bar{\omega}_W = \omega_{WX} \hat{i}_W + \omega_{WY} \hat{j}_W + \omega_{WZ} \hat{k}_W \quad (A.5)$$

where

$$\omega_{WX} = \dot{\phi}_{SE} + \dot{\phi}_W$$

$$\omega_{WY} = \Omega + \beta$$

$$\omega_{WZ} = -\frac{V}{R} + \dot{\psi}_W$$

Since a wheelset is symmetric about the $\hat{i}_W - \hat{k}_W$ plane, the yaw and spin moments of inertia are identical. The angular momentum of the wheelset is given by

$$\bar{H}_W = I_{WZ} \omega_{WX} \hat{i}_W + I_{WY} \omega_{WY} \hat{j}_W + I_W \omega_{WZ} \hat{k}_W \quad (A.6)$$

The time rate of change of the angular momentum is expressed by

$$\frac{D \bar{H}_W}{D t} = \frac{d \bar{H}_W}{d t} + \bar{\omega}_{AXIS} \times \bar{H}_W \quad (A.7)$$

Since the axis system does not spin with the wheelset, its angular velocity is described by the expression

$$\bar{\omega}_{\text{AXIS}} = \omega_{\text{WX}} \hat{i}_W + \omega_{\text{WZ}} \hat{k}_W \quad (\text{A. 8})$$

Substituting equations A.5, A.6 and A.8 into A.7 and neglecting small terms gives

$$\begin{aligned} \frac{D \bar{H}_W}{D t} &= (I_{\text{WX}} (\ddot{\phi}_{\text{SE}} + \ddot{\phi}_W) - I_{\text{WY}} (\Omega + \beta) (\dot{\psi}_W \frac{V}{R})) \hat{i}_W \\ &+ (I_{\text{WY}} \ddot{\beta}) \hat{j}_W \\ &+ (I_{\text{WX}} (\dot{\psi}_W - V \frac{d}{dt} (\frac{1}{R})) + I_{\text{WY}} (\Omega + \beta) (\dot{\phi}_{\text{SE}} + \dot{\phi}_W)) \hat{k}_W \end{aligned} \quad (\text{A. 9})$$

A.5 FORCES AND MOMENTS

A freebody diagram of a wheelset is shown in Figure A.2. The moments due to the external weight and the creep, normal and suspension forces are defined by the equation

$$\frac{D \bar{H}_W}{D t} = \bar{R}_R \times (\bar{F}_R + \bar{N}_R) + \bar{R}_L \times (\bar{F}_L + \bar{N}_L) + \bar{M}_L + \bar{M}_R + \bar{M}_{\text{SUSP}} + \bar{M}_{\text{EXT}} \quad (\text{A. 10})$$

$$\text{where } \bar{R}_R = a \hat{v}_W \hat{i}_T - a \hat{j}_T - r_R \hat{k}_T$$

$$\bar{R}_L = -a \hat{v}_W \hat{i}_T + a \hat{j}_T - r_L \hat{k}_T$$

$$\bar{M}_{\text{EXT}} = -h W_{\text{EXT}} (\phi_d - \phi_W) \hat{i}_W$$

The force expression is

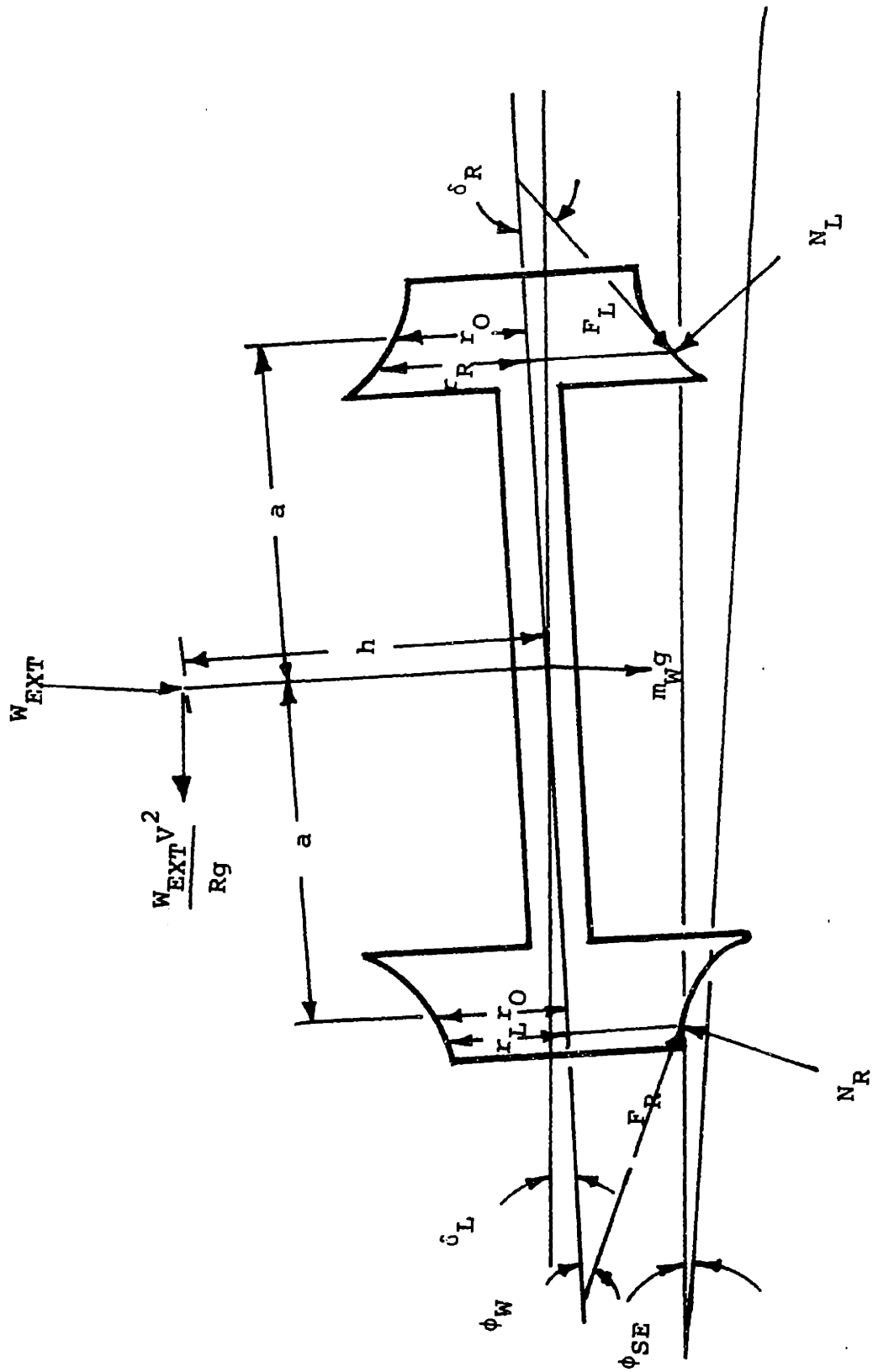


FIGURE A.2 FREEBODY DIAGRAM OF WHEELSET

$$\bar{m}_W \bar{a}_W = \bar{F}_R + \bar{F}_L + \bar{F}_{SUSP} + \bar{N}_R + \bar{N}_L + \bar{L}_A \quad (A.11)$$

where

$$\bar{L}_A = \left(\frac{W_{EXT} V^2}{Rg} - (W_W + W_{EXT}) \phi_{SE} \right) \hat{j}_T - \left((W_W + W_{EXT}) + \frac{W_{EXT} V^2}{Rg} \phi_{SE} \right) \hat{k}_T$$

Applying Newton's law to the track reference axis system yields the following six equations.

Longitudinal Equation

$$m_W \ddot{x}_W = F_{RX} + F_{LX} \quad (A.12)$$

Lateral Equation

$$m_W (\ddot{y}_W - r_0 \ddot{\phi}_{SE}) - (W_W + W_{EXT}) \phi_d = F_{RY} + F_{LY} + F_{SUSP_Y} + N_{RY} + N_{LY} \quad (A.13)$$

Vertical Equation

$$m_W (\ddot{z}_W + a \ddot{\phi}_{SE}) + (W_W + W_{EXT}) \left(1 + \frac{V^2}{Rg} \phi_{SE} \right) = F_{RZ} + F_{LZ} + N_{RZ} + N_{LZ} \quad (A.14)$$

Roll Equation

$$\begin{aligned} I_{WX} (\ddot{\phi}_W + \ddot{\phi}_{SE}) - I_{WY} (\dot{\alpha} + \dot{\beta}) \left(\dot{\psi}_W - \frac{V}{R} \right) - h W_{EXT} (\phi_d - \phi_W) = \\ r_R (F_{RY} + N_{RY}) + r_L (F_{LY} + N_{LY}) + M_{LX} + M_{LY} \\ + a (F_{LZ} - F_{RZ} + N_{LZ} - N_{RZ}) \end{aligned} \quad (A.15)$$

Yaw Equation

$$\begin{aligned} I_{WZ} \left(\ddot{\psi}_W - V \frac{d}{dt} \left(\frac{1}{R} \right) \right) - I_{WY} (\dot{\alpha} + \dot{\beta}) (\dot{\phi}_W + \dot{\phi}_{SE}) = \\ a (F_{RX} - F_{LX}) + a \psi_W (F_{RY} - F_{LY} + N_{RY} - N_{LY}) \\ + M_{LZ} + M_{RZ} + M_{SUSP_Z} \end{aligned} \quad (A.16)$$

Spin Equation

$$I_{WY} \ddot{\beta} = -r_R F_{RX} - r_L F_{LX} + M_{LY} + M_{RY} \quad (A.17)$$

A.5.1 NORMAL FORCES

The normal forces at the left and right contact points are

$$\bar{N}_L = -N_L \sin(\delta_L + \phi_W) \hat{j}_T + N_L \cos(\delta_L + \phi_W) \hat{k}_T \quad (A.18)$$

and

$$\bar{N}_R = N_R \sin(\delta_R - \phi_W) \hat{j}_T + N_R \cos(\delta_R - \phi_W) \hat{k}_T \quad (A.19)$$

where

$$N_L = |\bar{N}_L|$$

$$N_R = |\bar{N}_R|$$

The normal forces are obtained from the vertical and roll equations. Simultaneous solution of equations A.14 and A.15 furnishes the following expressions for the vertical components of the normal forces

$$N_R \cos(\delta_R - \phi_W) = \frac{-M_\phi^* + F_z^*(a - r_L \tan(\delta_L + \phi_W))}{2a - r_R \tan(\delta_R - \phi_W) - r_L \tan(\delta_L + \phi_W)} \quad (A.20)$$

and

$$N_L \cos(\delta_L + \phi_W) = \frac{M_\phi^* + F_z^*(a - r_R \tan(\delta_R - \phi_W))}{2a - r_R \tan(\delta_R - \phi_W) - r_L \tan(\delta_L + \phi_W)} \quad (A.21)$$

where

$$M_\phi^* = I_{WZ}(\ddot{\phi}_W + \ddot{\phi}_{SE}) - I_{WY}(\dot{\Omega} + \dot{\beta})\left(\dot{\psi}_W - \frac{V}{R}\right) - a(F_{LZ} - F_{RZ}) - r_R F_{RY} - r_L F_{LY} + hW_{EXT}(\phi_d - \phi_W)$$

$$F_z^* = m_W(\ddot{z}_W + a\ddot{\phi}_{SE} + \frac{V^2}{R}\phi_{SE}) - F_{RZ} - F_{LZ} + (W_W + W_{EXT}) + \frac{W_{EXT}V^2}{Rg}\phi_{SE}$$

The gravitaional stiffness force is defined as the net lateral component of the normal forces.

$$F_{\text{GRAV}} = - N_R \sin(\delta_R - \phi_W) + N_L \sin(\delta_L + \phi_W) \quad (\text{A} . 22)$$

The gravitaional stiffness is defined by

$$M_{\text{GRAV}} = - a \psi_W (N_R \sin(\delta_R - \phi_W) - N_L \sin(\delta_L + \phi_W)) \quad (\text{A} . 23)$$

A.5.2 CREEP FORCES AND MOMENTS

Two axis systems, shown in Figure A.3, are attached to the left and right rail contact points. These axes are used to represent the direction of the wheel/rail contact forces. The relations between the contact point axes and the body axis are given by

$$\begin{bmatrix} \hat{i}_{\text{CL}} \\ \hat{j}_{\text{CL}} \\ \hat{k}_{\text{CL}} \end{bmatrix} = \begin{bmatrix} 1 & 0 & 0 \\ 0 & \cos \delta_L & \sin \delta_L \\ 0 & -\sin \delta_L & \cos \delta_L \end{bmatrix} \begin{bmatrix} \hat{i}_W \\ \hat{j}_W \\ \hat{k}_W \end{bmatrix} \quad (\text{A} . 24)$$

and

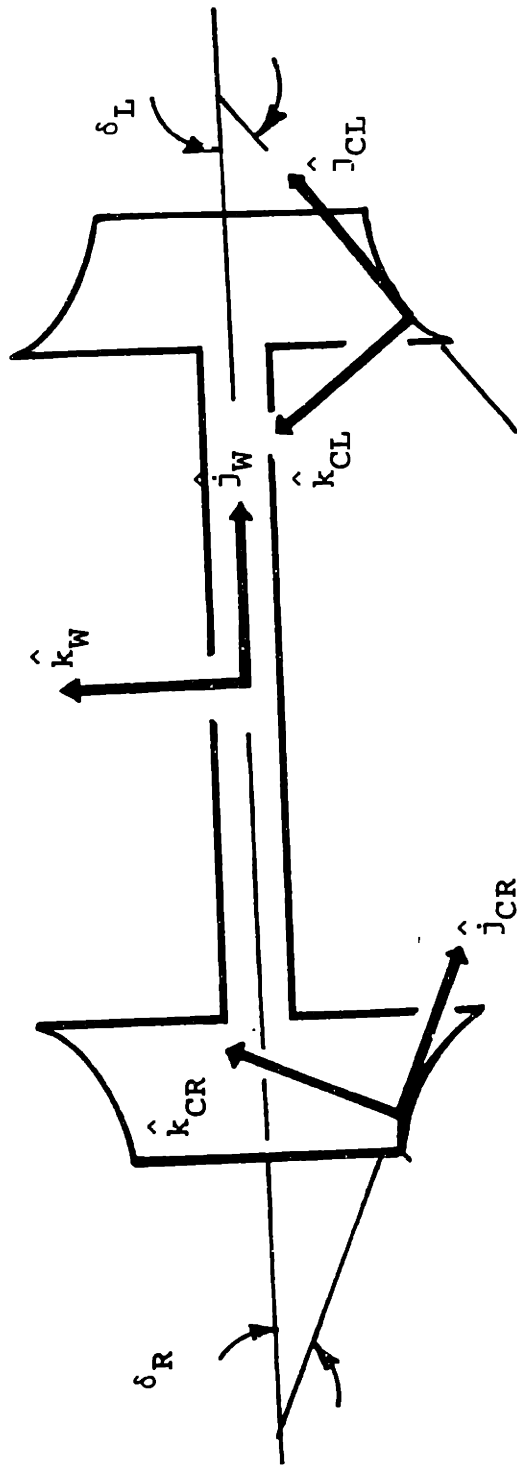


FIGURE A.3 DEFINITION OF CONTACT PLANE AXIS SYSTEMS

$$\begin{bmatrix} \hat{i}_{CR} \\ \hat{j}_{CR} \\ \hat{k}_{CR} \end{bmatrix} = \begin{bmatrix} 1 & 0 & 0 \\ 0 & \cos \delta_R & -\sin \delta_R \\ 0 & \sin \delta_R & \cos \delta_R \end{bmatrix} \begin{bmatrix} \hat{i}_W \\ \hat{j}_W \\ \hat{k}_W \end{bmatrix} \quad (A . 25)$$

After coordinate transformations, the creep forces and moments in the track reference frame for large contact angles and small yaw angles can be written as

Left Wheel:

$$F_{LX} = F_{LX^\circ} - F_{LY^\circ} \psi_W \cos(\delta_L + \phi_W) \quad (A . 26)$$

$$F_{LY} = F_{LX^\circ} \psi_W + F_{LY^\circ} \cos(\delta_L + \phi_W) \quad (A . 27)$$

$$F_{LZ} = F_{LY^\circ} \sin(\delta_L + \phi_W) \quad (A . 28)$$

$$M_{LX} = M_{LZ^\circ} \psi_W \sin(\delta_L + \phi_W) \quad (A . 29)$$

$$M_{LY} = -M_{LZ^\circ} \sin(\delta_L + \phi_W) \quad (A . 30)$$

$$M_{LZ} = M_{LZ^\circ} \cos(\delta_L + \phi_W) \quad (A . 31)$$

Right Wheel:

$$F_{RX} = F_{RX^\circ} - F_{RY^\circ} \psi_W \cos(\delta_R - \phi_W) \quad (A . 32)$$

$$F_{RY} = F_{RX^\circ} \psi_W + F_{RY^\circ} \cos(\delta_R - \phi_W) \quad (A . 33)$$

$$F_{RZ} = -F_{RY^\circ} \sin(\delta_R - \phi_W) \quad (A . 34)$$

$$M_{RX} = -M_{RZ^\circ} \psi_W \sin(\delta_R - \phi_W) \quad (A . 35)$$

$$M_{RY} = M_{RZ} \cdot \sin(\delta_R - \phi_W) \quad (A . 36)$$

$$M_{RZ} = M_{RZ} \cdot \cos(\delta_R - \phi_W) \quad (A . 37)$$

where F_{Ri} and F_{Li} are the i^{th} component of creep forces resolved in the contact plane.

M_{Ri} and M_{Li} are the i^{th} component of creep forces resolved in the contact plane.

Kalker linear creep theory defines the relation between the creep forces and creepages as

Lateral Creep Force:

$$F_Y = - f_{11} \xi_Y - f_{12} \xi_{SP} \quad (A . 38)$$

Longitudinal Creep Force:

$$F_X = - f_{33} \xi_X \quad (A . 39)$$

Spin Creep Moment:

$$M_Z = f_{12} \xi_Y - f_{22} \xi_{SP} \quad (A . 40)$$

where

$$\xi_{LX} = \frac{1}{V} \left(V \left(1 + \frac{a}{R} - \frac{r_L}{r_0} \right) - a \dot{\varphi}_W - r_L \dot{\beta} \right) \quad (A . 41)$$

$$\xi_{LY} = \frac{1}{V} \left(\cos \delta_L (\dot{y}_W - V \dot{\varphi}_W + r_L \dot{\phi}_W) + \sin \delta_L (\dot{z}_W + a \dot{\phi}_W) \right) \quad (A . 42)$$

$$\xi_{LZ} = \frac{1}{V} \left(-\sin \delta_L (\dot{y}_W - V \dot{\varphi}_W + r_L \dot{\phi}_W) + \cos \delta_L (\dot{z}_W + a \dot{\phi}_W) \right) \quad (A . 43)$$

$$\xi_{LSP} = \frac{1}{V} \left(-\sin \delta_L (\dot{\alpha} + \dot{\beta}) + \cos \delta_L \left(\dot{\varphi}_W - \frac{V}{R} \right) \right) \quad (A . 44)$$

$$\xi_{RX} = \frac{1}{V} \left(V \left(1 - \frac{a}{R} - \frac{r_R}{r_0} \right) + a \dot{\varphi}_W - r_R \dot{\beta} \right) \quad (A . 45)$$

$$\xi_{RY} = \frac{1}{V} \left(\cos \delta_R (\dot{y}_W - V \dot{\varphi}_W + r_R \dot{\phi}_W) + \sin \delta_R (a \dot{\phi}_W) \right) \quad (A . 46)$$

$$\xi_{RZ} = \frac{1}{V} (-\sin \delta_R (\dot{y}_W - V\dot{\psi}_W + r_R \dot{\phi}_W) + \cos \delta_R (\dot{z}_W + a\dot{\phi}_W)) \quad (A . 47)$$

$$\xi_{RSP} = \frac{1}{V} (\sin \delta_R (\dot{\alpha} + \dot{\beta}) + \cos \delta_R (\dot{\psi}_W - \frac{V}{R})) \quad (A . 48)$$

Assuming no wheel lift, the vertical creepages are zero.

Substitution of equations A.43 and A.47 into A.42 and A.46

gives new expressions for the lateral creepages.

$$\xi_{LY} = \sec \delta_L (\dot{y}_W - V\dot{\psi}_W + r_L \dot{\phi}_W) \quad (A . 49)$$

$$\xi_{RY} = \sec \delta_R (\dot{y}_W - V\dot{\psi}_W + r_R \dot{\phi}_W) \quad (A . 50)$$

APPENDIX B

DERIVATION OF THE EQUATIONS OF MOTION FOR THE
FREIGHT CAR MODELB.1 INTRODUCTION

This section contains the derivations of the equations of motion for a freight car moving along curved track with varying radius and constant forward speed. Schematics of the complete model showing the degrees of freedom and dimensions are shown in Figures 2.5-8. The complete set of equations are listed in section B.6.

The model is comprised of two trucks, with two wheelsets each, supporting a carbody. Each wheelset has two degrees of freedom, lateral and yaw, and an additional state to describe the spin perturbation rate. The truck has three degrees of freedom, lateral, yaw and warp. Warp is defined as the relative yaw of the bolster with respect to the sideframes. This motion causes the sideframes to rotate about the truck centerline and assume a skewed parallelogram shape. The carbody has three degrees of freedom, lateral, yaw and roll. Since the centerplate restricts the lateral and roll motion of the bolster relative to the carbody, the bolster is included in the carbody lateral and roll equations. The truck components and the carbody are assumed to be rigid bodies.

The equations of motion for a single wheelset, derived in Appendix A, are modified to include longitudinal and lateral suspension elements and wheelset interconnections. The front truck and carbody equations are derived explicitly. The front truck equations are modified to describe the rear truck

The degrees of freedom include:

- y_{W1} - lateral excursion of lead wheelset of lead truck relative to track centerline
- ψ_{W1} - angle of attack of lead wheelset of the lead truck
- $\dot{\beta}_1$ - spin perturbation rate of lead wheelset of lead truck
- y_{W2} - lateral excursion of trailing wheelset of lead truck relative to track centerline
- ψ_{W2} - angle of attack of trailing wheelset of the lead truck
- $\dot{\beta}_2$ - spin perturbation rate of trailing wheelset of lead truck
- y_{W3} - lateral excursion of lead wheelset of trailing truck relative to track centerline
- ψ_{W3} - angle of attack of lead wheelset of the trailing truck
- $\dot{\beta}_3$ - spin perturbation rate of trailing wheelset of lead truck
- y_{W4} - lateral excursion of trailing wheelset of trailing truck relative to track centerline
- ψ_{W4} - angle of attack of trailing wheelset of the trailing truck
- $\dot{\beta}_4$ - spin perturbation rate of trailing wheelset of trailing truck

- Y_{T1} - lateral excursion of lead truck relative to the truck reference position (centered over the track at lead and trailing wheelset connection points)
- ψ_{T1} - yaw angle of lead truck with respect to radial line passing half way between lead and trailing wheelsets of truck
- θ_{W1} - warp angle of lead truck
- Y_{T2} - lateral excursion of trailing truck relative to the truck reference position (centered over the track at lead and trailing wheelset connection points)
- ψ_{T2} - yaw angle of trailing truck with respect to radial line passing half way between lead and trailing wheelsets of truck
- θ_{W2} - warp angle of trailing truck
- Y_C - lateral excursion of the carbody relative to track centerline
- ϕ_C - roll angle of carbody
- ψ_C - yaw angle of the carbody

B.2 AXIS SYSTEMS

Four moving axis systems defined in Figure B.1 are used to describe the motion of the vehicle. As in section A.2, a track reference frame is constructed to describe the inertial acceleration of the vehicle. A set of \hat{i}_S , \hat{j}_S and \hat{k}_S axes are fixed to the center of gravity of the sideframes. These axes translate, yaw and roll with the sideframes. The sideframe roll angle is assumed to be the average of its wheelset's roll angles. For small angles, the sideframe axis system is related to the track reference axis system by the relationship

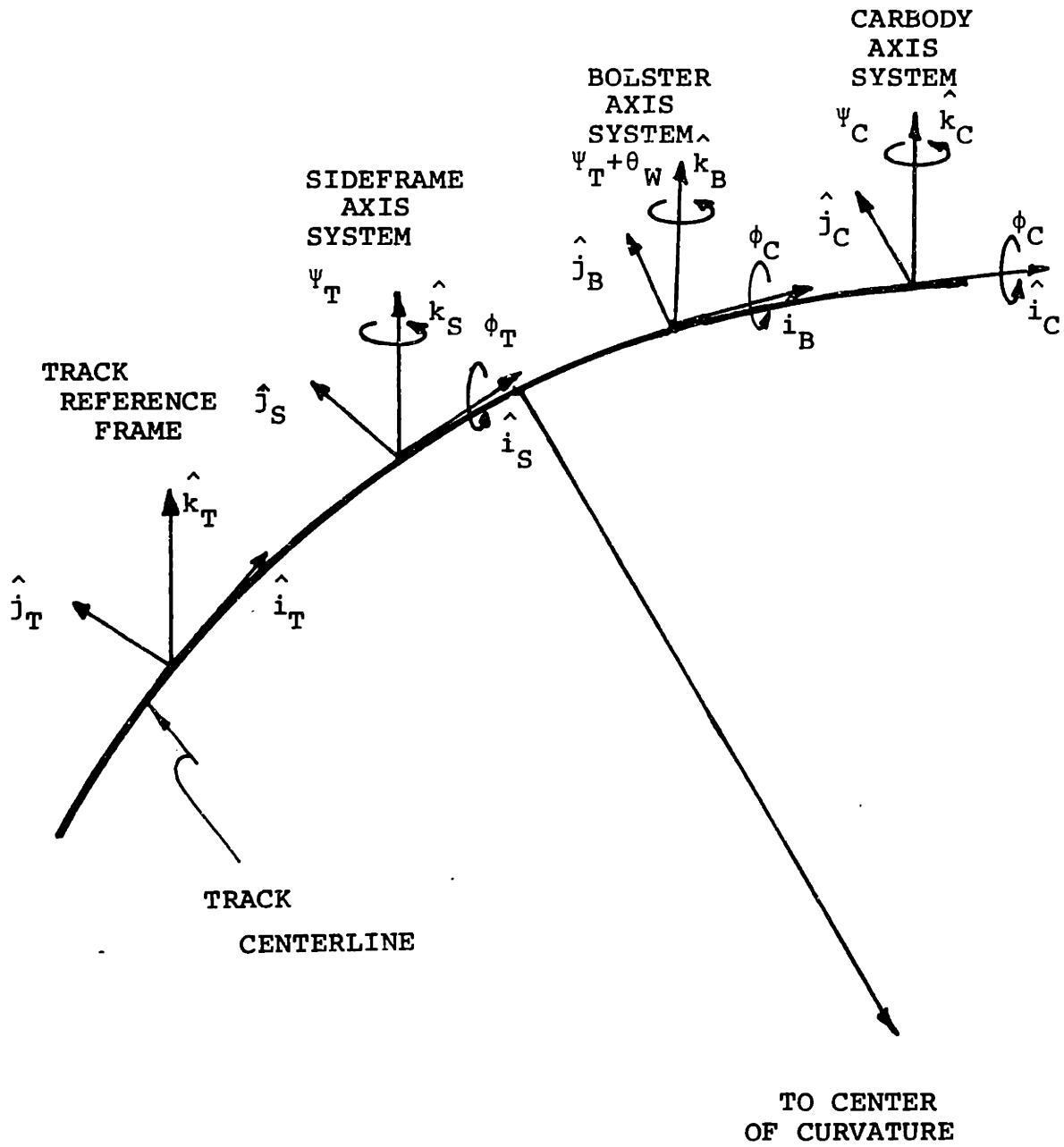


FIGURE B.1 DEFINITION OF COORDINATE SYSTEMS

$$\begin{bmatrix} \hat{i}_S \\ \hat{j}_S \\ \hat{k}_S \end{bmatrix} = \begin{bmatrix} 1 & \psi_T & 0 \\ -\psi_T & 1 & \frac{1}{2}(\phi_{W1} + \phi_{W2}) \\ 0 & -\frac{1}{2}(\phi_{W1} + \phi_{W2}) & 1 \end{bmatrix} \begin{bmatrix} \hat{i}_T \\ \hat{j}_T \\ \hat{k}_T \end{bmatrix} \quad (B.1)$$

The \hat{i}_B , \hat{j}_B and \hat{k}_B axes are fixed to the bolster center of gravity. This axes system warps and yaws but does not roll with the bolster since the bolster rolls about the carbody hinge point.

$$\begin{bmatrix} \hat{i}_B \\ \hat{j}_B \\ \hat{k}_B \end{bmatrix} = \begin{bmatrix} 1 & (\psi_T + \theta_W) & 0 \\ -(\psi_T + \theta_W) & 1 & 0 \\ 0 & 0 & 1 \end{bmatrix} \begin{bmatrix} \hat{i}_T \\ \hat{j}_T \\ \hat{k}_T \end{bmatrix} \quad (B.2)$$

The \hat{i}_C , \hat{j}_C and \hat{k}_C axes are constructed at the hinge point of the carbody. The hinge point is the point about which the carbody rotates. It is not necessarily the carbody center of gravity. The equations of motion of the carbody are derived about the hinge point. The C-axis system translates, yaws and rolls with the carbody. For small angles, the carbody axes are defined by

$$\begin{bmatrix} \hat{i}_C \\ \hat{j}_C \\ \hat{k}_C \end{bmatrix} = \begin{bmatrix} 1 & \psi_C & 0 \\ -\psi_C & 1 & \phi_C \\ 0 & -\phi_C & 1 \end{bmatrix} \begin{bmatrix} \hat{i}_T \\ \hat{j}_T \\ \hat{k}_T \end{bmatrix} \quad (B . 3)$$

B.3 ACCELERATION

The inertial accelerations of the sideframe, bolster and carbody are defined by the expression

$$\bar{a} = \bar{a}_T + \dot{\bar{\omega}}_T \times \bar{R} + \bar{\omega}_T \times (\bar{\omega}_T \times \bar{R}) + 2 \bar{\omega}_T \times \dot{\bar{R}} + \ddot{\bar{R}} \quad (B . 4)$$

where the track reference frame acceleration and angular velocity are given by equation A.2 and \bar{R} is the relative displacement of the center of gravity from the track reference frame.

B.3.1 SIDEFAME ACCELERATION

The displacements of the right and left sideframe center of gravity relative to the track are given by

$$\bar{R}_{SR,SL} = x_{SR,SL} \hat{i}_T + y_T \hat{j}_T + z_{SR,SL} \hat{k}_T \quad (B . 5)$$

Since there is no vertical or roll motion of the sideframes relative to the wheelsets, the vertical displacement of the sideframes can be expressed in terms of wheelset rollangles.

Assuming no wheel lift

$$z_{RS,LS} = \frac{1}{2} d (\phi_{W1} + \phi_{W2}) + h_S + r_0 \quad (B.6)$$

Because the sideframes are assumed to always form a parallelogram, the longitudinal motions of the sideframes are constrained by the expression

$$-x_{RS} = x_{LS} = -d (\dot{\nu}_{T1} + \dot{\theta}_{W1}) \quad (B.7)$$

The displacement of the sideframes may be written as

$$\begin{aligned} \bar{R}_{SR,SL} = & (\pm d (\dot{\nu}_{T1} + \dot{\theta}_{W1})) \hat{i}_T + y_T \hat{j}_T \\ & + \left(\frac{1}{2} (\phi_{W1} + \phi_{W2}) + r_0 + h_S \right) \hat{k}_T \end{aligned} \quad (B.8)$$

Substitution into equation B.4 gives the acceleration of the right and left sideframes.

$$\begin{aligned} \bar{a}_{SR,SL} = & (\pm d (\ddot{\nu}_{T1} + \ddot{\theta}_{W1})) \hat{i}_T \\ & + \left(\ddot{y}_T - \frac{v^2}{R} - (r_0 + h_S) \ddot{\phi}_{SE} \right) \hat{j}_T \\ & + \left(\frac{1}{2} d (\ddot{\phi}_{W1} + \ddot{\phi}_{W2}) + a \ddot{\phi}_{SE} + \frac{v^2}{R} \phi_{SE} \right) \hat{k}_T \end{aligned} \quad (B.9)$$

B.3.2 ACCELERATION OF THE BOLSTER CENTER OF GRAVITY

Since the bolsters translate with the carbody, the displacement of the front bolster relative to the track reference frame is given by

$$\bar{R}_B = (y_C + h_T \phi_C - L \nu_C) \hat{j}_T + (h_B + r_0) \hat{k}_T \quad (B.10)$$

By substituting this expression into equation B.4, the bolster acceleration is obtained.

$$\begin{aligned} \bar{a}_B = & \left(\ddot{y}_C + h_T \ddot{\phi}_C - \frac{v^2}{R} - (r_0 + h_B) \ddot{\phi}_{SE} \right) \hat{j}_T \quad (B . 11) \\ & + \left(a_{\phi_{SE}} + \frac{v^2}{R} \phi_{SE} \right) \hat{k}_T \end{aligned}$$

B.3.3 ACCELERATION OF THE CARBODY

The displacement of the carbody center of gravity relative to the track reference frame is given by

$$\bar{r}_C = (y_C + (h_T - h_C) \phi_C) \hat{j}_T + (r_0 + h_B + h_C) \hat{k}_T \quad (B . 12)$$

Substitution into equation B.4 gives the carbody acceleration.

$$\begin{aligned} \bar{a}_C = & \left(\ddot{y}_C + (h_T - h_C) \ddot{\phi}_C - \frac{v^2}{R} - (r_0 + h_C + h_B) \ddot{\phi}_{SE} \right) \hat{j}_T \quad (B . 13) \\ & + \left(a_{\phi_{SE}} + \frac{v^2}{R} \phi_{SE} \right) \hat{k}_T \end{aligned}$$

B.4 ANGULAR MOMENTUM

B.4.1 SIDEFAME

The angular velocity of the sideframes of the front truck is defined by

$$\bar{\omega}_S = \dot{\phi}_{SE} \hat{i}_I - \frac{v}{R} \hat{k}_I + \frac{1}{2} (\dot{\phi}_{W1} + \dot{\phi}_{W2}) \hat{i}_S + \dot{\psi}_T \hat{k}_S \quad (B . 14)$$

Transformations and small angle approximations reduce this expression to

$$\bar{\omega}_S = \omega_{SX} \hat{i}_S + \omega_{SY} \hat{j}_S + \omega_{SZ} \hat{k}_S \quad (B . 15)$$

where

$$\omega_{SX} = \dot{\phi}_{SE} + \frac{1}{2}(\dot{\phi}_{W1} + \dot{\phi}_{W2})$$

$$\omega_{SY} = -\dot{\phi}_{SE} \frac{V}{R}$$

$$\omega_{SZ} = \dot{\psi}_T - \frac{V}{R}$$

The time rate of change of the angular momentum of the sideframe center of gravity is defined by

$$\frac{D \bar{H}_S}{D t} = \frac{d \bar{H}_S}{d t} + \bar{\omega}_S \times \bar{H}_S \quad (B . 16)$$

where

$$\bar{H}_S = I_{SX} \omega_{SX} \hat{i}_S + I_{SY} \omega_{SY} \hat{j}_S + I_{SZ} \omega_{SZ} \hat{k}_S$$

Substitution of the appropriate terms into equation B.16 yields the following expression

$$\begin{aligned} \frac{D \bar{H}_S}{D t} = & I_{SX} (\ddot{\phi}_{SE} + \frac{1}{2}(\ddot{\phi}_{W1} + \ddot{\phi}_{W2})) \hat{i}_S \\ & + I_{SZ} (\ddot{\psi}_{T1} - V \frac{d}{dt}(\frac{1}{R})) \hat{k}_S \end{aligned} \quad (B . 17)$$

B.4.2 BOLSTER

Since the bolster is assumed to yaw with the truck and roll with the carbody, its angular velocity can be described by

$$\bar{\omega}_B = \omega_{BX} \hat{i}_C + \omega_{BY} \hat{j}_B + \omega_{BZ} \hat{k}_B \quad (B . 18)$$

where

$$\omega_{BX} = \dot{\phi}_{SE} + \dot{\phi}_C$$

$$\omega_{BY} = -\frac{V}{R} \dot{\phi}_{SE}$$

$$\omega_{BZ} = \dot{\psi}_{T1} + \dot{\phi}_{W1} - \frac{V}{R}$$

The yaw component of the rotational equation about the bolster center of gravity is defined by

$$\frac{D \bar{H}_B}{D t} \cdot \hat{k}_B = I_{BZ} (\ddot{\psi}_{T1} + \ddot{\theta}_{W1}) \quad (B . 19)$$

The roll component of the rotational equation about the carbody hinge point is defined by

$$\begin{aligned} \frac{D \bar{H}_B}{D t} \cdot \hat{i}_C = & I_{BX} (\ddot{\phi}_{SE} + \ddot{\phi}_C) \\ & + m_b h_T (\ddot{y}_C + h_T \ddot{\phi}_C \frac{V^2}{R} + (r_0 + h_S) \ddot{\phi}_{SE}) \end{aligned} \quad (B . 20)$$

B.4.3 CARBODY

The angular velocity of the carbody is described by the expression

$$\bar{\omega}_C = \dot{\phi}_{SE} \hat{i}_I - \frac{V}{R} \hat{k}_I + \dot{\phi}_C \hat{i}_C + \dot{\psi}_C \hat{k}_C \quad (B . 21)$$

In carbody coordinates, this expression reduces to

$$\bar{\omega}_C = \omega_{CX} \hat{i}_C + \omega_{CZ} \hat{k}_C \quad (B . 22)$$

$$\text{where } \omega_{CX} = \dot{\phi}_{SE} + \dot{\phi}_C$$

$$\omega_{CZ} = -\frac{V}{R} + \dot{\psi}_C$$

The time rate of change of the angular momentum of the carbody about its hinge point is defined by

$$\frac{D \bar{H}_C}{D t} = \frac{D \bar{H}_O}{D t} + m_C \bar{R}_O \times \bar{a}_C \quad (B . 23)$$

where

$$\begin{aligned} \frac{D \bar{H}_0}{D t} &= I_{CX} \dot{\omega}_{CX} \hat{i}_C \\ &+ I_{CX} \omega_{CX} \omega_{CZ} - I_{CZ} \omega_{CX} \omega_{CZ} \hat{j}_C \\ &+ I_{CZ} \dot{\omega}_{CZ} \hat{k}_C \\ \bar{R}_0 &= (h_C - h_T) \hat{k}_C \\ \bar{a}_0 &= \left(\ddot{y}_C + (h_T - h_C) \ddot{\phi}_C - \frac{V^2}{R} \right) \hat{j}_C \end{aligned}$$

Substitution reduces this expression to

$$\begin{aligned} \frac{D \bar{H}_C}{D t} &= \left(I_{CX} (\ddot{\phi}_{SE} + \ddot{\phi}_C) + m_C (h_T - h_C) (\ddot{y}_C + (h_T - h_C) \ddot{\phi}_C \right. \\ &\quad \left. - \frac{V^2}{R} - (r_0 + h_B + h_C) \ddot{\phi}_{SE} \right) \hat{i}_C \\ &+ (I_{CZ} - I_{CX}) (\dot{\phi}_{SE} + \dot{\phi}_C) \frac{V}{R} \hat{j}_C \\ &+ I_{CZ} \left(\ddot{y}_C - V \frac{d}{dt} \left(\frac{1}{R} \right) \right) \hat{k}_C \end{aligned} \quad (B . 24)$$

B.5 FORCES AND MOMENTS

Free body diagrams for the wheelsets, sideframes and bolster of the front truck and the carbody are shown in Figures B.2-4. The equations of motion for each rigid body are determined from these.

B.5.1 ROLLER BEARING CONNECTIONS

The sideframe/wheelset bearing connections are modelled as parallel combinations of linear springs and viscous dampers in the longitudinal and lateral directions. The longitudinal

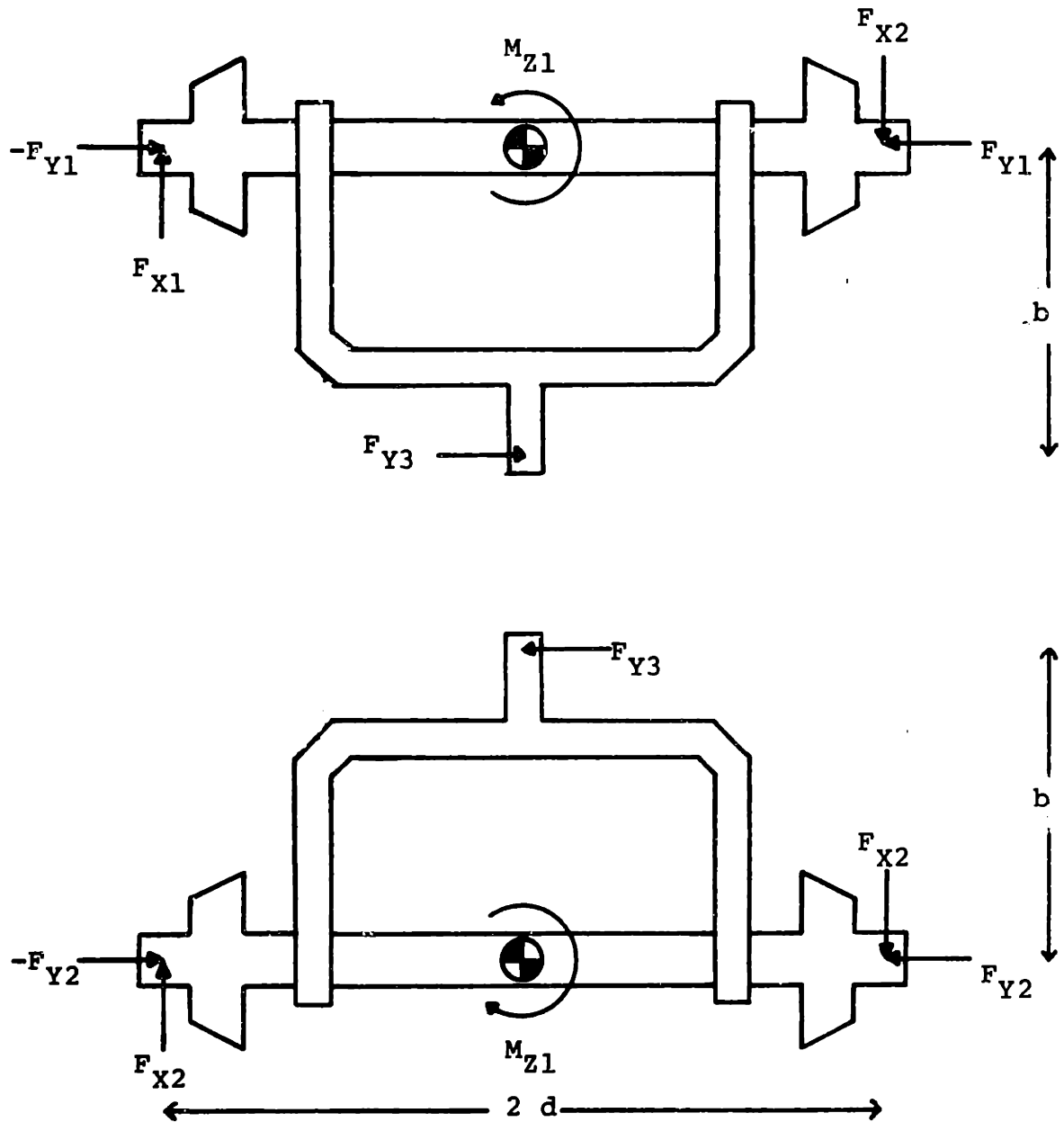


FIGURE B.2 FREEBODY DIAGRAM OF WHEELSET SUSPENSION FORCES

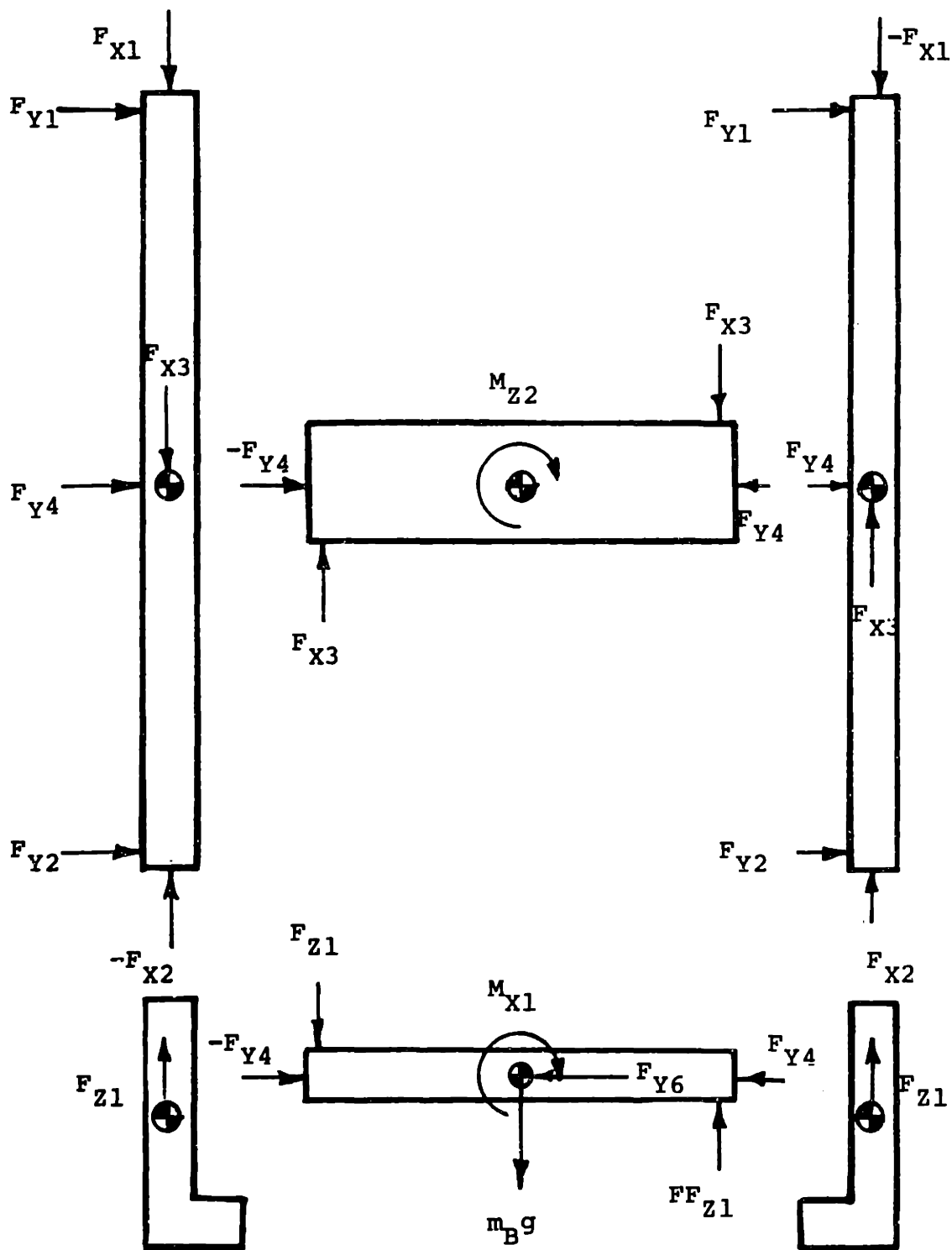


FIGURE B.3 FREEBODY DIAGRAM OF SIDEFAMES ANL BOLSTER

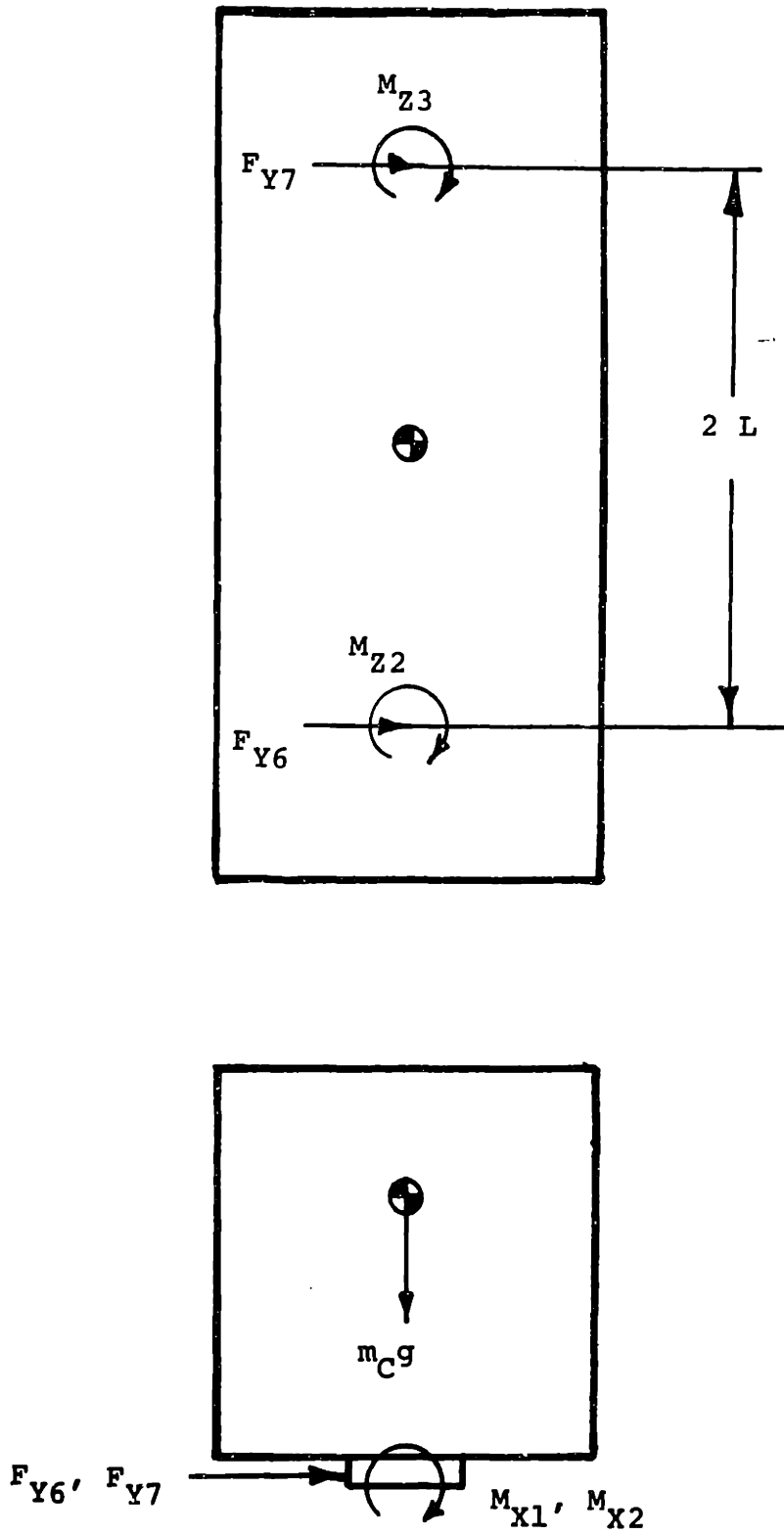


FIGURE B.4 FREEBODY DIAGRAM OF THE CARBODY

forces exerted by the front and rear wheelsets on the sideframes are

$$F_{X1} = d_{PX} \dot{d}(\dot{\psi}_{W1} - \dot{\psi}_{T1} - \dot{\theta}_{W1}) + k_{PX} d(\psi_{W1} - \psi_{T1} - \theta_{W1}) \quad (B . 25)$$

and

$$F_{X2} = d_{PX} \dot{d}(\dot{\psi}_{W2} - \dot{\psi}_{T1} - \dot{\theta}_{W1}) + k_{PX} d(\psi_{W2} - \psi_{T1} - \theta_{W1}) \quad (B . 26)$$

The lateral forces exerted by the front and rear wheelsets on the sideframes are

$$F_{Y1} = -d_{PY} \dot{d}(\dot{\psi}_{W1} - \dot{\psi}_{T1} - b\dot{\psi}_{T1}) - k_{PY} (y_{W1} - y_{T1} - b\psi_{T1}) \quad (B . 27)$$

and

$$F_{Y2} = -d_{PY} \dot{d}(\dot{\psi}_{W2} - \dot{\psi}_{T1} - b\dot{\psi}_{T1}) - k_{PY} (y_{W2} - y_{T1} - b\psi_{T1}) \quad (B . 28)$$

B.5.2. INTERWHEELSET CONNECTIONS

The radial connections of each wheelset pair are modelled by a lateral and torsional spring pair connecting the two wheelsets at their midpoints. The forces and moments are described by

$$F_{Y3} = k_S (y_{W1} - y_{W2} - b(\psi_{W1} + \psi_{W2}) + 2b\psi_{T1}) \quad (B . 29)$$

and

$$M_{Z1} = k_B (\psi_{W2} - \psi_{W1} + 2\frac{b}{R}) \quad (B . 30)$$

B.5.3 SECONDARY SUSPENSION

The suspension between the sideframes, bolster and carbody consists of vertical and lateral linear springs and coulomb friction elements in parallel at each bolster/sideframe interface. Additionally, there is a torsional spring and damper combination at each bolster/sideframe connection which resists warp motion. The lateral forces exerted by the bolster and carbody on the sideframe are

$$F_{Y4} = k_{SY}(y_{T1} - y_C - L\dot{v}_C - h_T\dot{\phi}_C - \frac{1}{2}(h_B - h_S)(\dot{\phi}_{W1} + \dot{\phi}_{W2})) \quad (B.31)$$

$$+ F_{Y0} \operatorname{sgn}(\dot{y}_{T1} - \dot{y}_C - L\dot{v}_C - h_T\dot{\phi}_C - \frac{1}{2}(h_B - h_S)(\dot{\phi}_{W1} + \dot{\phi}_{W2}))$$

and

$$F_{Y5} = k_{SY}(y_{T2} - y_C + L\dot{v}_C - h_T\dot{\phi}_C - \frac{1}{2}(h_B - h_S)(\dot{\phi}_{W3} + \dot{\phi}_{W4})) \quad (B.32)$$

$$+ F_{Y0} \operatorname{sgn}(\dot{y}_{T2} - \dot{y}_C + L\dot{v}_C - h_T\dot{\phi}_C - \frac{1}{2}(h_B - h_S)(\dot{\phi}_{W3} + \dot{\phi}_{W4}))$$

The vertical forces exerted on the carbody and bolster by the sideframes are

$$F_{Z1} = k_{SZ}d(\dot{\phi}_C - \frac{1}{2}(\dot{\phi}_{W1} + \dot{\phi}_{W2})) \quad (B.33)$$

$$+ F_{Z0} \operatorname{sgn} d(\dot{\phi}_C - \frac{1}{2}(\dot{\phi}_{W1} + \dot{\phi}_{W2}))$$

and

$$F_{Z2} = k_{SZ}d(\dot{\phi}_C - \frac{1}{2}(\dot{\phi}_{W3} + \dot{\phi}_{W4})) \quad (B.34)$$

$$+ F_{Z0} \operatorname{sgn} d(\dot{\phi}_C - \frac{1}{2}(\dot{\phi}_{W3} + \dot{\phi}_{W4}))$$

The moment exerted on the bolster resisting warp is defined by

$$M_{Z2} = k_W \theta_{W1} + T_{W0} \operatorname{sgn}(\dot{\theta}_{W1}) \quad (B.35)$$

B.5.4 CENTERPLATE

The carbody/bolster centerplate connection is modelled by a torsional linear spring and coulomb friction element in parallel which resists relative yaw motion. The yaw moments acting on the front and rear bolster due to the carbody are

$$M_{Z3} = T_{CP0} \operatorname{sgn}(\dot{\psi}_C + L \frac{d}{dt}(\frac{1}{R}) - \dot{\psi}_{T1} - \dot{\theta}_{W1}) \quad (B.36)$$

and

$$M_{Z4} = T_{CP0} \operatorname{sgn}(\dot{\psi}_C - L \frac{d}{dt}(\frac{1}{R}) - \dot{\psi}_{T2} - \dot{\theta}_{W2}) \quad (B.37)$$

B.6 EQUATIONS OF MOTION

B.6.1 WHEELSET

The equations of motion for a typical wheelset are developed in Appendix A. Modifications have been made to include the suspension forces and moments developed in the previous section. The lateral equation for the *i*th wheelset is given by

$$\begin{aligned} m_W (\ddot{y}_{Wi} - r_0 \ddot{\theta}_{SE}) &= (m_W + \frac{1}{2}m_b + m_s + \frac{1}{4}m_c) g (\phi_d - \phi_{Wi}) \\ &+ F_{RYi} + F_{LYi} + N_{LYi} + N_{RYi} \\ &+ F_{SUSP_{Yi}} \end{aligned} \quad (B.38)$$

$$\begin{aligned}
\text{where } F_{\text{SUSP}_{Y1}} &= -2k_{PY}(y_{W1} - y_{T1} - b_{\psi_{T1}} - h_S \phi_{W1}) \\
&\quad - 2d_{PY}(\dot{y}_{W1} - \dot{y}_{T1} - \dot{b}_{\psi_{T1}} - \dot{h}_S \dot{\phi}_{W1}) \\
&\quad - k_S(y_{W1} - b_{\psi_{W1}} - y_{W2} - b_{\psi_{W2}}) \\
F_{\text{SUSP}_{Y2}} &= -2k_{PY}(y_{W2} - y_{T1} + b_{\psi_{T1}} - h_S \phi_{W2}) \\
&\quad - 2d_{PY}(\dot{y}_{W2} - \dot{y}_{T1} + \dot{b}_{\psi_{T1}} - \dot{h}_S \dot{\phi}_{W2}) \\
&\quad + k_S(y_{W1} - b_{\psi_{W1}} - y_{W2} - b_{\psi_{W2}}) \\
F_{\text{SUSP}_{Y3}} &= -2k_{PY}(y_{W3} - y_{T2} - b_{\psi_{T2}} - h_S \phi_{W3}) \\
&\quad - 2d_{PY}(\dot{y}_{W3} - \dot{y}_{T2} - \dot{b}_{\psi_{T2}} - \dot{h}_S \dot{\phi}_{W3}) \\
&\quad - k_S(y_{W3} - b_{\psi_{W3}} - y_{W4} - b_{\psi_{W4}}) \\
F_{\text{SUSP}_{Y4}} &= -2k_{PY}(y_{W4} - y_{T2} + b_{\psi_{T2}} - h_S \phi_{W4}) \\
&\quad - 2d_{PY}(\dot{y}_{W4} - \dot{y}_{T2} + \dot{b}_{\psi_{T2}} - \dot{h}_S \dot{\phi}_{W4}) \\
&\quad + k_S(y_{W3} - b_{\psi_{W3}} - y_{W4} - b_{\psi_{W4}})
\end{aligned}$$

The yaw equation for the i th wheelset is given by

$$\begin{aligned}
I_{WZ}(\ddot{\psi}_{Wi} - v \frac{d}{dt}(\frac{1}{R})) &= I_{WY}(\alpha + \beta_i)(\dot{\phi}_{Wi} + \dot{\phi}_{SE}) \quad (B.39) \\
&\quad + a(F_{RXi} - F_{LXi}) + a_{\psi_W}(F_{RYi} - F_{LYi} + N_{RYi} - N_{LYi}) \\
&\quad + M_{LZi} + M_{RZi} + M_{\text{SUSP}_{Zi}}
\end{aligned}$$

$$\begin{aligned}
\text{where } M_{\text{SUSP}_{Z1}} &= bk_S(y_{W1} - b_{\psi_{W1}} - y_{W2} - b_{\psi_{W2}}) - k_B(\psi_{W1} - \psi_{W2}) \\
&\quad - 2d^2 k_{PX}(\psi_{W1} - \psi_{T1} - \theta_{W1}) \\
&\quad - 2d^2 d_{PX}(\dot{\psi}_{W1} - \dot{\psi}_{T1} - \dot{\theta}_{W1}) \\
M_{\text{SUSP}_{Z2}} &= bk_S(y_{W1} - b_{\psi_{W1}} - y_{W2} - b_{\psi_{W2}}) - k_B(\psi_{W2} - \psi_{W1}) \\
&\quad - 2d^2 k_{PX}(\psi_{W2} - \psi_{T1} - \theta_{W1}) \\
&\quad - 2d^2 d_{PX}(\dot{\psi}_{W2} - \dot{\psi}_{T1} - \dot{\theta}_{W1})
\end{aligned}$$

$$\begin{aligned}
 M_{SUSP_{Z3}} &= bk_S(y_{W3} - b\psi_{W3} - y_{W4} - b\psi_{W4}) - k_B(\psi_{W3} - \psi_{W4}) \\
 &\quad - 2d^2 k_{PX}(\psi_{W3} - \psi_{T2} - \theta_{W2}) \\
 &\quad - 2d^2 d_{PX}(\dot{\psi}_{W3} - \dot{\psi}_{T2} - \dot{\theta}_{W2}) \\
 M_{SUSP_{Z4}} &= bk_S(y_{W3} - b\psi_{W3} - y_{W4} - b\psi_{W4}) - k_B(\psi_{W4} - \psi_{W3}) \\
 &\quad - 2d^2 k_{PX}(\psi_{W4} - \psi_{T2} - \theta_{W2}) \\
 &\quad - 2d^2 d_{PX}(\dot{\psi}_{W4} - \dot{\psi}_{T2} - \dot{\theta}_{W2})
 \end{aligned}$$

The spin equation for the i th wheelset is given by

$$I_{WY}^{\beta_i} \ddot{\beta}_i = -r_R^F R X_i - r_L^F L X_i \quad (B . 40)$$

B.6.2 TRUCK FRAME

The equations of motion for the lead truck are derived in two parts. The equations of motion for the sideframes and the bolster yaw equation are initially independently derived. The physical constraints are then incorporated to form the combined truck equations. The derivations for the trailing truck follow in a similar manner.

The summation of the forces and moments of the leading truck frame freebody diagrams of Figure B.3 yield the following equations.

Lateral Motion of Sideframes:

$$2m_S \left(\ddot{y}_{T1} - \frac{V^2}{R} - (r_0 + h_S) \ddot{\phi}_{SE} \right) = -2F_{Y1} - 2F_{Y4} - 2m_S g \left(\phi_{SE} + \frac{1}{2}(\phi_{W1} + \phi_{W2}) \right) \quad (B . 41)$$

Longitudinal Motion of the Sideframes:

$$2m_S d(\ddot{v}_{T1} + \ddot{\theta}_{W1}) = 2F_{X1} + 2F_{X2} + 2F_{X3} \quad (B . 42)$$

Yaw Motion of the Sideframes:

$$2I_{SZ} (\ddot{\theta}_{W1} - v \frac{d}{dt}(\frac{1}{R})) = M_{Z2} + 2b(F_{Y2} - F_{Y1}) \quad (B . 43)$$

Yaw Motion of the Bolster:

$$I_{BZ} (\ddot{v}_{T1} + \ddot{\theta}_{W1} - v \frac{d}{dt}(\frac{1}{R})) = -M_{Z2} - M_{Z3} - 2dF_{X3} \quad (B . 44)$$

Since the sideframes translate laterally independent of the bolster, the truck lateral equation is described solely by B.41. The bolster is lumped with the sideframes to describe the yaw and warp of the truck assembly. The warp equation is obtained by adding the bolster yaw equation to the sideframe longitudinal equation times half the distance between the sideframes. The yaw motion is described by adding the truck warp equation to the sideframe yaw equation.

Lateral Equation for Front Truck

$$\begin{aligned} 2m_S (\ddot{y}_{T1} - g(\phi_d + \frac{1}{2}(\phi_{W1} + \phi_{W2}))) - (r_0 + h_S) \ddot{\phi}_{SE} = \\ 2k_{PY} (y_{W1} + y_{W2} - 2y_{T1} - 2b\dot{v}_{T1}) \\ + 2d_{PY} (\dot{y}_{W1} + \dot{y}_{W2} - 2\dot{y}_{T1} - 2b\dot{v}_{T1}) \quad (B . 45) \\ - 2k_{SY} (y_{T1} - y_C - h_T \phi_C + \frac{1}{2}(\phi_{W1} + \phi_{W2})) \\ - 2F_{Y0} \operatorname{sgn}(y_{T1} - y_C - h_T \phi_C + \frac{1}{2}(\phi_{W1} + \phi_{W2})) \end{aligned}$$

Yaw Equation for the Front Truck

$$\begin{aligned}
(2I_{SZ} + 2m_S d^2 + I_{BZ}) (\ddot{\varphi}_{T1} - v \frac{d}{dt} (\frac{1}{R})) + (2m_S d^2 + I_{BZ}) \ddot{\theta}_{W1} = \\
2bk_{PY}(y_{W1} - y_{W2}) + 2bd_{PY}(\dot{y}_{W1} - \dot{y}_{W2}) \\
+ 2d^2 k_{PX}(\varphi_{W1} + \varphi_{W2} - 2\varphi_{T1} - 2\theta_{W1}) \\
+ 2d^2 d_{PX}(\dot{\varphi}_{W1} + \dot{\varphi}_{W2} - 2\dot{\varphi}_{T1} - 2\dot{\theta}_{W1}) \\
- T_{CP0} \operatorname{sgn}(\dot{\varphi}_{T1} + \dot{\theta}_{W1})
\end{aligned} \tag{B.46}$$

Warp Equation for the Front Truck

$$\begin{aligned}
(2m_S d^2 + I_{BZ}) (\ddot{\varphi}_{T1} + \ddot{\theta}_{W1}) - I_{BZ} v \frac{d}{dt} (\frac{1}{R}) = \\
2d^2 k_{PX}(\varphi_{W1} + \varphi_{W2} - 2\varphi_{T1} - 2\theta_{W1}) \\
+ 2d^2 d_{PX}(\dot{\varphi}_{W1} + \dot{\varphi}_{W2} - 2\dot{\varphi}_{T1} - 2\dot{\theta}_{W1}) \\
- k_W \theta_{W1} - T_{W0} \operatorname{sgn}(\dot{\theta}_{W1}) - T_{CP0} \operatorname{sgn}(\dot{\theta}_{W1} + \dot{\varphi}_{T1})
\end{aligned} \tag{B.47}$$

Lateral Equation for the Trailing Truck

$$\begin{aligned}
2m_S (\ddot{y}_{T2} - g(\phi_d + \frac{1}{2}(\phi_{W3} + \phi_{W4}))) - (r_0 + h_S) \ddot{\phi}_{SE} = \\
2k_{PY}(y_{W3} + y_{W4} - 2y_{T2} - 2b\varphi_{T2}) \\
+ 2d_{PY}(\dot{y}_{W3} + \dot{y}_{W4} - 2\dot{y}_{T2} - 2b\dot{\varphi}_{T2}) \\
- 2k_{SY}(y_{T2} - y_C - h_T \phi_C + \frac{1}{2}(\phi_{W3} + \phi_{W4})) \\
- 2F_{Y0} \operatorname{sgn}(y_{T2} - y_C - h_T \phi_C + \frac{1}{2}(\phi_{W3} + \phi_{W4}))
\end{aligned} \tag{B.48}$$

Yaw Equation for the Trailing Truck

$$\begin{aligned}
(2I_{SZ} + 2m_S d^2 + I_{BZ}) (\ddot{\varphi}_{T2} - v \frac{d}{dt} (\frac{1}{R})) + (2m_S d^2 + I_{BZ}) \ddot{\theta}_{W2} = \\
2bk_{PY}(y_{W3} - y_{W4}) + 2bd_{PY}(\dot{y}_{W3} - \dot{y}_{W4}) \\
+ 2d^2 k_{PX}(\varphi_{W3} + \varphi_{W4} - 2\varphi_{T2} - 2\theta_{W2}) \\
+ 2d^2 d_{PX}(\dot{\varphi}_{W3} + \dot{\varphi}_{W4} - 2\dot{\varphi}_{T2} - 2\dot{\theta}_{W2}) \\
+ T_{CP0} \operatorname{sgn}(\dot{\varphi}_{T2} + \dot{\theta}_{W2})
\end{aligned} \tag{B.49}$$

Warp Equation for the Trailing Truck

$$\begin{aligned}
 (2m_S d^2 + I_{BZ}) (\ddot{\psi}_{T2} + \ddot{\theta}_{W2}) - I_{BZ} V \frac{d}{dt} \left(\frac{1}{R} \right) = \\
 2d^2 k_{PX} (\psi_{W3} + \psi_{W4} - 2\psi_{T2} - 2\theta_{W2}) \\
 + 2d^2 d_{PX} (\dot{\psi}_{W3} + \dot{\psi}_{W4} - 2\dot{\psi}_{T2} - 2\dot{\theta}_{W2}) \\
 - k_{W\theta} \theta_{W2} - T_{W0} \operatorname{sgn}(\dot{\theta}_{W2}) - T_{CP0} \operatorname{sgn}(\dot{\theta}_{W2} + \dot{\psi}_{T2})
 \end{aligned} \tag{B.50}$$

B.6.3 CARBODY

Summation of the forces and moments of the freebody diagrams of figures B.3 and B.4 yield the equations of motion for the carbody and the roll and lateral motion of the bolster.

Lateral Motion of the Front Bolster

$$m_B (\ddot{y}_C + h_T \ddot{\phi}_C - \frac{V^2}{R} + L \ddot{\psi}_x - (r_0 + h_B) \ddot{\phi}_{SE}) = 2F_{Y4} + F_{Y6} - m_B g (\phi_C + \phi_{SE}) \tag{B.51}$$

Roll Motion of the Front Bolster

$$\begin{aligned}
 I_{BX} (\ddot{\phi}_{SE} + \ddot{\phi}_C) + m_B h_T (\ddot{y}_C + h_T \ddot{\phi}_C - \frac{V^2}{R} + (r_0 + h_B) \ddot{\phi}_{SE}) = \\
 2dF_{Z1} + M_{X1} - m_B g h_T (\phi_{SE} + \phi_C)
 \end{aligned} \tag{B.52}$$

Lateral Motion of the Rear Bolster

$$m_B (\ddot{y}_C - L \ddot{\psi}_C + h_T \ddot{\phi}_C - \frac{V^2}{R} - (r_0 + h_B) \ddot{\phi}_{SE}) = 2F_{Y5} + F_{Y7} \tag{B.53}$$

Roll Motion of the Rear Bolster

$$\begin{aligned}
 I_{BX} (\ddot{\phi}_{SE} + \ddot{\phi}_C) + m_B h_T (\ddot{y}_C + h_T \ddot{\phi}_C - \frac{V^2}{R} + (r_0 + h_B) \ddot{\phi}_{SE}) = \\
 2dF_{Z2} + M_{X2} - m_B g h_T (\phi_{SE} + \phi_C)
 \end{aligned} \tag{B.54}$$

Lateral Motion of Carbody

$$m_C(\ddot{y}_C + (h_T - h_C)\ddot{\phi}_C \frac{v^2}{R} - (r_0 + h_B + h_C)\ddot{\phi}_{SE}) = -F_{Y6} - F_{Y7} - m_C g(\phi_{SE} + \phi_C) \quad (B.55)$$

Roll Motion of Carbody

$$I_{CX}(\ddot{\phi}_C + \ddot{\phi}_{SE}) + m_C(h_T - h_C)(\ddot{y}_C + (h_T - h_C)\ddot{\phi}_C \frac{v^2}{R} - (r_0 + h_B + h_C)\ddot{\phi}_{SE}) = -M_{X1} - M_{X2} + m_C g h_C(\phi_{SE} + \phi_C) \quad (B.56)$$

Yaw Motion of the Carbody

$$I_{CZ}(\ddot{\psi}_C - v \frac{d}{dt}(\frac{1}{R})) = -M_{Z3} - M_{Z4} + L F_{Y7} - L F_{Y6} \quad (B.57)$$

The lateral forces, F_{Y6} and F_{Y7} , and the roll moments, M_{X1} and M_{X2} , exerted by the bolster on the carbody are defined by equations B.51-54. Substitution of the suspension forces and moments results in the carbody equations.

Lateral Equation for Carbody

$$\begin{aligned} & (m_C + 2m_B)(\ddot{y}_C - g(\phi_d - \phi_C)) + (2m_B h_T + (m_C(h_T - h_C)))\ddot{\phi}_C \\ & - (m_C(r_0 + h_B + h_C) + 2m_B(r_0 + h_B))\ddot{\phi}_{SE} = \quad (B.58) \\ & 2k_{SY}(y_{T1} + y_{T2} - 2y_C - 2h_T\phi_C - \frac{1}{2}(h_B - h_S)(\phi_{W1} + \phi_{W2} + \phi_{W3} + \phi_{W4})) \\ & + 2F_{Y0} \operatorname{sgn}(\dot{y}_{T1} - \dot{y}_C - L\dot{\psi}_C - h_T\dot{\phi}_C - \frac{1}{2}(h_B - h_S)(\dot{\phi}_{W1} + \dot{\phi}_{W2})) \\ & + 2F_{Y0} \operatorname{sgn}(\dot{y}_{T2} - \dot{y}_C + L\dot{\psi}_C - h_T\dot{\phi}_C - \frac{1}{2}(h_B - h_S)(\dot{\phi}_{W3} + \dot{\phi}_{W4})) \end{aligned}$$

Roll Equation for the Carbody

$$\begin{aligned}
& (I_{CX} + 2I_{BX} + 2m_B h_T^2 + m_C (h_T - h_C)^2) \ddot{\phi}_C + (I_{CX} + 2I_{BX} + 2m_B h_T (r_0 + h_B) \\
& \quad + m_C (h_T - h_C) (r_0 + h_B + h_C)) \ddot{\phi}_{SE} + (2m_B h_T + m_C (h_T - h_C)) (\ddot{y}_C - \frac{V^2}{R}) \\
& \quad + (2m_B g h_T - m_C g h_C) (\phi_C + \phi_{SE}) = \\
& 2k_{SY} h_T (y_{T1} + y_{T2} - 2y_C - 2h_T \phi_C - \frac{1}{2}(h_B - h_S) (\phi_{W1} + \phi_{W2} + \phi_{W3} + \phi_{W4})) \\
& \quad + 2h_T F_{Y0} \operatorname{sgn}(\dot{y}_{T1} - \dot{y}_C - L\dot{v}_C - h_T \dot{\phi}_C - \frac{1}{2}(h_B - h_S) (\dot{\phi}_{W1} + \dot{\phi}_{W2})) \\
& \quad + 2h_T F_{Y0} \operatorname{sgn}(\dot{y}_{T2} - \dot{y}_C + L\dot{v}_C - h_T \dot{\phi}_C - \frac{1}{2}(h_B - h_S) (\dot{\phi}_{W1} + \dot{\phi}_{W2})) \quad (B. 59) \\
& \quad - 2d^2 k_{SZ} (2\dot{\phi}_C - \frac{1}{2}(\dot{\phi}_{W1} + \dot{\phi}_{W2} + \dot{\phi}_{W3} + \dot{\phi}_{W4})) \\
& \quad - 2dF_{Z0} \operatorname{sgn} d(\dot{\phi}_C - \frac{1}{2}(\dot{\phi}_{W1} + \dot{\phi}_{W2})) \\
& \quad - 2dF_{Z0} \operatorname{sgn} d(\dot{\phi}_C - \frac{1}{2}(\dot{\phi}_{W3} + \dot{\phi}_{W4}))
\end{aligned}$$

Yaw Equation of the Carbody

$$\begin{aligned}
& (I_{CZ} + 2L^2 m_B) (\ddot{v}_C - v \frac{d}{dt}(\frac{1}{R})) = T_{CP0} \operatorname{sgn}(\dot{v}_C + L \frac{d}{dt}(\frac{1}{R}) - \dot{v}_{T1} - \dot{\theta}_{W1}) \\
& \quad + T_{CP0} \operatorname{sgn}(\dot{v}_C + L \frac{d}{dt}(\frac{1}{R}) - \dot{v}_{T2} - \dot{\theta}_{W2}) \\
& \quad + Lk_{SY} (y_{T1} - y_{T2} - 2L\dot{v}_C - \frac{1}{2}(h_B - h_S) (\dot{\phi}_{W1} + \dot{\phi}_{W2} + \dot{\phi}_{W3} + \dot{\phi}_{W4})) \quad (B. 60) \\
& \quad + LF_{Y0} \operatorname{sgn}(\dot{y}_{T1} - \dot{y}_C - L\dot{v}_C - h_T \dot{\phi}_C - \frac{1}{2}(h_B - h_S) (\dot{\phi}_{W1} + \dot{\phi}_{W2})) \\
& \quad + LF_{Y0} \operatorname{sgn}(\dot{y}_{T2} - \dot{y}_C + L\dot{v}_C - h_T \dot{\phi}_C - \frac{1}{2}(h_B - h_S) (\dot{\phi}_{W3} + \dot{\phi}_{W4}))
\end{aligned}$$


```

C           wheelset connection points)
C   Y(16) = YLT(2) = yaw angle of truck wrt radial line passing half
C           way between lead and trailing wheelsets of truck
C   Y(17) = YLT(3) = warp angle of the truck
C   Y(18) = YLT(4) = lateral velocity of truck
C   Y(19) = YLT(5) = yaw angle rate of truck
C   Y(20) = YLT(6) = warp angle rate of truck
C
C   * Car Body (C.B.)
C
C   Y(21) = YCB(1) = lateral excursion of carbody with respect
C           to track centerline
C   Y(22) = YCB(2) = roll angle of carbody
C   Y(23) = YCB(3) = yaw angle of carbody
C   Y(24) = YCB(4) = lateral velocity of carbody
C   Y(25) = YCB(5) = roll angle rate of carbody
C   Y(26) = YCB(6) = yaw angle rate of carbody
C
C   * Trailing Truck, Leading Wheelset (T.T.L.W.)
C
C   Y(27) = YPTLW(1) = = (same definition as L.T.L.W.)
C           . . .
C   Y(33) = YPTLW(7) = =
C
C   * Trailing Truck, Trailing Wheelset (T.T.T.W.)
C
C   Y(34) = YPTTW(1) = = (same definition as L.T.L.W.)
C           . . .
C   Y(40) = YPTTW(7) = =
C
C   * Trailing Truck (T.T.)
C
C   Y(41) = YPT(1) = = (same definition as L.T.)
C           . . .
C   Y(46) = YPT(6) = =
C
C   COMMON NEWDT, DT,DT1,DT2, FLANGE,N, T, FTIME
C   COMMON/OUTPUT1/IOUPTUT, ICOUNT,JPLT(12), IOUPT,NPTS
C   COMMON/STATES/Y(46),DY(46),YMAX(46),YMIN(46)
C
C   EQUIVALENCE (Y(1),YLT(1)),(DY(1),DYLT(1)),
1       (Y(8),YLT(8)),(DY(8),DYLT(8)),
2       (Y(15),YLT(15)),(DY(15),DYLT(15)),
3       (Y(21),YCB(1)),(DY(21),DYCB(1)),
4       (Y(27),YPTLW(1)),(DY(27),DYPTLW(1)),
5       (Y(34),YPTTW(1)),(DY(34),DYPTTW(1)),
6       (Y(41),YPT(1)),(DY(41),DYPT(1))
C
C   DIMENSION YLT(7),YLT(7),YLT(6),YCB(6),YPTLW(7),YPTTW(7),YPT(6),
1   DYLT(7),DYLT(7),DYLT(6),DYCB(6),DYPTLW(7),DYPTTW(7),DYPT(6)
C   DIMENSION SY(46),YO(46),Y1(46),Y2(46)
C
C   CALL INITIAL
C

```



```

C      NEWDT = -1          FLAGS THE FIRST TIMESTEP
C      NEWDT = 0          FLAGS RUNGE - KUTTA STEPS
C      NEWDT = 1          FLAGS A NEW TIMESTEP
C
C      NEWDT = -1
C
C      CALL EQUATION
20     CONTINUE
C
C      NEWDT = 0
C
C      DO 30 I=1,N
C      SY(I) = Y(I)
C      YO(I) = DY(I)
30     Y(I) = DT*DY(I)/2.0 + Y(I)
C      T = T + DT/2.0
C
C      CALL EQUATION
C
C      DO 40 I=1,N
C      Y1(I) = DY(I)
40     Y(I) = SY(I) + DT*DY(I)/2.0
C
C      CALL EQUATION
C
C      DO 50 I=1,N
C      Y2(I) = DY(I)
50     Y(I) = SY(I) + DT*DY(I)
C      T = T + DT/2.0
C
C      CALL EQUATION
C
C      DO 60 I=1,N
C      PRT1 = 2.0*(Y1(I) + Y2(I))
C      PRT2 = YO(I) + DY(I)
60     Y(I) = SY(I) + (PRT1 + PRT2)*DT/6.0
C      CONTINUE
C
C      SET COUNTERS FOR PRINTING AND PLOTTING
C
C      IF(ICOUNT.NE.IOOUTPUT)GO TO 70
C      NPTS = NPTS + 1
C      ICOUNT = 0
C      IF((NPTS.LT.1).OR.(NPTS.GT.105))GO TO 100
70     ICOUNT = ICOUNT + 1
C
C      NEWDT = 1
C
C      CALL EQUATION
C
C      SAVE MAXIMUM AND MINIMUM
C
C      DO 90 I=1,N
C      IF (Y(I) - YMIN(I).GE.0.0) GO TO 80
C      YMIN(I) = Y(I)

```

```
80     IF (Y(I) - YMAX(I).LE.0.0) GO TO 90
      YMAX(I) = Y(I)
90     CONTINUE
C
C     SAVE STATE ARRAYS IN ARRAYS FOR OUTPUT
C
      IF(IOUTPUT.EQ.ICOUNT)CALL OUTPUT
C
C     TEST FOR COMPLETION
C
      IF((T - FTIME).LT.0.0)GO TO 20
C
      CALL PLOT
      CALL PRINT
C
      STOP
C
C     TERMINATE PROGRAM & PRINT ERROR MESSAGE IF ARRAYS ARE OUT OF BOUND
C
100    WRITE(IOUT,110)NPTS
110    FORMAT(//° NUMBER OF PLOT POINTS (°,I4,°) OUT OF ARRAY RANGE °)
      END
```

C

SUBROUTINE INITIAL

C

INITIALIZES VARIABLES AND ECHOES INPUT DATA

C

COMMON NEWDT, DT, DT1,DT2, FLANGE,N,T, FTIME, ISUSP
COMMON/OUTPUT1/IOOUTPUT, ICOUNT, JPLT(12), IOUT1, NPTS
COMMON/STATES/Y(46), DY(46), YMAX(46), YMIN(46)
COMMON/CONSTANT/VEL, CANTD, G, PI
COMMON/GEOMETRY/A, B, D, L, HS, HB, HC, HT, RO
COMMON/INERTIA/MW, MB, MS, MC, MAPP, WIYY, WIZZ, BIXX, BIZZ,
1 CIXX, CIZZ, SIZZ
COMMON/TRACK/FPHISE, FRHO, DTANGENT, DSPIRAL, DCURVE
COMMON/RAIL/RAILK, RAILB
COMMON/SUSP/KS, KB, KPX, KPY, KSY, KSZ, KCP, KW, DPX, DPY
COMMON/DAMP/DSY, DSZ, DCP, DW
COMMON/COULOMB/FYO, TCP0, TWO, FZO, DEL1, DEL2, DEL3, DEL4
COMMON/CREEP/NO, MU, F110, F120, F330, F220
COMMON/GEOM/NDIM, XWINC, ARG(242), RRDAT(242), RLDAT(242),
1 DRDAT(242), DLDAT(242), PHIDAT(242), DPHI(242),
1 D2PHI(242)

C

INTEGER FRONT, CENTER, BACK

C

REAL MU, MAPP, NO, L, MW, MC, MB, MS, KS, KB, KPX, KPY, KSY,
1 KSZ, KCP, KW

C

CHARACTER*80 RAILFILE, DUMMY, DATE

C

DATA IDAT1, IDAT2, IOUT1/1, 2, 3/
DATA PI, G, T, ZERO, FRONT, CENTER, BACK/3.14156, 32.2, 0.0, 0.0, 1, 2, 3/

C

DIMENSION YLTLW(7), YLTTW(7), YLT(6), YCB(6), YTTLW(7), YTTTW(7), YTT(6),
1 DYTLW(7), DYTTW(7), DYLT(6), DYCB(6), DYTTW(7), DYTTW(7), DYTT(6)

C

EQUIVALENCE (Y(1), YLTLW(1)), (DY(1), DYTLW(1)),
1 (Y(8), YLTTW(1)), (DY(8), DYTTW(1)),
2 (Y(15), YLT(1)), (DY(15), DYLT(1)),
3 (Y(21), YCB(1)), (DY(21), DYCB(1)),
4 (Y(27), YTTLW(1)), (DY(27), DYTTW(1)),
5 (Y(34), YTTTW(1)), (DY(34), DYTTTW(1)),
6 (Y(41), YTT(1)), (DY(41), DYTT(1))

C

JPLT(1) = 0 NO PLOT
= 1 PLOTS TIME VERSES LAT. EXCURSION OF WHEELSETS

C

C

JPLT(2) = 0 NO PLOT
= 1 PLOTS TIME VERSES ANGLE OF ATTACK OF WHEELSETS

C

C

JPLT(3) = 0 NO PLOT
= 1 PLOTS TIME VERSES FLANGE FORCE OF WHEELSETS

C

C

JPLT(4) = 0 NO PLOT
= 1 PLOTS TIME VERSES L/V RATIO OF WHEELSETS

C

C

C

```

C      JPLT(5) = 0 NO PLOT
C          = 1 PLOTS TIME VERSES WORK OF WHEELSETS
C
C      JPLT(6) = 0 NO PLOT
C          = 1 PLOTS TIME VERSES ACCELERATION OF WHEELSETS
C
C      JPLT(7) = 0 NO PLOT
C          = 1 PLOTS TIME VERSES LATERAL EXCURSION OF TRUCK AND CARBODY
C
C      JPLT(8) = 0 NO PLOT
C          = 1 PLOTS TIME VERSES YAW ANGLE OF TRUCK AND CARBODY
C
C      JPLT(9) = 0 NO PLOT
C          = 1 PLOTS TIME VERSES WARP ANGLE OF TRUCK
C
C      JPLT(10) = 0 NO PLOT
C          = 1 PLOTS TIME VERSES ROLL ANGLE OF CARBODY
C
C      JPLT(11) = 0 NO PLOT
C          = 1 PLOTS TIME VERSES ACCELERATION OF TRUCK AND CARBODY
C
500    FORMAT(A80)
510    FORMAT(14I4)
520    FORMAT(8G15.5)
525    FORMAT(2X,F6.3,5F11.6)
      READ(IDAT1,500)DUMMY
      READ(IDAT1,500)DATE
      READ(IDAT1,500)DUMMY
      READ(IDAT1,520)DT1,FTIME,DT2
      READ(IDAT1,500)DUMMY
      READ(IDAT1,510)(JPLT(I),I=1,12)
      READ(IDAT1,500)DUMMY
      READ(IDAT1,520)A,B,D,L
      READ(IDAT1,500)DUMMY
      READ(IDAT1,520)HS,IB,HC,HT,FLANGE
      READ(IDAT1,500)DUMMY
      READ(IDAT1,520)MW,MB,MS,MC
      READ(IDAT1,500)DUMMY
      READ(IDAT1,520)WIYY,WIZZ,BIXX,BIZZ
      READ(IDAT1,500)DUMMY
      READ(IDAT1,520)CIXX,SIZZ,CIZZ
      READ(IDAT1,500)DUMMY
      READ(IDAT1,520)KPX,KPY,DPX,DPY
      READ(IDAT1,500)DUMMY
      READ(IDAT1,510)ISUSP
      READ(IDAT1,500)DUMMY
      IF(ISUSP.EQ.0)READ(IDAT1,520)KSY,KSZ,KCP, KW
      IF(ISUSP.EQ.1)READ(IDAT1,520)KSY,KSZ,KW
      IF(ISUSP.NE.1)GO TO 15
      READ(IDAT1,500)DUMMY
      READ(IDAT1,520)FYO,TCPO,TWO,FZO,DEL1,DEL2,DEL3,DEL4
      GO TO 20
15     CONTINUE
      READ(IDAT1,500)DUMMY
      READ(IDAT1,520)DSY, DSZ,DCP,DW

```

```

20     CONTINUE
      READ(IDAT1,500)DUMMY
      READ(IDAT1,520)KS,KB
30     CONTINUE
      READ(IDAT1,500)DUMMY
      READ(IDAT1,520)F110, F120, F220, F330
      READ(IDAT1,500)DUMMY
      READ(IDAT1,520)MU, RAILK, RAILB
      READ(IDAT1,500)DUMMY
      READ(IDAT1,520)DTANGENT, DSPIRAL, DCURVE
      READ(IDAT1,500)DUMMY
      READ(IDAT1,520)PPHISE, RRHO, CCANTD
      READ(IDAT1,500)DUMMY
      READ(IDAT1,520)(YLTW(I), I=1, 5)
      READ(IDAT1,520)(YLTTW(I), I=1, 5)
      READ(IDAT1,520)(YLT(I), I=1, 6)
      READ(IDAT1,520)(YCB(I), I=1, 6)
      READ(IDAT1,520)(YTTW(I), I=1, 5)
      READ(IDAT1,520)(YTTT(I), I=1, 5)
      READ(IDAT1,520)(YTT(I), I=1, 6)
      READ(IDAT2,500)RAILFILE
      READ(IDAT2,510)NDIM
      READ(IDAT2,525)XWINC
      READ(IDAT2,525)(ARG(I), RRDAT(I), RLDAT(I), DRDAT(I), DLLDAT(I),
1         PHIDAT(I), I=1, NDIM)

C
C     END OF DATA READ IN
C
C     DETERMINE FIRST AND SECOND DERIVATIVES OF ROLLANGLE W.R.T.
C     LATERAL EXCURSION USING VALUES OF ROLLANGLE (PHIDAT)
C
      DO 50 J = 2, NDIM
      DPHI(J) = (PHIDAT(J) - PHIDAT(J-1))/XWINC
50     CONTINUE
      DPHI(1) = DPHI(2)
      DO 60 J = 2, NDIM
      D2PHI(J) = (DPHI(J) - DPHI(J-1))/XWINC
60     CONTINUE
      D2PHI(1) = D2PHI(2)

C
C     DETERMINE THE NUMBER OF STATES
C
      N=46

C
C     INITIALIZE THE PLOT AND PRINT COUNTER
C
      IOUTPUT=INT(FTIME/(DT2*100.0)) + 1
      ICOUNT = IOUTPUT
      NPTS =1

C
C     CALCULATE VALUE OF ROLLING RADIUS
C
      CALL CONTACT(1, ZERO, RO, RL, DR, DO, PHI, DDPHI, DD2PHI)
      NO = G*(MW + MS + .5*MB + .25*MC)/COS(DO)
C

```

```

C   CHANGE FINAL SUPERELEVATION & CANT DEFICIENCY FROM DEG TO RADIANS
C
      FPHISE = PPHISE*PI/180.0
      CANTD = CCANTD*PI/180.0
C
C   DETERMINE FINAL RADIUS FROM FINAL TRACK CURVATURE (DEGREE CURVE)
C
      FRHO = SIN(RRHO*PI/360.0)/50.0
C
C   CALCULATE THE FORWARD VELOCITY
C
      VEL = (FPHISE*G/FRHO)**.5
C
C   INITIALIZE MINIMUM AND MAXIMUM STATE VARIABLES
C
      DO 70 I = 1,N
      YMIN(I) = 1.7E38
      YMAX(I) = -1.7E38
70  CONTINUE
C
C   WRITE OUT HEADINGS FOR OUTPUT
C
      WRITE(IOUT1,560)
560  FORMAT(1H1//20X,'DYNAMIC CURVING PERFORMANCE OF FULL CARBODY')
C
C   WRITE INPUT DATA
C
      WRITE (IOUT1,570) DATE,DT1,FTIME,DT2
570  FORMAT(/12X,A20,9X,'OFF FLANGE TIMESTEP = ',F6.4,
1 /12X,'FINAL TIME (SECS) = ',F6.2,4X,
1 'ON FLANGE TIMESTEP = ',F6.4)
      WRITE(IOUT1,600)A,B,D, L, HS,HB,HC, HT,FLANGE, RO,MW, MB,
1 MS,MC
      WRITE(IOUT1,605)WIYY,WIZZ,BIXX,BIZZ,CIXX,SIZZ
600  FORMAT(/12X,'GEOMETRY'
1 //12X,'A - TRACK GAGE (FT) = ',
1F8.3/12X,'B - HALF OF TRUCK WHEELBASE (FT) = ',
1F8.3/12X,'D - SPACING OF PRIMARY LONG. SUSPENSION (FT) = ',
1F8.3/12X,'L - HALF DIS. BTW. TRUCK BOLSTER (FT) = ',
1F8.3/12X,'HS - HEIGHT OF SIDEFRAE C.G. ABOVE WHEELSET (FT) = ',
1F8.3/12X,'HB - HEIGHT OF BOLSTER C. G. ABOVE WHEELSET (FT) = ',
1F8.3/12X,'HC - HEIGHT OF CARBODY C.G. ABOVE BOLSTER (FT) = ',
1F8.3/12X,'HT - HEIGHT OF CARBODY HINGE ABOVE BOLSTER(FT) = ',
1F8.3/12X,'FLANGE - FLANGE CLEARANCE (INCHES) = ',
1F8.3/12X,'RO - CENTERED ROLLING RADIUS (FT) = ',
1F8.3//12X,'MASSES AND INERTIAS'
1 //12X,'MW - WHEELSET MASS (SLUGS) = ',
1F8.1/12X,'MB - BOLSTER MASS (SLUGS) = ',
1F8.1/12X,'MS - SIDE FRAME MASS (SLUGS) = ',
1F8.1/12X,'MC - CARBODY MASS (SLUGS) = ',
1F8.1)
605  FORMAT(12X,
1 'WIYY - WHEELSET SPIN MOMENT OF INERTIA (SLUG-FT2) = ',
1F8.1/12X,'WIZZ - WHEELSET YAW MOMENT OF INERTIA (SLUG-FT2) = ',
1F8.1/12X,'BIXX - BOLSTER ROLL MOMENT OF INERTIA (SLUG-FT2) = ',

```

```

1F8.1/12X, °BIZZ - BOLSTER YAW MOMENT OF INERTIA (SLUG-FT2) = °,
1F8.1/12X, °CIXX - CARBODY ROLL MOMENT OF INERTIA (SLUG-FT2) = °,
1F8.1/12X, °SIZZ - SIDEFAME MOMENT OF INERTIA (SLUG-FT2) = °,
1F8.1)
WRITE(IOUT1,610)CIZZ
610 FORMAT(12X,
1 °CIZZ - CARBODY YAW MOMENT OF INERTIA (SLUG-FT2) = °,F8.1)
WRITE(IOUT1,620)KPX,KPY,DPX,DPY
620 FORMAT(/12X, °SUSPENSION PARAMETERS°
1 //12X, °KPX - LONGITUDINAL PRIMARY STIFFNESS (LB/FT) = °,
1F12.1/12X, °KPY - LATERAL PRIMARY STIFFNESS (LB/FT) = °,
1F12.1/12X, °DPX - LONGITUDINAL PRIMARY DAMPING (LB-SEC/FT) = °,
1F12.1/12X, °DPY - LATERAL PRIMARY DAMPING (LB-SEC/FT) = °,
1 F12.1)
WRITE(IOUT1,630)KS,KB
630 FORMAT(12X, °KS - INTERAXLE SHEAR STIFFNESS (LB/FT) = °,
1F12.1/12X, °KB - INTERAXLE BENDING STIFFNESS (FT-LB/RAD) = °,
1F12.1)
WRITE(IOUT1,640)KSY,KSZ,KW
640 FORMAT( 12X, °KSY - LATERAL SECONDARY STIFFNESS (LB/FT) = °,
1 F12.1/12X, °KSZ - VERTICAL SECONDARY STIFFNESS (LB/FT) = °,
1 F12.1/12X, °KW - SECONDARY WARP STIFFNESS (FT-LB/RAD) = °,
1 F12.1)
IF(ISUSP.NE.1)WRITE(IOUT1,650)KCP,DSY,DSZ,DCP,DW
650 FORMAT(12X, °KCP - CENTERPLATE YAW STIFFNESS (FT-LB/RAD) = °,
1 F12.1/12X, °DSY - LATERAL SECONDARY DAMPING (LB-SEC/FT) = °,
1 F12.1/12X, °DSZ - VERTICAL SECONDARY DAMPING (LB-SEC/FT) = °,
1 F12.1/12X, °DCP - CENTERPLATE YAW DAMPING (FT-LB-SEC/RAD) = °,
1 F12.1/12X, °DW - SECONDARY WARP DAMPING (FT-LB-SEC/RAD) = °,
1 F12.1)
IF(ISUSP.EQ.1)WRITE(IOUT1,660)FYO,TCPO,TWO,FZO
660 FORMAT(/12X, °COULOMB FRICTION °
1 //12X, °FYO - LATERAL FORCE BTW BOLSTER & SIDEFAME(LB) = °,
1F9.0/12X, °TWO - YAW TORQUE BTW BOLSTER & CARBODY (FT-LB) = °,
1F9.0/12X, °TCPO - WARP TORQUE BTW BOLSTER & SIDEFAME(FT-LB)=°,
1F9.1/12X, °FZO - VERTICAL FORCE BTW BOLSTER & SIDEFAME(LB)=°,
1F9.1)
WRITE(IOUT1,680)F110,F120,F220,F330,MU
680 FORMAT( /12X, °FRICTION AND KALKER CREEP COEFFICIENTS°
1 //12X, °F110 - LATERAL CREEP COEFFICIENT(LB/WHEEL) = °,
1F12.1/12X, °F120 - LATERAL/SPIN CREEP COEFFICIENT(FT-LB/WH)=°,
1F12.1/12X, °F220 - SPIN CREEP COEFFICIENT(FT2-LB/WH) = °,
1F12.1/12X, °F330 - LONGITUDINAL CREEP COEFFICIENT (LB/WH) = °,
1F12.1/12X, °MU - WH/RAIL COEFFICIENT OF FRICTION = °,
1F12.3)
WRITE(IOUT1,700)RAILK,RAILB
700 FORMAT(1H1//12X, °RAIL FLEXIBILITY PARAMETERS:°
1 //12X, °RAILK - RAIL STIFFNESS (LB/FT) = °,
1F12.0/12X, °RAILB - RAIL DAMPING (LB-SEC/FT) = °,
1F12.0)
WRITE(IOUT1,710)DTANGENT,DSPIRAL,DCURVE,PPHISE,RRHO,
1 CCANTD,VEL,RAILFILE
710 FORMAT(/12X, °CURVING PARAMETERS°
1 //12X, °LENGTH OF TANGENT TRACK (FT) = °,
1 F12.1/12X, °LENGTH OF SPIRAL TRACK (FT) = °,

```

```

1 F12.1/12X, °LENGTH OF CURVED TRACK (FT) = °,
1 F12.1/12X, °FINAL SUPERELEVATION ANGLE (DEG) = °,
1 F12.1/12X, °FINAL DEGREE CURVE = °,
1 F12.1/12X, °CANT DEFICIENCY (DEG) = °,
1 F12.1/12X, °VELOCITY (FT/SEC) = °,
1 F12.2//12X, °WHEEL/RAIL GEOMETRY PROFILE°/12X, A80)
WRITE(IOUT1, 720)
720 FORMAT(1H1///18X, °INITIAL VALUES OF STATE VARIABLES°)
WRITE(IOUT1, 740)
740 FORMAT(/12X, °LEAD WHEELSET OF LEAD TRUCK:°)
WRITE(IOUT1, 750) YLTLW(1), YLTLW(2), YLTLW(3), YLTLW(4), YLTLW(5)
750 FORMAT(12X, °LATERAL EXCURSION OF WHEELSET (INCHES) °, 7X, F12.6
1 /12X, °YAW ANGLE OF WHEELSET (DEGREES) °, 7X, F12.6
3 /12X, °LATERAL VELOCITY OF WHEELSET (INCHES/SEC) °, 7X, F12.6
4 /12X, °YAW ANGLE RATE OF WHEELSET (DEGREES/SEC) °, 7X, F12.6
2 /12X, °BETA DOT OF WHEELSET (DEGREES/SEC) °, 7X, F12.6)
WRITE(IOUT1, 760)
760 FORMAT(/12X, °TRAILING WHEELSET OF LEAD TRUCK:°)
WRITE(IOUT1, 750) (YLTIW(I), I=1, 5)
WRITE(IOUT1, 770)
770 FORMAT(/12X, °LEAD TRUCK:°)
WRITE(IOUT1, 780) (YLT(I), I=1, 6)
780 FORMAT(12X, °LATERAL EXCURSION OF TRUCK (INCHES) °, 7X, F12.6
1 /12X, °YAW ANGLE OF TRUCK (DEGREES) °, 7X, F12.6
1 /12X, °WARP ANGLE OF TRUCK (DEGREES) °, 7X, F12.6
1 /12X, °LATERAL VELOCITY OF TRUCK (INCHES/SEC) °, 7X, F12.6
1 /12X, °YAW ANGLE RATE OF TRUCK (DEGREES/SEC) °, 7X, F12.6
1 /12X, °WARP ANGLE RATE OF TRUCK (DEGREES/SEC) °, 7X, F12.6)
WRITE(IOUT1, 810) (YCB(I), I=1, 6)
810 FORMAT(/12X, °CARBODY:°)
1 /12X, °LATERAL EXCURSION OF CARBODY (INCHES) °, 7X, F12.6
1 /12X, °ROLL ANGLE OF CARBODY (DEGREES) °, 7X, F12.6
1 /12X, °YAW ANGLE OF CARBODY (DEGREES) °, 7X, F12.6
1 /12X, °LATERAL VELOCITY OF CARBODY (INCHES/SEC) °, 7X, F12.6
1 /12X, °ROLL ANGLE RATE OF CARBODY (DEGREES/SEC) °, 7X, F12.6
1 /12X, °YAW ANGLE RATE OF CARBODY (DEGREES/SEC) °, 7X, F12.6)
WRITE(IOUT1, 820)
820 FORMAT(/12X, °LEAD WHEELSET OF TRAILING TRUCK:°)
WRITE(IOUT1, 750) (YTTLW(I), I=1, 5)
WRITE(IOUT1, 830)
830 FORMAT(/12X, °TRAILING WHEELSET OF TRAILING TRUCK:°)
WRITE(IOUT1, 750) (YTTIW(I), I=1, 5)
WRITE(IOUT1, 840)
840 FORMAT(/12X, °TRAILING TRUCK:°)
WRITE(IOUT1, 780) (YTT(I), I=1, 6)

```

C
C
C

CONVERT INCHES TO FEET AND DEGREES TO RADIANS

```

YLTLW(1) = YLTLW(1)/12.0
YLTLW(2) = YLTLW(2)*PI/180.0
YLTLW(3) = YLTLW(3)/12.0
YLTLW(4) = YLTLW(4)*PI/180.0
YLTLW(5) = YLTLW(5)*PI/180.0
YLTIW(1) = YLTIW(1)/12.0
YLTIW(2) = YLTIW(2)*PI/180.0

```



```

YLTW(3) = YLTW(3)/12.0
YLTW(4) = YLTW(4)*PI/180.0
YLTW(5) = YLTW(5)*PI/180.0
YLT(1) = YLT(1)/12.0
YLT(2) = YLT(2)*PI/180.0
YLT(3) = YLT(3)*PI/180.0
YLT(4) = YLT(4)/12.0
YLT(5) = YLT(5)*PI/180.0
YLT(6) = YLT(6)*PI/180.0
YCB(1) = YCB(1)/12.0
YCB(2) = YCB(2)*PI/180.0
YCB(3) = YCB(3)*PI/180.0
YCB(4) = YCB(4)/12.0
YCB(5) = YCB(5)*PI/180.0
YCB(6) = YCB(6)*PI/180.0
YTTLW(1) = YTTLW(1)/12.0
YTTLW(2) = YTTLW(2)*PI/180.0
YTTLW(3) = YTTLW(3)/12.0
YTTLW(4) = YTTLW(4)*PI/180.0
YTTLW(5) = YTTLW(5)*PI/180.0
YTTW(1) = YTTW(1)/12.0
YTTW(2) = YTTW(2)*PI/180.0
YTTW(3) = YTTW(3)/12.0
YTTW(4) = YTTW(4)*PI/180.0
YTTW(5) = YTTW(5)*PI/180.0
YTT(1) = YTT(1)/12.0
YTT(2) = YTT(2)*PI/180.0
YTT(3) = YTT(3)*PI/180.0
YTT(4) = YTT(4)/12.0
YTT(5) = YTT(5)*PI/180.0
YTT(6) = YTT(6)*PI/180.0
FLANGE = FLANGE/12.0

```

C
C
C

```
IF EITHER WHEELSET IS ON THE FLANGE DECREASE TIME STEP
```

```

DT = DT1
IF( (ABS(YLTW(1)) .GT. FLANGE) .OR. (ABS(YTTW(1)) .GT. FLANGE) )DT=DT2
IF( (ABS(YTTLW(1)) .GT. FLANGE) .OR. (ABS(YTTW(1)) .GT. FLANGE) )DT=DT2
RETURN
END

```

SUBROUTINE EQUATION

C
C
C

CALCULATE THE DY(I) TO BE INTEGRATED IN MAIN PROGRAM

COMMON NEWDT, DT,DT1,DT2, FLANGE,N, T, FTIME
COMMON /STATES/ Y(46), DY(46), YMAX(46), YMIN(46)
COMMON/MATRIX/SUSP(17)

C

DIMENSION YLTLW(7),YLTTW(7),YLT(6),YCB(6),YTTLW(7),YTTTW(7),YTT(6),
1 DYTLW(7),DYLTTW(7),DYLT(6),DYCB(6),DYTTLW(7),DYTTTW(7),DYTT(6)

C

INTEGER FRONT, BACK, CENTER, TTLW, TTTW

C

DATA FRONT/1/, CENTER/2/, BACK/3/, LTLW/1/, LTTW/2/, TTLW/3/, TTTW/4/

C

EQUIVALENC (Y(1),YLTLW(1)),(DY(1),DYLTLW(1)),
1 (Y(8),YLTTW(1)),(DY(8),DYLTTW(1)),
2 (Y(15),YLT(1)),(DY(15),DYLT(1)),
3 (Y(21),YCB(1)),(DY(21),DYCB(1)),
4 (Y(27),YTTLW(1)),(DY(27),DYTTLW(1)),
5 (Y(34),YTTTW(1)),(DY(34),DYTTTW(1)),
6 (Y(41),YTT(1)),(DY(41),DYTT(1))

C

C

DETERMINE THE CURVE GEOMETRY

C

IF(NEWDT.EQ.0)GO TO 10
CALL CURVE(FRONT)
CALL CURVE(CENTER)
CALL CURVE(BACK)
CONTINUE

10

C

C

DETERMINE THE SUSPENSION FORCES AND MOMENTS

C

CALL FSUSP

C

C

DETERMINE FIRST ORDER EQUATIONS OF MOTION FOR WHEELSET, TRUCK AND CARBODY

C

CALL WHEELSET(FRONT, LTLW,SUSP(1),SUSP(2),YLTLW, DYLTLW)
CALL WHEELSET(FRONT, LTTW,SUSP(3), SUSP(4),YLTTW, DYLTTW)
CALL TRUCK(FRONT, SUSP(5),SUSP(6),SUSP(7),YLT, DYLT)
CALL CARBODY(SUSP(8), SUSP(9),SUSP(10), YCB,DYCB)
CALL WHEELSET(BACK, TTLW,SUSP(11),SUSP(12),YTTLW, DYTTLW)
CALL WHEELSET(BACK, TTTW,SUSP(13),SUSP(14),YTTTW, DYTTTW)
CALL TRUCK(BACK, SUSP(15),SUSP(16),SUSP(17),YTT,DYTT)

C

IF(NEWDT.EQ.0)GO TO 40

C

C

IF ANY WHEELSET IS NEAR THE FLANGE ADJUST THE TIMESTEP

C

IF((ABS(YLTLW(1)).LT.FLANGE).AND. (ABS(YLTTW(1)).LT.FLANGE))DT=DT1
IF((ABS(YLTLW(1)).GT.FLANGE).OR. (ABS(YLTTW(1)).GT.FLANGE))DT=DT2
IF((ABS(YTTLW(1)).LT.FLANGE).AND. (ABS(YTTTW(1)).LT.FLANGE))DT=DT1
IF((ABS(YTTLW(1)).GT.FLANGE).OR. (ABS(YTTTW(1)).GT.FLANGE))DT=DT2

C

40

CONTINUE

RETURN
END

SUBROUTINE CURVE(K)

```

C
C CALCULATES THE SUPEREVELATION ANGLE (PHISE)
C           FIRST DERIVATIVE OF PHISE (DPHISE)
C           SECOND DERIVATIVE OF PHISE (D2PHISE)
C           TRACK CURVATURE (RHO)
C           FIRST DERIVATIVE OF RHO (DRHO)
C
C FOR LEAD TRUCK AND ITS WHEELSETS      IF K = 1
C           CARBODY CENTER OF MASS      IF K = 2
C           TRAILING TRUCK AND ITS WHEELSETS IF K= 3
C
C CURVE GEOMETRY IS A FUNCTION OF DISTANCE THAT SECTION OF
C           VEHICLE HAS TRAVELED ALONG THE TRACK
C
C           COMMON NEWDT ,DT
C           COMMON/TRACK/FPHISE, FRHO, DTANGENT, DSPIRAL, DCURVE,
C           1           A, B, C, D, E
C           COMMON/CURVE/DIS(3), PHISE(3), DPHISE(3), D2PHISE(3),
C           1           RHO(3), DRHO(3)
C           COMMON/CONSTANT/VEL,CANTD,GG, PI
C           COMMON/GEOMETRY/AA,BB,DD,L
C
C DETERMINE THE COEFFICIENTS OF EQUATIONS
C
C           IF( (NEWDT.NE.-1) .OR. (DSPIRAL.EQ.0.0) )GO TO 100
C           A = 1.0/(.5*DSPIRAL*DSPIRAL)
C           B = -2.0*A*DTANGENT
C           C = A*(DTANGENT)**2
C           D = A*2.0*(DTANGENT + DSPIRAL)
C           E = -A*(DTANGENT + DSPIRAL)**2 + 1
C
C INITIAL AND INCREMENT THE DISTANCE TRAVELED BY EACH SECTION
C
C           DIS(1) = 0.0
C           DIS(2) = -L
C           DIS(3) = -2.*L
100    IF(NEWDT.NE.-1)DIS(K) = DIS(K) + DT*VEL
C
C TANGENT TRACK SECTION
C
C           X = DIS(K)
C           IF(DIS(K).GE.DTANGENT) GO TO 130
120    PHISE(K)= 0.0
C           DPHISE(K) = 0.0
C           D2PHISE(K) = 0.0
C           RHO(K) = 0.0
C           DRHO(K) = 0.0
C           GO TO 200
C
C SPIRAL - QUADRATIC FAIRING INTO CONSTANT RADIUS CURVE
C
130    IF(DIS(K).GE.(DTANGENT + .5*DSPIRAL) )GO TO 140
135    PHISE(K) = FPHISE*(A*X*X + B*X + C)

```

```

DPHISE(K) = VEL*FPHISE*(2.*A*X + B)
D2PHISE(K) = 2.0*A*VEL*VEL*FPHISE
RHO(K) = FRHO*(A*X*X + B*X + C)
DRHO(K) = FRHO*VEL*(2.*A*X + B)
GO TO 200
140  IF(DIS(K).GE.(DTANGENT + DSPIRAL))GO TO 150
145  PHISE(K) = FPHISE*(-A*X*X + D*X + E)
    DPHISE(K) = VEL*FPHISE*(-2.*A*X + D)
    D2PHISE(K) = -VEL*VEL*FPHISE*2.*A
    RHO(K) = FRHO*(-A*X*X + D*X + E)
    DRHO(K) = VEL*FRHO*(-2.*A*X + D)
    GO TO 200

C
C  CONSTANT RADIUS CURVE
C
150  IF(DIS(K).GE.(DCURVE + DTANGENT + DSPIRAL))GO TO 160
    PHISE(K) = FPHISE
    DPHISE(K) = 0.0
    D2PHISE(K) = 0.0
    RHO(K) = FRHO
    DRHO(K) = 0.0
    GO TO 200

C
C  CURVE EXIT
C
160  X = (2.0*DSPIRAL + 2.*DTANGENT + DCURVE - DIS(K))
    IF(DIS(K).GT.(DCURVE + 2.0*DSPIRAL + DTANGENT))GO TO 120
    IF(DIS(K).GT.(DCURVE + DTANGENT + 1.5*DSPIRAL))GO TO 135
    GO TO 145
200  CONTINUE
    RETURN
    END

```


$K(3,1) = KS$
 $K(3,2) = -B*KS$
 $K(3,3) = -KS - 2.*KPY$
 $K(3,4) = -B*KS$
 $K(3,5) = 2.*KPY$
 $K(3,6) = -2.0*B*KPY$
 $K(3,18) = 2.*KPY*HS$
 $C(3,3) = - 2.*DPY$
 $C(3,5) = 2.*DPY$
 $C(3,6) = -2.0*B*DPY$
 $C(3,18) = 2.0*DPY*HS$

C TRAILING WHEELSET, LEAD TRUCK - YAW

$K(4,1) = B*KS$
 $K(4,2) = -B**2*KS + KB$
 $K(4,3) = -B*KS$
 $K(4,4) = -B**2*KS - KB - 2.*D*D*KPX$
 $K(4,6) = 2.0*D*D*KPX$
 $K(4,7) = 2.0*D*D*KPX$
 $C(4,4) = -2.*D*D*DPX$
 $C(4,6) = 2.0*D*D*DPX$
 $C(4,7) = 2.0*D*D*DPX$

C LEAD TRUCK - LATERAL

$K(5,1) = 2.*KPY$
 $K(5,3) = 2.*KPY$
 $K(5,5) = -4.*KPY - 2.*KSY$
 $K(5,8) = 2.*KSY$
 $K(5,9) = 2.*KSY*HT + MS*G$
 $K(5,10) = 2.0*L*KSY$
 $K(5,18) = -4.0*KPY*HS + 2.0*KSY*(HB-HS)$
 $C(5,1) = 2.*DPY$
 $C(5,3) = 2.*DPY$
 $C(5,5) = -4.*DPY - 2.*DSY$
 $C(5,8) = 2.*DSY$
 $C(5,9) = 2.*DSY*HT$
 $C(5,10) = 2.0*L*DSY$
 $C(5,18) = -4.0*DPY*HS + 2.0*DSY*(HB-HS)$

C LEAD TRUCK - YAW

$K(6,1) = 2.0*B*KPY$
 $K(6,2) = 2.*KPX*D*D$
 $K(6,3) = -2.0*B*KPY$
 $K(6,4) = 2.*KPX*D*D$
 $K(6,6) = -KCP - 4.*KPX*D*D - 4.*B*B*KPY$
 $K(6,7) = -4.*KPX*D*D - KCP$
 $K(6,10) = KCP$
 $K(6,20) = KCP$
 $C(6,1) = 2.0*B*DPY$
 $C(6,2) = 2.*DPX*D*D$
 $C(6,3) = -2.0*B*DPY$
 $C(6,4) = 2.*DPX*D*D$
 $C(6,6) = -DCP - 4.*DPX*D*D - 4.*B*B*DPY$
 $C(6,7) = -4.*DPX*D*D - DCP$
 $C(6,10) = DCP$
 $C(6,20) = DCP$

C LEAD TRUCK - WARP

$K(7,2) = 2.*KPX*D*D$

$K(11,11) = -KS - 2.*KPY$
 $K(11,12) = B*KS$
 $K(11,13) = KS$
 $K(11,14) = B*KS$
 $K(11,15) = 2.*KPY$
 $K(11,16) = 2.*B*KPY$
 $K(11,19) = 2.*KPY *HS$
 $C(11,11) = -2.*DPY$
 $C(11,15) = 2.*DPY$
 $C(11,16) = 2.*B*DPY$
 $C(11,19) = 2.0*DPY*HS$

C LEAD WHEELSET, TRAILING TRUCK - YAW
 $K(12,11) = B*KS$
 $K(12,12) = -B**2*KS - KB - 2.*D*D*KPX$
 $K(12,13) = -B*KS$
 $K(12,14) = -B**2*KS + KB$
 $K(12,16) = 2.*D*D*KPX$
 $K(12,17) = 2.*D*D*KPX$
 $C(12,12) = -2.*D*D*DPX$
 $C(12,16) = 2.*D*D*DPX$
 $C(12,17) = 2.*D*D*DPX$

C TRAILING WHEELSET, TRAILING TRUCK - LATERAL
 $K(13,11) = KS$
 $K(13,12) = -B*KS$
 $K(13,13) = -KS - 2.*KPY$
 $K(13,14) = -B*KS$
 $K(13,15) = 2.*KPY$
 $K(13,16) = -2.*B*KPY$
 $K(13,19) = 2.*KPY*HS$
 $C(13,13) = -2.*DPY$
 $C(13,15) = 2.*DPY$
 $C(13,16) = -2.*B*DPY$
 $C(13,19) = 2.0*DPY*HS$

C TRAILING WHEELSET, TRAILING TRUCK - YAW
 $K(14,11) = B*KS$
 $K(14,12) = -B**2*KS + KB$
 $K(14,13) = -B*KS$
 $K(14,14) = -B**2*KS - KB - 2.*D*D*KPX$
 $K(14,16) = 2.*D*D*KPX$
 $K(14,17) = 2.*D*D*KPX$
 $C(14,14) = -2.*D*D*DPX$
 $C(14,16) = 2.*D*D*DPX$
 $C(14,17) = 2.*D*D*DPX$

C TRAILING TRUCK - LATERAL
 $K(15,8) = 2.*KSY$
 $K(15,9) = 2.*KSY*HS$
 $K(15,10) = -2.0*L*KSY$
 $K(15,11) = 2.*KPY$
 $K(15,13) = 2.*KPY$
 $K(15,15) = -4.*KPY - 2.*KSY$
 $K(15,19) = -4.0*KPY*HS + 2.0*KSY*(HB-HS)$
 $C(15,8) = 2.*DSY$
 $C(15,9) = 2.*DSY*HS$
 $C(15,10) = -2.0*L*DSY$
 $C(15,11) = 2.*DPY$

$C(15,13) = 2.*DPY$
 $C(15,15) = -4.*DPY - 2.*DSY$
 $C(15,19) = -4.0*DPY*HS + 2.0*DSY*(HB-HS)$
C TRAILING TRUCK - YAW
 $K(16,10) = KCP$
 $K(16,11) = 2.*B*KPY$
 $K(16,12) = 2.*D*D*KPX$
 $K(16,13) = -2.*B*KPY$
 $K(16,14) = 2.*KPX*D*D$
 $K(16,16) = -KCP -4.*KPX*D*D -4.*B*B*KPY$
 $K(16,17) = -4.*KPX*D*D - KCP$
 $K(16,20) = KCP$
 $C(16,10) = DCP$
 $C(16,11) = 2.*B*DPY$
 $C(16,12) = 2.*D*D*DPX$
 $C(16,13) = -2.*B*DPY$
 $C(16,14) = 2.*DPX*D*D$
 $C(16,16) = -DCP -4.*DPX*D*D -4.*B*B*DPY$
 $C(16,17) = -4.*DPX*D*D - DCP$
 $C(16,20) = -DCP$
C TRAILING TRUCK - WARP
 $K(17,10) = KCP$
 $K(17,12) = 2.*KPX*D*D$
 $K(17,14) = 2.*KPX*D*D$
 $K(17,16) = -4.*KPX*D*D - KCP$
 $K(17,17) = -4.*KPX*D*D - KCP - KW$
 $C(17,10) = DCP$
 $C(17,12) = 2.*DPX*D*D$
 $C(17,14) = 2.*DPX*D*D$
 $C(17,16) = -4.*DPX*D*D - DCP$
 $C(17,17) = -4.*DPX*D*D - DCP - DW$
CONTINUE

20
C
C
C

DEFINE STATE DISPLACEMENT VECTOR FOR LINEAR SUSPENSION ELEMENTS

$X(1) = Y(1)$
 $X(2) = Y(2) - B*RHO(FRONT)$
 $X(3) = Y(8)$
 $X(4) = Y(9) + B*RHO(FRONT)$
 $X(5) = Y(15)$
 $X(6) = Y(16)$
 $X(7) = Y(17)$
 $X(8) = Y(21)$
 $X(9) = Y(22)$
 $X(10) = Y(23)$
 $X(11) = Y(27)$
 $X(12) = Y(28) - B*RHO(BACK)$
 $X(13) = Y(34)$
 $X(14) = Y(35) + B*RHO(BACK)$
 $X(15) = Y(41)$
 $X(16) = Y(42)$
 $X(17) = Y(43)$
 $X(18) = .5*(PHI(LTTW) + PHI(LTLW))$
 $X(19) = .5*(PHI(TTTW) + PHI(TTLW))$
 $X(20) = L*RHO(CENTER)$

C
C
C

DEFINE VELOCITY VECTOR

$Z(1) = Y(3)$
 $Z(2) = Y(4) - B*DRHO(FRONT)$
 $Z(3) = Y(10)$
 $Z(4) = Y(11) + B*DRHO(FRONT)$
 $Z(5) = Y(18)$
 $Z(6) = Y(19)$
 $Z(7) = Y(20)$
 $Z(8) = Y(24)$
 $Z(9) = Y(25)$
 $Z(10) = Y(26)$
 $Z(11) = Y(29)$
 $Z(12) = Y(30) - B*DRHO(BACK)$
 $Z(13) = Y(36)$
 $Z(14) = Y(37) + B*DRHO(BACK)$
 $Z(15) = Y(44)$
 $Z(16) = Y(45)$
 $Z(17) = Y(46)$
 $Z(18) = .5*(DPHI(LTLW) + DPHI(LTTW))$
 $Z(19) = .5*(DPHI(TTLW) + DPHI(TTTW))$
 $Z(20) = L*DRHO(CENTER)$

C
C
C
CMULTIPLY K AND C MATRICES WITH DISPLACEMENT AND VELOCITY VECTORS
TO DETERMINE LINEAR SUSPENSION

50

DO 50 I=1,M
 SUSP(I)=0.0
 DO 50 JJ=1,J
 SUSP(I)=SUSP(I) + K(I,JJ)*X(JJ) + C(I,JJ)*Z(JJ)
 CONTINUE
 IF(ISUSP.NE.1)GO TO 70

C
C
C
C
C

DETERMINE SUSPENSION FORCES AND MOMENTS DUE TO COULOMB FRICTION

LATERAL FORCE BETWEEN SIDEFAME AND BOLSTER OF LEAD TRUCK

$LAT = Y(24) + HT*Y(25) + L*Y(26) - Y(18) + (HB-HS)*Z(18)$
 $FY1 = 2.0*LAT*FYO/DEL1$
 $IF(ABS(LAT).GT.DEL1)FY1 = 2.0*FYO*(LAT/ABS(LAT))$

C
C

YAW MOMENT BETWEEN BOLSTER OF LEAD TRUCK AND CARBODY

$YAW = Y(26) + L*DRHO(CENTER) - Y(20) - Y(19)$
 $TCP1 = YAW*TCPO/DEL2$
 $IF(ABS(YAW).GT.DEL2)TCP1 = TCPO*(YAW/ABS(YAW))$

C
C
C

WARP MOMENT BETWEEN BOLSTER AND SIDEFAMES OF LEAD TRUCK

$TW1 = -Y(20)*TWO/DEL3$
 $IF(ABS(Y(20)).GT.DEL3)TW1 = -TWO*Y(20)/ABS(Y(20))$

C
C
C

VERTICAL FORCE BETWEEN BOLSTER AND SIDEFAME

```

Z1 = D*(Y(25) - .5*(DPHI(LTLW) + DPHI(LTW)))
FZ1 = 2.0*Z1*FZO/DELA
IF(ABS(Z1).GT.DELA)FZ1 = 2.0*FZO*Z1/ABS(Z1)

```

C
C
C

LATERAL FORCE BETWEEN BOLSTER AND SIDEFAMES OF TRAILING TRUCK

```

LAT = Y(24) + HT*Y(25) - L*Y(26) - Y(44) + (HB-HS)*Z(19)
FY2 = 2.0*LAT*FYO/DEL1
IF(ABS(LAT).GT.DEL1)FY2 = 2.0*FYO*(LAT/ABS(LAT))

```

C
C
C

YAW MOMENT BETWEEN BOLSTER OF LEAD TRUCK AND CARBODY

```

YAW = Y(26) - L*DRHO(CENTER) - Y(45) - Y(46)
TCP2 = YAW*TCPO/DEL2
IF(ABS(YAW).GT.DEL2)TCP2 = TCPO*(YAW/ABS(YAW))

```

C
C
C

WARP MOMENT BETWEEN BOLSTER AND SIDEFAMES OF LEAD TRUCK

```

TW2 = -Y(46)*TWO/DEL3
IF(ABS(Y(46)).GT.DEL3)TW2 = -TWO*Y(46)/ABS(Y(46))

```

C
C
C

VERTICAL FORCE BETWEEN BOLSTER AND SIDEFAME OF TRAILING TRUCK

```

Z2 = D*(Y(25) - .5*(DPHI(TTLW) + DPHI(TTW)))
FZ2 = 2.0*Z2*FZO/DELA
IF(ABS(Z2).GT.DELA)FZ2 = 2.0*FZO*Z2/ABS(Z2)

```

C
C
C

ADD COULOMB SUSP. ELEMENTS IN PARALLEL TO LINEAR SUSP. ELEMENTS

```

SUSP(5) = SUSP(5) + FY1
SUSP(6) = SUSP(6) + TCP1
SUSP(7) = SUSP(7) + TCP1 + TW1
SUSP(8) = SUSP(8) - (FY1 + FY2)
SUSP(9) = SUSP(9) - HT*(FY1 + FY2) - D*(FZ1 + FZ2)
SUSP(10) = SUSP(10) + L*(FY2 - FY1) - TCP1 - TCP2
SUSP(15) = SUSP(15) + FY2
SUSP(16) = SUSP(16) + TCP2
SUSP(17) = SUSP(17) + TCP2 + TW2

```

C
70

```

CONTINUE
RETURN
END

```

SUBROUTINE WHEELSET(L, K, SUSP1, SUSP2, YW, DYW)

ESTABLISHES THE FIRST ORDER EQUATIONS OF MOTION FOR WHEELSET
TO BE INTEGRATED BY MAIN

L = 1 LEAD TRUCK
= 3 TRAILING TRUCK
K = 1 LEAD WHEELSET LEAD TRUCK
= 2 TRAILING WHEELSET OF LEAD TRUCK
= 3 LEAD WHEELSET OF TRAILING TRUCK
= 4 TRAILING WHEELSET OF TRAILING TRUCK

COMMON NEWDT, DT,DT1,DT2, FLANGE,N, T, FTIME
COMMON/CONSTANT/ VEL ,CANTD,G,PI
COMMON/GEOMETRY/A,B,D,LT,HT,HS,HP,HC,RO
COMMON/WHGEOM/RR(4),RL(4),PHI(4),DPHI(4)
COMMON/INERTIA/MW, MB, MS, MC,MAPP, WIYY, WIZZ, BIXX, BIZZ,
1 CIXX, CIZZ, SIZZ
COMMON/CURVE/DIS(3),PHISE(3),DPHISE(3),D2PHISE(3),RHO(3),
1 DRHO(3)
COMMON/RAIL/RAILK, RAILB

DIMENSION YW(7),DYW(7),FORCE(5)

REAL LT,MAPP,MS, MC, MB, MW

DETERMINE THE WHEEL/RAIL GEOMETRY

IF(NEWDT.NE.0)CALL WHGEOM(K,YW,DYW)

DETERMINE THE WHEEL/RAIL FORCES

CALL WHFORCE(L,K, YW, FORCE)

FIRST ORDER EQUATIONS OF MOTION FOR WHEELSET

AXLEL = (.25*MC + MW + .5*MB + MS)*G
DYW(1) = YW(3)
DYW(2) = YW(4)
DYW(3) = (SUSP1 + FORCE(1))/MW
1 + CANTD*(AXLEL)/MW + RO*D2PHISE(L)
DYW(4) = (SUSP2 + FORCE(2))/WIZZ + VEL*DRHO(L)
1 - (VEL/RO + YW(5))*(DPHI(K) + DPHISE(L))*WIYY/WIZZ
DYW(5) = (FORCE(3))/WIYY

FIRST ORDER EQUATIONS GOVERNING RAIL MOTION

IF(RAILB.EQ.0.0) GO TO 20
DYW(6) = - (RAILK*YW(6) + FORCE(4))/RAILB
DYW(7) = - (RAILK*YW(7) + FORCE(5))/RAILB
GO TO 30
CONTINUE

AN ALTERNATE METHOD FOR DETERMINING RAIL MOTION WITHOUT DAMPING

```
IF( (RAILK.EQ.0.0).OR.(NEWDT.EQ.0) )GO TO 30  
YW(6) = -(FORCE(4))/RAILK  
YW(7) = -(FORCE(5))/RAILK  
30 CONTINUE  
RETURN  
END
```

```

SUBROUTINE WHGEOM(K,YW,DYW)
C
C DETERMINES WHEEL/RAIL CONTACT GEOMETRY
C
COMMON NEWDT,DT
COMMON/WHGEOM/RR(4),RL(4),PHI(4),DPHI(4),D2PHI(4)
COMMON/TRIG/COSRP(4),COSLP(4),SINRP(4),SINLP(4),COSR(4),
1          COSL(4),SINR(4),SINL(4)
C
DIMENSION YW(7),DYW(7)
C
C FIND EFFECTIVE LAT. EXCURS. = EXCURS. OF WHEELSET - EXCURS. OF RAIL
C
      YWL = YW(1) - YW(6)
      YWR = YW(1) - YW(7)
C
C DETERMINE THE CONTACT GEOMETRY GEOMETRY OF EACH CONTACT PATCH
C
      CALL CONTACT(K,YWL,DUM1,RL(K),DUM2,DL,PHIL,DPDYL,D2PDYL)
      CALL CONTACT(K,YWR,RR(K),DUM1,DR,DUM2,PHIR,DPDYR,D2PDYR)
      PHI(K) = .5*(PHIL + PHIR)
C
C DETERMINE THE DERIVATIVES OF ROLLANGLE W. R. T. TIME
C
      DPHI(K) = .5*(DPDYL + DPDYR)*DYW(1)
      D2PHI(K) = .5*(D2PDYL + D2PDYR)*DYW(3)
C
C DETERMINE USEFUL TRIGONOMETRIC FUNCTIONS USED IN WHFORCE
C
      COSRP(K) = COS(DR-PHI(K))
      COSLP(K) = COS(DL + PHI(K))
      SINRP(K) = SIN(DR-PHI(K))
      SINLP(K) = SIN(DL + PHI(K))
      COSR(K) = COS(DR)
      COSL(K) = COS(DL)
      SINR(K) = SIN(DR)
      SINL(K) = SIN(DL)
C
      RETURN
      END

```

SUBROUTINE CONTACT(K, XW, RR, RL, DR, DL, PHI, DPDY, D2PDY)

THIS IS A SUBROUTINE DETERMINES THE WHEEL/RAIL CONTACT GEOMETRY
AS A FUNCTION OF LATERAL EXCURSION BY INTERPOLATING FROM TABLES

COMMON/GEOM/NDIM, XWINC, ARG(242), RRDAT(242), RLDAT(242),
1 DRDAT(242), DLDAT(242), PHIDAT(242), DDPHI(242),
1 DD2PHI(242)
IOUT=3

DETERMINE LATERAL EXCURSION IN INCHES

XW = XW*12.0

DETERMINE IF LATERAL EXCURSION IS WITHIN RANGE OF DATA TABLE

IF(XW.LT.ARG(1)) .OR. (XW.GT.ARG(NDIM)) GO TO 20

DETERMINE THE INDEX FOR DATA

IF(XW.EQ.0.0) XW = .000000001
IF(XW.LE.0.) J = INT(XW + ARG(NDIM) + XWINC)/XWINC
IF(XW.GT.0.) J = INT(XW + ARG(NDIM) + XWINC)/XWINC + 1

DETERMINE CONTACT GEOMETRY BY LINEAR INTERPOLATION

IF(J.NE.51) GO TO 25

RR = RRDAT(J)

RL = RLDAT(J)

DR = DRDAT(J)

DL = DLDAT(J)

PHI = PHIDAT(J)

DPDY = DDPHI(J)

D2PDY = DD2PHI(J)

GO TO 30

25 CONTINUE

Z = 1.0/(ARG(J+1) - ARG(J))*(XW - ARG(J))

RR = (RRDAT(J+1) - RRDAT(J))*Z + RRDAT(J)

RL = (RLDAT(J+1) - RLDAT(J))*Z + RLDAT(J)

DR = (DRDAT(J+1) - DRDAT(J))*Z + DRDAT(J)

DL = (DLDAT(J+1) - DLDAT(J))*Z + DLDAT(J)

PHI = (PHIDAT(J+1) - PHIDAT(J))*Z + PHIDAT(J)

DPDY = (DDPHI(J+1) - DDPHI(J))*Z + DDPHI(J)

D2PDY = (DD2PHI(J+1) - DD2PHI(J))*Z + DD2PHI(J)

30 CONTINUE

CHANGE RIGHT AND LEFT ROLLING RADII FROM INCHES TO FEET

RR = RR/12.0

RL = RL/12.0

RETURN

PRINT OUT WARNING AND TERMINATES PROGRAM

20 CONTINUE

```
35  WRITE (IOUT,35)XW,K
      FORMAT(///10X,°WHEEL EXCURSION (°,F9.6,°INCHES ) OF AXLE°,
1     I4,° IS OUTSIDE WHEEL-RAIL PROFILE TABLE°//
1     20X,      °PROGRAM EXECUTION IS STOPPED°)
      CALL PRINT
      STOP
      END
```


SUBROUTINE WHFORCE(L, K, YW, FORCE)

C
C
C
C
C

AN ITERATIVE APPROACH IS USED TO CALCULATE WHEEL/RAIL FORCES

ITERATION TERMINATES WHEN NORMAL FORCE VARIES BY § 10%

COMMON NEWDT,DT,DT1,DT2, FLANGE,N, T, FTIME
 COMMON/CONSTANT/VEL,CANTD,G,PI
 COMMON/GEOMETRY/A,B,D,LT,HS,HB,HC,HT,RO
 COMMON/SAVE/CRP(4,4)
 COMMON/WHGEOM/RR(4),RL(4),PHI(4),DPHI(4),D2PHI(4)
 COMMON/CURVE/DIS(3),PHISE(3),DPHISE(3),D2PHISE(3),RHO(3),
 1 DRHO(3)
 COMMON/INERTIA/MW,MB,MS,MC,MAPP,WIYY,WIZZ,BIXX,BIZZ,
 1 CIXX,CIZZ,SIZZ
 COMMON/TRIG/COSRP(4),COSLP(4),SINRP(4),SINLP(4),COSR(4),COSL(4),
 1 SINR(4),SINL(4)
 COMMON/OUTPUT1/IOOUTPUT,ICOUNT,JPLT(12),IOUT,NPTS
 COMMON/OUTPUT2/XPRINT(12,105),PLOT1(13,105),
 1 PLOT2(13,105),PLOT3(13,105)
 COMMON/STATES/Y(46),DY(46),YMIN(46),YMAX(46)

C

DIMENSION FORCE(5),YW(7)

C

DATA ITER/10/

C

REAL LT, MAPP, MB, MC, MLZ, MPHI, MRZ,MS, MU, MW, NL, NLY, NLZ,
 1 NO, NR, NRY, NRZ

C

FRY= CRP(K,1)
 FLY= CRP(K,2)
 FRZ= CRP(K,3)
 FLZ= CRP(K,4)

C

C

C

CALCULATE THE CREEPAGES

CLX = 1.0 + A*RHO(L) - RL(K)/RO - A*YW(4)/VEL
 1 - RL(K)*YW(5)/VEL
 CRK = 1.0 - A*RHO(L) - RR(K)/RO + A*YW(4)/VEL
 1 - RR(K)*YW(5)/VEL
 CLY = (YW(3)/VEL - YW(2) + RL(K)*DPHI(K)/VEL)/COSL(K)
 CRY = (YW(3)/VEL - YW(2) + RR(K)*DPHI(K)/VEL)/COSR(K)
 CLSP = -SINL(K)*(1.0/RO + YW(5)/VEL) + COSL(K)*(YW(4)/VEL
 1 - RHO(L))
 CRSP = SINR(K)*(1.0/RO + YW(5)/VEL) + COSR(K)*(YW(4)/VEL
 1 - RHO(L))

C

C

C

DETERMINE THE AXLE LOAD AND MOMENT

YT = Y(15)
 IF(L.EQ.2)YT = Y(41)
 AXLEM = (HT*MS*G + (HS+HC)*(0.25*MC + 0.5*MB)*G)*(CANTD - PHI(K))
 1 +G* (0.25*MC + 0.5*MB)*(Y(21) - HP*Y(22) - YW(1))
 1 + G*MS*(YT-YW(1))
 AXLEL = (MW + MS + 0.25*MC + 0.5*MB)*G

```

C
C CALCULATE THE ROLL MOMENT AND VERTICAL FORCE WITHOUT CREEP FORCES
C
  XMPHI = WIZZ*(D2PHI(K) + D2PHISE(L)) + AXLEM
  1      - WIYY*(VEL/RO + YW(5))*(YW(4)-VEL*RHO(L))
XFZ = AXLEL + MW*(A*D2PHISE(L) + VEL*VEL*RHO(L)*PHISE(L))
  1      + WEXT*VEL*VEL*RHO(L)*PHISE(L)/G
DENOM = 2*A - RR(K)*(SINRP(K)/COSRP(K)) - RL(K)*(SINLP(K)/COSLP(K))
XNL=0.0

C
C ITERATE TO DETERMINE NORMAL FORCE WITHIN 10 PERCENT
C
  DO 100 I=1, ITER

C
C CALCULATE THE ROLL MOMENT AND VERTICAL FORCE WITH CREEP FORCES
C
  MPHI = XMPHI + A*(FRZ - FLZ) - RR(K)*FRY - RL(K)*FLY
  FZ = XFZ - (FRZ + FLZ)

C
C CALCULATE THE NORMAL FORCES
C
  NL = (MPHI + FZ*(A - RR(K)*(SINRP(K)/COSRP(K)))) / (DENOM * COSLP(K))
  NR = (FZ*(A - RL(K)*(SINLP(K)/COSLP(K))) - MPHI) / (DENOM * COSRP(K))

C
C IF NORMAL FORCE § ZERO DURING FIRST ITERATION SET IT TO ONE
C
  IF(I.NE.1)GO TO 12
  IF(NL.LT.0.0)NL = 1.0
  IF(NR.LT.0.0)NR=1.0
12  CONTINUE

C
C IF NORMAL FORCE IS LESS THAN ZERO STOP PROGRAM EXECUTION
C
  IF ((NL.LT.0.0).OR.(NR.LT.0.0)) GO TO 150
  IF(ABS(NL-XNL).LT..1*ABS(NL))GO TO 120
  XNL=NL

C
C CALCULATE THE CREEP FORCES
C
  CALL FCREEP(NL, CLX, CLY, CLSP, XFLX, XFLY, XMLZ)
  CALL FCREEP(NR, CRX, CRY, CRSP, XFRX, XFRY, XMRZ)

C
C RESOLVE CREEP FORCES IN THE WHEELSET REFERENCE FRAME
C
  FLX = XFLX - XFLY *YW(2) *COSLP(K)
  FLY = XFLX*YW(2) + XFLY *COSLP(K)
  FLZ = XFLY *SINLP(K)
  MLZ = XMLZ *COSLP(K)
  FRX = XFRX - XFRY *YW(2) *COSRP(K)
  FRY = XFRX *YW(2) + XFRY *COSRP(K)
  FRZ = -XFRY *SINRP(K)
  MRZ = XMRZ *COSRP(K)

C
100 CONTINUE
C

```

```

120  CONTINUE
      NRZ = NR*COSRP(K)
      NRY = NR*SINRP(K)
      NLZ = NL*COSLP(K)
      NLY = -NL*SINLP(K)
C
      CRP(K,1) = FRY
      CRP(K,2) = FLY
      CRP(K,3) = FRZ
      CRP(K,4) = FLZ
C
C      CALCULATE FORCES TO BE USED IN WHEELSET
C
      FORCE(1) = NRY + NLY + FRY + FLY
      FORCE(2) = A*(FRX-FLX)
      FORCE(3) = -RL(K)*FLX - RR(K)*FRX
      FORCE(4) = FLY + NLY
      FORCE(5) = FRY + NRY
      WORK = ABS(XFLX*CLX) + ABS(XFLY*CLY) + ABS(XMLZ*CLSP)
            1 + ABS(XFRX*CRX) + ABS(XFRY*CRY) + ABS(XMRZ*CRSP)
C
C      SAVE VARIABLES FOR OUTPUT
C
      IF( (NEWDT.EQ.0) .OR. (IOUTPUT.NE.ICOUNT) )GO TO 300
      IF( (K.NE.1) .AND. (K.NE.3) ) GO TO 250
      IF(K.EQ.3)K=2
      XPRINT(K*6-2,NPTS) = NLY
      XPRINT(K*6-1,NPTS) = (FLY + NLY)/(FLZ + NLZ)
      XPRINT(K*6 ,NPTS) = WORK
      IF(K.EQ.2)K=3
250  CONTINUE
      PLOT1(K*3+1,NPTS) = NLY
      PLOT2(K*3-1,NPTS) = (NLY + FLY)/(FLZ + NLZ)
      PLOT2(K*3 ,NPTS) = WORK
300  CONTINUE
      RETURN
C
C      IF NORMAL FORCES ARE LESS THAN ZERO PRINT ERROR MESSAGE
C      AND TERMINATE PROGRAM
150  CONTINUE
      CALL PRINT
      CALL PLOT
      WRITE(IOUT,155)K,NL,NR,
155  FORMAT(/15X, ° NORMAL FORCE § ZERO FOR WHEELSET °,I4,
1     /25X, ° PROGRAM TERMINATED°,
1     //20X, °NL =°, F12.1,12X, °NR =°, F12.1/)
      STOP
      END

```

SUBROUTINE FCREEP(N,CX,CY,CSP,XFX,XFY,XMZ)

DETERMINES CREEP FORCES USING CREEPPAGES AND NORMAL FORCES
FROM WHFORCE AND MODIFIED VERMEULEN- JOHNSON TECHNIQUE

COMMON/CREEP/NO,MJ,F110,F120,F330,F220

REAL NO,MJ,N,MZ, MJN

ADJUST CREEP COEFFICIENTS WITH RESPECT TO NORMAL LOAD

$F11 = F110 * (N/NO) ** (2./3.)$

$F12 = F120 * (N/NO)$

$F33 = F330 * (N/NO) ** (2./3.)$

$F22 = F220 * (N/NO) ** (4./3.)$

CALCULATE CREEP FORCES AND MOMENTS IN CONTACT PATCH

$XFX = -F33 * CX$

$XFY = -F11 * CY - F12 * CSP$

$XMZ = F12 * CY - F22 * CSP$

DETERMINE THE CREEP SATURATION COEFFICIENT

$MJN = MJ * N$

$FF = (XFX**2 + XFY**2)**.5$

$F = MJN$

$IF(FF.LT.(3.*MJN)) F = MJN*(FF/MJN -(FF/MJN)**2/3.+(FF/MJN)**3/27.)$

SATURATE CREEP FORCES AND MOMENTS

$XFX = XFX * F / FF$

$XFY = XFY * F / FF$

$XMZ = XMZ * F / FF$

RETURN

END

SUBROUTINE TRUCK(K,SUSP1,SUSP2,SUSP3,YT,DYT)

C
C
C
C

ESTABLISHES THE FIRST ORDER EQUATIONS OF MOTION FOR THE TRUCK
WHICH ARE INTEGRATED IN MAIN

COMMON NEWDT,DT,DT1,DT2,FLANGE,N,T,FTIME
COMMON/INERTIA/MW,MB,MS,MC,MAPP,WIYY,WIZZ,BIXX,BIZZ,
1 CIOX,CIZZ,SIZZ
COMMON/CONSTANT/VEL,CANTD,G,PI
COMMON/GEOMETRY/A,B,D,L,HS,HB,HC,HT,RO
COMMON/CURVE/DIS(3),PHISE(3),DPHISE(3),D2PHISE(3),RHO(3),
1 DRHO(3)

C

DIMENSION YT(6),DYT(6)

C

REAL LT,MW,MS,MC,MB,MAPP

C

DYT(1) = YT(4)
DYT(2) = YT(5)
DYT(3) = YT(6)
DYT(4) = SUSP1/(2.*MS) + G*CANTD + (RO + HS)*D2PHISE(K)
DYT(5) = (SUSP2 + VEL*DRHO(K)*(2.*SIZZ + 2.0*MS*D*D + BIZZ)
1 - SUSP3 - BIZZ*VEL*DRHO(K))/(2.0*SIZZ)
DYT(6) = -DYT(5) + (SUSP3 + BIZZ*VEL*DRHO(K))/(2.*MS*D*D+ BIZZ)

C

RETURN
END

SUBROUTINE CARBODY(SUSP1,SUSP2,SUSP3,YC,DYC)

ESTABLISHES THE FIRST ORDER EQUATIONS OF MOTION FOR CARBODY
TO BE INTEGRATED BY MAIN

COMMON NEWDT, DT,DTL,DT2, FLANGE, T,N, FTIME
COMMON/INERTIA/MW,MB,MS,MC,MAPP,WIYY,WIZZ,BIXX, BIZZ,
1 CIXX, CIZZ, SIZZ
COMMON/CONSTANT/VEL,CANTD,G,PI
COMMON/GEOMETRY/A,B,D,LT,HS,HB,HC,HT,RO
COMMON/CURVE/DIS(3),PHISE(3),DPHISE(3),D2PHISE(3),RHO(3),
1 DRHO(3)

DIMENSION YC(6), DYC(6)

REAL LT,MAPP,MW,MS,MC,MB

EQUATIONS OF MOTION FOR FULL CARBODY MODEL

ACCEL1 = - (MC*(RO + HB + HC) + 2.*MB*(RO + HB))*D2PHISE(2)
1 - G*CANTD
ACCEL2 = (CIZZ + 2.*BIZZ + 2.*MB*HT*(RO + HB) + MC*(HT-HB))*
1 (RO + HC + HB))*D2PHISE(2)
1 + (2.*MB*G*HT - MC*G*HC)*PHISE(2)
1 - (2.*MB*HT + MC*(HT-HC))*VEL*VEL*RHO(2)
ACCEL3 = - VEL*DRHO(2)*CIZZ
Q1 = 1.0/(CIXX + 2.*BIXX + 2.*MB*HT*HT + MC*(HT-HC)**2)
Q2 = 2.*MB*HT + MC*(HT-HC)
Q3 = MC + 2.*MB + Q1*Q2*Q1
DYC(1) = YC(4)
DYC(2) = YC(5)
DYC(3) = YC(6)
DYC(4) = (SUSP1-ACCEL1 - (SUSP2-ACCEL2)*Q2*Q1)/Q3
DYC(5) = (-Q2*DYC(4) + SUSP2-ACCEL2)*Q1
DYC(6) = (SUSP3 - ACCEL3)/(CIZZ + 2.*L*L*MB)

RETURN
END

SUBROUTINE OUTPUT

COMMON NEWDT,DT,DT1,DT2,FLANGE,N,T,FTIME

COMMON/CONSTANT/VEL,CANTD,G,PI

COMMON/STATES/Y(46),DY(46)

COMMON/OUTPUT1/IOOUTPUT,ICOUNT,JPLT(12),IOUT,NPTS

COMMON/OUTPUT2/XPRINT(12,105),PLOT1(13,105),

1 PLOT2(13,105),PLOT3(13,105)

C
C
C

SAVE STATE VARIABLES IN ARRAY FOR PRINTOUT

```

XPRINT(1,NPTS) = T
XPRINT(2,NPTS) = Y(1)*12.0
XPRINT(3,NPTS) = Y(2)*180.0/PI
XPRINT(7,NPTS) = T
XPRINT(8,NPTS) = Y(8)*12.0
XPRINT(9,NPTS) = Y(9)*180.0/PI
PLOT1(1,NPTS) = T
PLOT1(2,NPTS) = Y(1)*12.0
PLOT1(3,NPTS) = Y(2)*180.0/PI
PLOT1(5,NPTS) = Y(8)*12.0
PLOT1(6,NPTS) = Y(9)*180.0/PI
PLOT1(8,NPTS) = Y(27)*12.0
PLOT1(9,NPTS) = Y(28)*180.0/PI
PLOT1(11,NPTS) = Y(34)*12.0
PLOT1(12,NPTS) = Y(35)*180.0/PI
PLOT2(1,NPTS) = T
PLOT2(4,NPTS) = DY(3)*12.0
PLOT2(7,NPTS) = DY(10)*12.0
PLOT2(10,NPTS) = DY(29)*12.0
PLOT2(13,NPTS) = DY(36)*12.0
PLOT3(1,NPTS) = T
PLOT3(2,NPTS) = Y(15)*12.0
PLOT3(3,NPTS) = Y(16)*180.0/PI
PLOT3(4,NPTS) = Y(17)*180.0/PI
PLOT3(5,NPTS) = DY(18)*12.0
PLOT3(6,NPTS) = Y(41)*12.0
PLOT3(7,NPTS) = Y(42)*180.0/PI
PLOT3(8,NPTS) = Y(43)*180.0/PI
PLOT3(9,NPTS) = DY(44)*12.0
PLOT3(10,NPTS) = Y(24)*12.0
PLOT3(11,NPTS) = Y(25)*180.0/PI
PLOT3(12,NPTS) = Y(26)*180.0/PI
PLOT3(13,NPTS) = DY(27)*12.0

```

C

RETURN
END

```

SUBROUTINE PRINT
COMMON/OUTPUT1/IOOUTPUT,ICOUNT,JPLT(12),IOUT,NPTS
COMMON/OUTPUT2/XPRINT(12,105),PLOT1(13,105),
1   PLOT2(13,105),PLOT3(13,105)

```

C

C

PRINT OUT FOR LEAD WHEELSET OF LEAD TRUCK

C

```

WRITE(IOUT,10)
10  FORMAT(1H1 //25X, °LEAD WHEELSET OF LEAD TRUCK°//
1   15X, °TIME      LAT      ATTACK      FLANGE      L/V      WORK°/
1   15X, °          EXCUR   ANGLE      FORCE        RATIO    °/
1   15X, °SECS     INCH     DEGREE     LBS        °/ )
DO 30 J = 1,NPTS-1
IF(J.EQ.50)WRITE(IOUT,10)
WRITE(IOUT,20) (XPRINT(I,J),I=1,6)
20  FORMAT(12X,F8.4,1X,F9.4,1X,F9.5,1X,F9.1,1X,F9.4,1X,F9.4)
30  CONTINUE

```

C

C

PRINT OUT FOR TRAILING WHEELSET OF TRAILING TRUCK

C

```

WRITE(IOUT,15)
15  FORMAT(1H1 //25X, °TRAILING WHEELSET OF LEAD TRUCK°//
1   15X, °TIME      LAT      ATTACK      FLANGE      L/V      WORK°/
1   15X, °          EXCUR   ANGLE      FORCE        RATIO    °/
1   15X, °SECS     INCH     DEGREE     LBS        °/      )
DO 35 J = 1,NPTS-1
IF(J.EQ.50)WRITE(IOUT,15)
WRITE(IOUT,20) (XPRINT(I,J),I=7,12)
35  CONTINUE

```

C

C

PRINT MAX AND MIN

C

```

CALL PRIMAXMIN
RETURN
END

```


SUBROUTINE PRIMAXMIN

```

C
C PRINTS OUT THE MIN AND MAX VALUES OF STATE VARIABLES
C
COMMON/STATES/Y(46),DY(46),YMAX(46),YMIN(46)
C
DATA IOUT,PI/3,3.1416/
WRITE(IOUT,100)
100 FORMAT(1H1/// 24X, °EXTREME VALUES OF STATE VARIABLES°//
1 T54, °MINIMIUM°, T64, °MAXIMIUM°)
C
WRITE(IOUT,110)
110 FORMAT(/12X, °LEAD WHEELSET OF LEAD TRUCK°)
C
WRITE(IOUT,120)YMIN(1)*12.0, YMAX(1)*12.0, YMIN(2)*180.0/PI,
1 YMAX(2)*180.0/PI, YMIN(3)*12.0, YMAX(3)*12.0,
2 YMIN(4)*180.0/PI, YMAX(4)*180.0/PI,
3 YMIN(5)*180.0/PI, YMAX(5)*180.0/PI,
4 YMIN(6)*12.0, YMAX(6)*12.0, YMIN(7)*12.0,
5 YMAX(7)*12.0
120 FORMAT(12X, °LATERAL EXCURSION OF WHEELSET (INCHES) °
1 ,F8.4,2X,F8.4
2 /12X, °YAW ANGLE OF WHEELSET (DEGREES) °
1 ,F8.4,2X,F8.4
3 /12X, °LATERAL VELOCITY OF WHEELSET (IN/SEC) °
1 ,F8.4,2X,F8.4
4 /12X, °YAW ANGLE RATE OF WHEELSET (DEG/SEC) °
1 ,F8.4,2X,F8.4
5 /12X, °SPIN PERTURBATION OF WHEELSET (DEG/SEC) °
1 ,F8.4,2X,F8.4
6 /12X, °LEFT RAIL LATERAL DISPLACEMENT (INCHES) °
1 ,F8.4,2X,F8.4
7 /12X, °RIGHT RAIL LATERAL DISPLACEMENT (INCHES)°
1 ,F8.4,2X,F8.4)
C
WRITE(IOUT,130)
130 FORMAT(/12X, °TRAILING WHEELSET OF LEAD TRUCK:°)
WRITE(IOUT,120)YMIN(8)*12.0, YMAX(8)*12.0, YMIN(9)*180.0/PI,
1 YMAX(9)*180.0/PI, YMIN(10)*12.0, YMAX(10)*12.0,
2 YMIN(11)*180.0/PI, YMAX(11)*180.0/PI,
3 YMIN(12)*180.0/PI, YMAX(12)*180.0/PI,
4 YMIN(13)*12.0, YMAX(13)*12.0, YMIN(14)*12.0,
5 YMAX(14)*12.0
C
WRITE(IOUT,140)
140 FORMAT(/12X, °LEAD TRUCK:°)
WRITE(IOUT,150)YMIN(15)*12.0, YMAX(15)*12.0,
1 YMIN(16)*180.0/PI, YMAX(16)*180.0/PI,
2 YMIN(17)*180.0/PI, YMAX(17)*180.0/PI,
3 YMIN(18)*12.0, YMAX(18)*12.0,
4 YMIN(19)*180.0/PI, YMAX(19)*180.0/PI,
5 YMIN(20)*180.0/PI, YMAX(20)*180.0/PI
150 FORMAT(12X, °LATERAL EXCURSION OF TRUCK (INCHES) °
1 ,F8.4,2X,F8.4
2 /12X, °YAW ANGLE OF TRUCK (DEGREES) °

```

```

1      , F8.4, 2X, F8.4
3      /12X, °WARP ANGLE OF TRUCK (DEGREES)
1      , F8.4, 2X, F8.4
4      /12X, °LATERAL VELOCITY OF TRUCK (IN/SEC)
1      , F8.4, 2X, F8.4
5      /12X, °YAW ANGLE RATE OF TRUCK (DEG/SEC)
1      , F8.4, 2X, F8.4
6      /12X, °WARP ANGLE RATE OF TRUCK (RAD/SEC)
1      , F8.4, 2X, F8.4

C
WRITE(IOUT,160)
160   FORMAT(/12X, °CARBODY:°)
C
WRITE(IOUT,180)YMIN(21)*12.0,YMAX(21)*12.0,
1      YMIN(22)*180.0/PI,YMAX(22)*180.0/PI,
2      YMIN(23)*180.0/PI,YMAX(23)*180.0/PI,
3      YMIN(24)*12.0,YMAX(24)*12.0,
4      YMIN(25)*180.0/PI,YMAX(25)*180.0/PI,
5      YMIN(26)*180.0/PI,YMAX(26)*180.0/PI
180   FORMAT(12X, °LATERAL EXCURSION OF CARBODY (INCHES)
1      , F8.4, 2X, F8.4
2      /12X, °ROLL ANGLE OF CARBODY (DEGREES)
1      , F8.4, 2X, F8.4
3      /12X, °YAW ANGLE OF CARBODY (DEGREES)
1      , F8.4, 2X, F8.4
5      /12X, °LATERAL VELOCITY OF CARBODY (IN/SEC)
1      , F8.4, 2X, F8.4
6      /12X, °ROLL ANGLE RATE OF CARBODY (DEG/SEC)
1      , F8.4, 2X, F8.4
7      /12X, °YAW ANGLE RATE OF CARBODY (DEG/SEC)
1      , F8.4, 2X, F8.4

C
WRITE(IOUT,190)
190   FORMAT(/12X, °LEAD WHEELSET OF TRAILING TRUCK:°)
WRITE(IOUT,120)YMIN(27)*12.0,YMAX(27)*12.0,YMIN(28)*180.0/PI,
1      YMAX(28)*180.0/PI,YMIN(29)*12.0,YMAX(29)*12.0,
2      YMIN(30)*180.0/PI,YMAX(30)*180.0/PI,
3      YMIN(31)*180.0/PI,YMAX(31)*180.0/PI,
4      YMIN(32)*12.0,YMAX(32)*12.0,YMIN(33)*12.0,
5      YMAX(33)*12.0
WRITE(IOUT,210)
210   FORMAT(/12X, °TRAILING WHEELSET OF TRAILING TRUCK:°)
WRITE(IOUT,120)YMIN(34)*12.0,YMAX(34)*12.0,YMIN(35)*180.0/PI,
1      YMAX(35)*180.0/PI,YMIN(36)*12.0,YMAX(36)*12.0,
2      YMIN(37)*180.0/PI,YMAX(37)*180.0/PI,
3      YMIN(38)*180.0/PI,YMAX(38)*180.0/PI,
4      YMIN(39)*12.0,YMAX(39)*12.0,YMIN(40)*12.0,
5      YMAX(40)*12.0
WRITE(IOUT,220)
220   FORMAT(1H1 ///12X, °TRAILING TRUCK:°)
WRITE(IOUT,150)YMIN(41)*12.0,YMAX(41)*12.0,
1      YMIN(42)*180.0/PI,YMAX(42)*180.0/PI,
2      YMIN(43)*180.0/PI,YMAX(43)*180.0/PI,
3      YMIN(44)*12.0,YMAX(44)*12.0,
4      YMIN(45)*180.0/PI,YMAX(45)*180.0/PI,

```

155

5
RETURN
END

YMIN(46)*180.0/PI, YMAX(46)*180.0/PI

SUBROUTINE PLOT

```

COMMON/OUTPUT1/IOOUTPUT, ICOUNT, JPLT(12), IOUT, NPTS
COMMON/OUTPUT2/XPRINT(12,105), PLOT1(13,105),
1      PLOT2(13,105), PLOT3(13,105)
CHARACTER*40 XLAB1, YLAB1, YLAB2, YLAB3, YLAB4,
1      YLAB5, YLAB6, YLAB7, YLAB8, YLAB9, YLAB10
XLAB1 = °          TIME (SEC) °
YLAB1 = ° LATERAL EXCURSION OF WHEELSET (IN) °
YLAB2 = ° ANGLE OF ATTACK OF WHEELSETS (DEG) °
YLAB3 = ° FLANGE FORCE ON OUTER WHEELS (LB) °
YLAB4 = ° L/V RATIO FOR WHEELSETS °
YLAB5 = ° WORK ON WHEELSET (FT-LB) °
YLAB6 = ° ACCEL. OF WHEELSETS (IN/SEC2) °
YLAB7 = ° LAT EXCUR. OF TRUCK AND CARBODY (IN) °
YLAB8 = ° YAW ANGLE OF TRUCK AND CARBODY (DEG) °
YLAB9 = ° WARP ANGLE OF TRUCKS (DEG) °
YLAB10 = ° ROLL ANGLE OF CARBODY (DEG) °
YLAB11 = ° ACCEL. OF TRUCK AND CARBODY (IN/SEC2) °
NPTS=NPTS-1
IF(JPLT(1).EQ.1)CALL OPICTR( PLOT1, 13, NPTS, QY(2,5,8,11),
1      QX(1),QXLAB(XLAB1), QYLAB(YLAB1), QMOVE(00),QLABEL(4))
IF(JPLT(2).EQ.1)CALL OPICTR( PLOT1, 13, NPTS, QY(3,6,9,12),
1      QX(1),QMOVE(00),QLABEL(4),QXLAB(XLAB1), QYLAB(YLAB2))
IF(JPLT(3).EQ.1)CALL OPICTR( PLOT1, 13, NPTS, QY(4,7,10,13),
1      QX(1),QMOVE(00),QLABEL(4),QXLAB(XLAB1),QYLAB(YLAB3))
IF(JPLT(4).EQ.1)CALL OPICTR( PLOT2, 13, NPTS,QY(2,5,8,11),
1      QX(1),QMOVE(00),QLABEL(4),QXLAB(XLAB1),QYLAB(YLAB4))
IF(JPLT(5).EQ.1)CALL OPICTR( PLOT2, 13, NPTS, QY(3,6,9,12),
1      QX(1),QMOVE(00),QLABEL(4),QXLAB(XLAB1),QYLAB(YLAB5))
IF(JPLT(6).EQ.1)CALL OPICTR( PLOT2, 13, NPTS, QY(4,7,10,13),
1      QX(1),QMOVE(00),QLABEL(4),QXLAB(XLAB1),QYLAB(YLAB6))
IF(JPLT(7).EQ.1)CALL OPICTR( PLOT3, 13, NPTS, QY(2,6,10),
1      QX(1),QMOVE(00),QLABEL(4),QXLAB(XLAB1),QYLAB(YLAB7))
IF(JPLT(8).EQ.1)CALL OPICTR( PLOT3, 13, NPTS, QY(3,7,12),
1      QX(1),QMOVE(00),QLABEL(4),QXLAB(XLAB1),QYLAB(YLAB8))
IF(JPLT(9).EQ.1)CALL OPICTR( PLOT3, 13, NPTS, QY(4,8),
1      QX(1),QMOVE(00),QLABEL(4),QXLAB(XLAB1),QYLAB(YLAB9))
IF(JPLT(10).EQ.1)CALL OPICTR( PLOT3, 13, NPTS, QY(11),QX(1),
1      QMOVE(00),QLABEL(4),QXLAB(XLAB1),QYLAB(YLAB10))
IF(JPLT(11).EQ.1)CALL OPICTR(PLOT3,13,NPTS,QY(5,9,13),
1      QX(1),QMOVE(00),QLABEL(4),QXLAB(XLAB1),QYLAB(YLAB11))
CONTINUE
RETURN
END

```